

**Geophysical Constraints on Mechanisms of Ocean
Plateau Formation from Shatsky Rise,
Northwest Pacific**

**Cruise Report
MGL1004
R/V Marcus G. Langseth
Honolulu to Honolulu
17 July - 13 September, 2010**

Jun Korenaga
Department of Geology and Geophysics
Yale University
New Haven, CT 06520

William Sager
Department of Oceanography
Texas A&M University
College Station, TX, 77843

Table of Contents

SUMMARY	4
EXECUTIVE SUMMARY	4
SCIENTIFIC OBJECTIVES	5
OPERATIONAL OBJECTIVES.....	6
PRELIMINARY CRUISE ASSESSMENT	7
PROJECT PRINCIPAL INVESTIGATORS	9
PERSONNEL	10
SCIENCE COMPLEMENT	10
R/V MARCUS G. LANGSETH CREW	11
NARRATIVE	12
INTRODUCTION AND BACKGROUND	22
SCIENTIFIC BACKGROUND: OCEANIC PLATEAU FORMATION.....	22
ORIGIN OF SHATSKY RISE	24
WHY STUDY SHATSKY RISE?	25
TESTING PLUME AND RIDGE MODELS.....	26
PRIOR RESEARCH ON SHATSKY RISE	28
INITIAL SURVEY PLAN	30
OPERATION DETAILS	32
NAVIGATION	32
SEISMIC REFRACTION SHOOTING OPERATIONS	33
MULTICHANNEL SEISMIC SHOOTING OPERATIONS	33
OCEAN BOTTOM SEISMOMETER OPERATIONS	35
WHOI D2 – DEPLOYMENT	35
WHOI D2 – RECOVERY	36
UNDERWAY GEOPHYSICS	37
MULTIBEAM BATHYMETRY.....	37
TOWED MAGNETOMETER	37
GRAVIMETER.....	37
FLUXGATE MAGNETOMETER	37
WEATHER INFORMATION	38
SHIPBOARD COMPUTING ENVIRONMENT	39
SHIPBOARD DATA PROCESSING	39
MULTICHANNEL SEISMIC PROFILES	39
MULTIBEAM BATHYMETRY.....	41
INITIAL OCEAN BOTTOM SEISMOMETER DATA PROCESSING.....	42
OCEAN BOTTOM SEISMOMETER SEG Y DATA PROCESSING.....	42
SURVEY OUTCOME AND ASSESSMENT	44

PRELIMINARY DATA REVIEW	48
MULTICHANNEL SEISMIC PROFILES	48
OCEAN BOTTOM SEISMOMETER DATA	60
MULTIBEAM BATHYMETRY	62
UNDERWAY GEOPHYSICAL DATA	67
REFERENCES	69
APPENDICES.....	73
DATA LIST.....	73
MCS LOGS.....	74
MCS PROCESSING PARAMETERS OUTLINE	74
LITTLE SCRIPTS FOR MCS PROCESSING.....	79
PYTHON SCRIPT FOR P190 FILES: P190_SHOT_DIST_XEND.PY.....	79
GMT SCRIPT FOR PLOTTING BLACK WHITE SEISMIC SECTIONS: PLOTSEGY.GMT	80
GMT SCRIPT FOR PLOTTING COLOR SEISMIC SECTIONS: SEGY2GRD.GMT	81
WHOI D2 SEISMIC RECEIVER INSTRUMENT DESCRIPTION	82
OCEAN BOTTOM SEISMOMETER DEPLOYMENT RECORD	84
OCEAN BOTTOM SEISMOMETER RECOVERY RECORD	85
OCEAN BOTTOM SEISMOMETER DATA QUALITY	86
WEEKLY REPORTS TO NSF.....	87
NOTES ON OUTREACH EFFORTS	100
SUMMARY OF PRE-CRUISE TWISTS AND TURNS.....	101
INCIDENTAL HARASSMENT AUTHORIZATION (IHA)	102

Summary

Executive Summary

R/V *Marcus G. Langseth* cruise MGL1004 formed the major data acquisition phase of the NSF-funded project, "Geophysical Constraints on Mechanisms of Ocean Plateau Formation from Shatsky Rise, Northwest Pacific" (OCE-0926611; OCE-0926945). Deciphering the origins of large oceanic plateaus is a critical element for understanding mantle dynamics and its relation to terrestrial magmatism, and Shatsky Rise was chosen as a high-priority target because it provides a unique tectonic setting to distinguish between various models proposed for the formation of oceanic plateaus. The purpose of this survey was to provide critical missing information on (1) the thickness, velocity structure, and composition of the Shatsky Rise crust, and (2) the history of magmatic emplacement and later tectonic development of the Rise. This was planned to be achieved by acquiring seismic data along two refraction lines over the Tamu Massif, which represents the early, most voluminous phase of the Rise construction, and over 3,000 km of seismic reflection lines covering both the Tamu and Ori Massifs, the latter of which corresponds to the intermediate phase of the plateau evolution.

The cruise was unfortunately hampered by two medical diversions, which took ~16 days in total, and even with a seven-day extension provided by NSF, the survey had to be scaled down to focus on the southern part, leaving the northern part to be completed in another cruise tentatively scheduled for spring 2012. The southern part includes all of refraction lines and ~1800 km of reflection transects, all on the Tamu Massif. The work remaining to be done includes the rest of reflection transects, which extend from the northern flank of the Tamu Massif to the center of the Ori Massif.

The *Langseth* fired over 47,000 shots from its 36-gun tuned airgun source into an array of seismic receivers: the *Langseth*'s 6-km-long multichannel streamer and 28 Woods Hole Oceanographic Institution ocean-bottom seismometers (OBSs). As far as the southern part of the survey is concerned, the operational goals of the experiment were achieved in full. All of 28 OBSs deployed were recovered successfully, and all instruments returned high-quality data. Multichannel seismic (MCS) profiling was also conducted with no major issues, yielding high-quality reflection data. Migrated MCS lines were produced during the cruise, exhibiting intriguing intrabasement reflectors as well as revealing the true lateral extent of Shatsky Rise. OBS data show spectacular wide-angle refraction and reflection arrivals with the source-receiver distance often exceeding 200 km. The data collected during this experiment are sufficient to accurately determine the entire crustal structure of the Tamu Massif and will provide key information on the early magmatic construction of Shatsky Rise. By combining with future seismic data from the northern part of the survey, this information will provide an important tectonic framework for synthesizing existing geological, geophysical, and geochemical data and for resolving the formation mechanism of this large igneous province.

Scientific Objectives

The Shatsky Rise active-source seismic project is designed to make accurate measurements of crustal thickness and velocity structure over the most prominent volcanic feature of the Rise, the Tamu massif, by wide-angle refraction and reflection recorded by OBS, and to map out basement topography and fine-scale upper crustal structure over a significant fraction of the rise, covering both the Tamu and Ori Massifs, by MCS profiling.

Oceanic plateaus belong to the so-called large igneous provinces (LIPs), the largest of which represent terrestrial magmatism of vast spatial extents yet formed only in a relatively short period. The origins of such extraordinary geological phenomena are still poorly understood, but the scale of magmatism requires that the source mantle must have been in a thermally, chemically, or dynamically anomalous state. Models put forward for the formation of oceanic plateaus include the impingement of a mantle plume head rising from the core-mantle boundary, tapping of a broad upper-mantle thermal anomaly by spreading centers, and the upwelling of fertile mantle driven by plate-tectonic stresses. Resolving the mechanism of plateau formation is thus directly connected to the first-order issues in mantle dynamics. Contrasting to the abundance of hypotheses, however, field observations that can distinguish between these models are conspicuously missing. Oceanic plateaus have scarcely been surveyed with modern geophysical methods. Shatsky Rise was chosen as a prime target because, compared to other plateaus in the Pacific, its tectonic environment is well understood thanks to its formation during a period of frequent magnetic polarity reversals. This seismic survey thus forms a major steppingstone to the new generation of exploring oceanic large igneous provinces.

The Shatsky Rise survey consists of two crossing perpendicular OBS refraction lines over the Tamu Massif and over 3,000-km-long MCS reflection transects that run along and across the major axis of Shatsky Rise. The resulting data will provide answers to several questions regarding the origin of the Rise, including:

1. What is the structure and volume of Shatsky Rise crust? How deep is the Moho discontinuity beneath the Rise? How does topography and crustal thickness correlate?
2. Was Shatsky Rise formed over a thermal or chemical anomaly? Does crustal velocity correlate with crustal thickness positively (thermal origin) or negatively (chemical origin)?
3. How was Shatsky Rise construction modulated by spreading ridges? What is the relation between the ridge-ridge-ridge triple junction and plateau formation?
4. Did a plume head create Shatsky Rise? Did the Rise form rapidly as expected from the melting of a mantle plume head? Or did it form in a prolonged time as predicted by tapping of anomalous mantle by plate tectonics?

Operational Objectives

Cruise MGL1004 was comprised of two parts: (1) a seismic survey of the Shatsky Rise along two crossing perpendicular OBS refraction lines over the Tamu Massif (a 410-km-long line across the rise axis and a 160-km-long line along the axis) and (2) a series of MCS reflection transects over the Tamu Massif totaling ~2000 km in length. Wide-angle seismic data were recorded by 28 Woods Hole Oceanographic Institution OBSs, and vertical-incidence data were recorded by the *Langseth's* 6-km-long towed hydrophone streamer. Shots were fired using the *Langseth's* 108-liter (6600 cubic inch) airgun array.

The primary operational goals were to:

- Deploy and recover 28 OBSs on two refraction lines over the Tamu Massif.
- Fire the 36-gun array into the OBSs at a shot interval of ~70s on all of refraction lines (two "2-D" lines directly over the OBSs and four additional "3-D" segments displaced horizontally from the OBS lines) and into the MCS streamer at an interval of 50 m on all of reflection transects.
- Collect multibeam bathymetry, magnetic, and gravity data along all seismic transects as well as during transits. Magnetic data include both those from a towed cesium-vapor magnetometer and from a shipboard fluxgate magnetometer.
- Produce SEGY archive files for the OBS data.
- Produce pseudo-real-time near-trace plots of all MCS data to monitor data quality.
- Produce preliminary stacks of all MCS data.
- Produce CDP-sorted data for all MCS data.
- Copy all raw and processed navigation, seismic, and underway geophysics data to PIs' hard drives.

Preliminary Cruise Assessment

The southern part of the original survey plan includes all of the OBS refraction lines and ~1800 km of MCS reflection transects, all on the Tamu Massif. The part of the survey that was not completed is the MCS reflection transects covering from the northern flank of the Tamu Massif to the center of the Ori Massif and crossing IODP drill Sites U1348, U1349, and U1350. Because of the scaling down of the survey caused by two medical diversions, the northern part was left for a second leg.

With regard to the southern part, we achieved completely our principal goal of acquiring both OBS and MCS data over the southern and central Tamu Massif. Key factors in this success include: (1) the highly professional *Langseth* crew, LEDO science tech group, and WHOI OBS team, (2) good fortune with weather (we were hit by no typhoons), (3) low biological productivity in the survey area (only one encounter with marine mammals during shooting), and (4) the flexibility of the original survey plan that allowed us to redesign quickly when confronted with a historical chain of unlikely incidents.

The reliability of the WHOI OBS operations contributed substantially to our success: no contingency time had to be used for OBS deployment and recovery. All instruments lifted off from the seafloor on command; only one instrument required two burn commands, and others were released by just one command. Sea conditions were good throughout recovery, all instruments were identified shortly after their expected arrival time on surface, and they were brought on deck smoothly thanks to skillful ship maneuvering. All instruments returned data. Though the geophone components are found to be of variable quality, the hydrophone component, which is sufficient for the reading of travel time data, is consistently of excellent quality.

MCS recording was also successful, and we acquired high-quality data along all transects. Streamer balancing was in a nearly perfect condition, and the steady firing of the airgun array was achieved without major problems. Occasional gun malfunctions were always fixed in a timely manner by the LDEO tech group during the preventive gun maintenance time that was scheduled at major waypoints. Good weather throughout the MCS shooting also helped us to acquire data with low ambient noise.

Shipboard processing was a success for both MCS and OBS data. Jacqueline Floyd streamlined the MCS data processing as well as mentoring watchstanders so that we were able to see a near-trace plot soon after finishing every MCS transect. Brute stack images quickly followed, which played a critical role in the planning of additional MCS line to be shot with unused contingency time. Peter Lemmond of WHOI provided SEGY files for all of refraction and reflection lines soon after the OBS recovery. Velocity reduction, band-pass filtering, and predictive deconvolution were applied to all OBS data for initial quality control.

Preliminary scientific results from MGL1004 include:

1. The basement morphology of Shatsky Rise and its intrabasement structure suggest the construction of the Rise by the massive outpouring of magma onto the surrounding seafloor, rather than by incremental accretion as seen for Iceland.
2. Seismic lines crossing Tamu Massif show no evidence of subaerial erosion, even though dredging and drilling data imply the edifice summit was in shallow water. These profiles also show the shape of the massif and demonstrate that it is a massive central volcano with

anomalously low flank slopes, probably resulting from massive eruptions that traveled long distances.

3. The spatial extent of Shatsky Rise is greater than previously thought. Even at the 5500-m contour, which was believed to outline the Rise, crust is found to be ~9-10-km thick. The transition to normal oceanic crust appears to take place at the depth of ~5700-5800 m.
4. *PmP* travel times from OBS data suggest that crustal thickness probably reaches ~28 km beneath the Tamu Massif, which is 40% thicker than the maximum thickness of ~20 km suggested by the previous seismic study conducted in 1960s.

Project Principal Investigators

Jun Korenaga (jun.korenaga@yale.edu)
Department of Geology and Geophysics
Yale University
New Haven, CT 06520

William W. Sager (wsager@ocean.tamu.edu)
Department of Oceanography
Texas A&M University
College Station, TX 77843

John B. Diebold* (johnd@ldeo.columbia.edu)
Lamont-Doherty Earth Observatory
Columbia University
Palisades, NY 10964

*Deceased on July 1, 2010.

Personnel

Science Complement

Jun Korenaga	Chief Scientist	Yale
William W. Sager	Co-Chief Scientist	TAMU
Jacqueline S. Floyd	Scientist	Yale
David L. Dubois	OBS	WHOI
James R. Elsenbeck II	OBS	WHOI
Timothy V. Kane	OBS	WHOI
Peter C. Lemmond	OBS	WHOI
Caroline K. Brooks	Graduate Student	TAMU
Kai Gao	Graduate Student	TAMU
Dan'l M. Lewis	Graduate Student	TAMU
Tolulope Olugboji	Graduate Student	Yale
Christopher F. Paul	Graduate Student	TAMU
Duayne M. Rieger	Graduate Student	Yale
Jinchange Zhang	Graduate Student	TAMU
Diana M. Antochiw	MMO	RPS
Joseph A. Beland	MMO	LGL
Amanda E. Dubuque	MMO	RPS
Claudio Fossati	MMO	U. Pavia
John R. Nicolas*	MMO	RPS
Robert J. Steinhaus	Chief Science Officer	LDEO
David M. Martinson	Science Officer	LDEO
Bernard K. McKiernan	Science Tech	LDEO
Michael P. Tatro	Science Tech	LDEO
Zhi Qiang Zhang	Science Tech	LDEO
David Ng-Li	Science Tech	LDEO
Thomas R. Spoto	Airgun Technician	LDEO
Robert C. Gunn	Airgun Technician	LDEO
Carlos D. Gutierrez	Airgun Technician	LDEO
Timothy M. Finn	Airgun Technician	LDEO

*Deceased on July 30, 2010

R/V Marcus G. Langseth Crew

Mark C. Landow	Captain
Patrick O'Leary	Chief Mate
Breckenridge C. Crum	2nd Mate
Rachel A. Widerman	3rd Mate
Jason J. Woronowicz	Boatswain
Ricardo M. Redito	A/B
George G. Cereno	A/B
Marcus B. Nadler	O/S
Jeromiel J. Webster	O/S
Nicky R. Applewhite	O/S
Albert D. Karlyn	Chief Engineer
Peter A. Chizmar	1st Engineer
Ryan P. Vetting	2nd Engineer
Trevor M. Lapham	3rd Engineer
Jack C. Billings	Oiler
Guillermo F. Uribe	Oiler
Meagan E. Fahey	Oiler
Hervin McLean Fuller	Steward
Michael J. Duffy*	Cook
John H. Schwartz	Electrician

*Disembarked on August 19, 2010

Narrative

July 13, 2010 (Tue)

Korenaga arrived at R/V Langseth, which was at the University of Hawaii Marine Facility, around 9 a.m. The WHOI OBS team had already arrived (half an hour before). Korenaga met with Captain Mark Landow, Anthony Johnson, and Dave Martinson. Sager arrived shortly after. Sager and Korenaga decided to have a first science-party meeting before noon tomorrow (~11AM).

July 14, 2010 (Wed)

All students were on board before 12 p.m. Safety orientation was given by Chief Science Officer Steinhaus at 2 p.m, followed by a tour around the ship. At 4 p.m, Sager and Korenaga had a pre-cruise meeting with the captain, the WHOI team, and science officers. IHA draft were expected to be issued on 15 July, a teleconference was scheduled for 8:30 a.m Friday (local time). An overall survey plan was briefed. Acquisition parameters were given to the LDEO tech group. The caption told us to use 10 knots as a transit speed. Peter Lemmond explained what to expect for OBS deployment and recovery. Deployment is quick and usually is completed within <10 minutes. Recovery will take 15 minutes (times # of trials) for release and 15-30 minutes from expected time on surface to onboard. Most instruments have been released on a first trial; they will try eight trials at most (i.e., 2 hours) before giving up. In case of rough sea, guns will be pulled up if waves are > 10 feet and streamers if > 15 feet.

July 15, 2010 (Thu)

In the morning Langseth moved to the navy yard at Pearl Harbor for fueling, which was completed before 5 p.m. local, and the ship returned to the UH pier at ~7 p.m.

The IHA draft was received. It contained standard contents, and nothing special was noticed. Korenaga gathered passports from the science party and handed them to the captain. Dan'l Lewis did not bring his, and just in case we end up with a foreign port, his passport was asked to be delivered to the agent in Honolulu and will be kept there during the cruise.

July 16, 2010 (Fri)

At 8:30 a.m. local, Sager, Korenaga, science officers, the captain, and the MMO team had conference call with Lamont regarding the IHA draft. Given its straightforward nature (compared to previous ones), it went well with not many questions. Later, NMFS finally issued a signed IHA to Lamont (~4 p.m. EDT). The limiting factor for the sail time turned out to be one of airgun technicians (Robby Gunn), who was late due to a flight delay. Based on this fact, the captain set the sailing time at 3 p.m. local on 17 July. At ~8 p.m. EDT, sailing orders were issued by LDEO. The return date of the cruise is set to September 7, 2010, so the net cruise days is 52.

Steinhaus set up the triaxial fluxgate magnetometer system on the roof of the winch office in the afternoon.

July 17, 2010 (Sat)

In the morning, Sager and Korenaga determined watchstanding shifts. Steinhaus informed us that full watch would start Monday midnight until when he will be busy starting up all instruments. He will give students an orientation sometime tomorrow. At 1 p.m., the science party had a meeting to be briefed on expected watchstanding tasks and the overall survey plan. Gunn has arrived in Honolulu at ~3 p.m., but unfortunately his luggage did not. He went to a nearby Kmart to buy clothes, and at 4:35 p.m. local, we were finally able to sail. Later, Korenaga had a meeting with the

WHOI OBS team. They recommended to use 8 knots for transit between OBS locations, so the cruise plan was revised slightly.

July 18, 2010 (Sun)

Thanks to good weather and trade winds pushing us ahead, the ship has been steaming at a nice speed of ~11 knots since departure. At 10:20AM we had fire & boat drill. At 1 p.m., we had a watchstanders orientation. The science party was also given more explanations on the logistics of the survey plan as well as its scientific background. A plan about blogging at <http://lifeonshatsky.blogspot.com/> (for outreach) was also explained. Interference between the multibeam and Knudsen echosounders was noted, and we decided to decrease the sampling rate of Knudsen.

July 19, 2010 (Mon)

At midnight, full watchstanding started. We continue to have good weather, and the ship is steaming at ~11 knots. At ~1:40 p.m. local, the main engine was set off line to investigate the cause of vibrations; sailing was continued with the port engine at the speed of ~6 knots. The problem (faulty fuel pump) was resolved at 2:50 p.m. local, and the speed returned to ~12 knots. Google Analytics for the cruise blog site was set up to gather access information. At midnight, the clock was retarded by an hour (now GMT-11).

July 20, 2010 (Tue)

Transit continues, with average speed being probably ~10.5 knots.

July 21, 2010 (Wed)

At ~3:20 a.m. local, power for multibeam, mag, gravity, and Knudsen was lost, due to an UPS failure. Everything besides multibeam was restored quickly. At ~3:54 a.m. local, multibeam was also restored. Transit continues at ~10.5 knots, with nice weather.

July 22, 2010 (Thu)

Transit continues at ~11 knots, still with nice weather. We have passed half way of transit today. Crossed over the International Date Line around 12 p.m. local.

July 23, 2010 (Fri)

LDEO requested to conduct BIST (system test of EM122) more frequently than its regular weekly schedule. According to Chris Paul, more frequent tests are a good thing, and each test takes only a few minutes, so the request was approved. Transit continues at ~11 knots, still with nice weather. There is nothing to complain about. At midnight, the clock was retarded by an hour (now GMT-12).

July 24, 2010 (Sat)

Sample MCS data were given from the science tech, and Floyd and students started to prepare for shipboard data processing with the training data, using ProMAX on Sager's computer. Dave Ng successfully completed the installation of ProMax on the computer "proc1" (one of Langseth linux machines), which took a few days because of the limited speed of Internet access.

Transit continues at ~10.5 knots, with nice weather. We passed by the bent of the Hawaii-Emperor seamount chain. The estimated time of arrival at the first OBS deployment point is Monday 6 p.m. local. The A-Frame was exercised in and out for OBS deployment as well as winches and turning blocks rigged on main deck.

July 25, 2010 (Sun)

Transit continues at slightly slower speed (~10 knots) than before; the engine pitch is the same, but the ship started to encounter larger waves. At 11 a.m. local, we had a pre-operational meeting to prepare for OBS deployment and subsequent shooting. Peter Lemmond informed that one of two spare OBSs turned out to be non-functional, so we have only one spare. Korenaga informed the captain about the details of turning operations expected at waypoints for refraction lines. Each turn will probably takes 1.5 hour or so. One of these turns should be part of planned gun maintenance. From Steinhaus, Korenaga found out that shot-time randomization is not possible, so instead of shooting on time (at 70s), we will shoot on distance (at 162 m for 4.5 knots), which should result in natural shot time randomization. We had a BBQ lunch on the deck.

July 26, 2010 (Mon)

Transit continues at ~11 knots. The fluxgate magnetometer was found to have stopped recording (no record for ~8hours). The PC was rebooted and a new log was initiated. At ~2:45 p.m. local, the towed magnetometer was pulled up to prepare for OBS deployment. At ~3:50 p.m. local, the first OBS deployment was done. Sea conditions are actually better than yesterday, and everything went smoothly. WHOI OBS ("D2") needs ~4 hours for its geophone to be dropped onto the seafloor; even if gun deployment goes smoothly, we should have at least 4 hours between the last OBS deployment and the first shot.

Sea surface temperature map (from Steinhaus) shows a gradient right around the northernmost MCS line. Most of the survey area is at ~27°C, but the temperature drops to ~23°C at the northern edge of the survey area. The streamer control is expected to be most difficult there.

July 27, 2010 (Tue)

Steinhaus informed the PIs that the starboard-side compressor was inoperable and it could not be used during this cruise. The port-side compressor is fine, and the whole survey can be done with it, but we just don't have a spare. (But we could use parts of the starboard-side compressor to fix the port-side if needed, so situations are not terribly desperate.)

OBS deployment continues smoothly, with average deployment time of ~10 minutes. At ~1:30 p.m. local, the 14th OBS was deployed, and we're halfway through. We anticipate the completion of the OBS deployment by a similar time in the afternoon tomorrow, so we should be able to start gun deployment (and firing) during the day.

July 28, 2010 (Wed)

OBS deployment went smoothly all the way up and was completed at ~11:30 a.m. local. After the towed magnetometer and the passive animal monitoring (PAM) hydrophone were deployed, gun deployment started before noon local. Gun deployment and tuning were completed at ~2 p.m. local, and we started to fire the entire gun array along the main refraction line at ~3:30 p.m. (but still an hour away from the first way point B). All guns worked well. They were towed at 12 m depth and fired at an interval of 162 m. Shooting on the refraction line B to E (line MGL1004_RL_B) started at 4:23 p.m. local.

Around 8 p.m. local, the latter part of gun string #4 died, and four guns are not functioning. By bringing 3 spare guns up, we're now shooting with a 35-gun array (one spare gun was dead from the beginning). The total volume is still 6520 cubic inch (only 80 cubic inch less, or 98.8%), so we decided to keep shooting with this configuration until further problems show up.

July 29, 2010 (Thu)

Shooting on the main refraction line (MGL1004_RL_B) continues with the 35-gun array. At ~6:30 p.m. local, the B-E shooting was completed successfully and started to turn to the E-DD line (line MGL1004_RL_E). During turning, shooting was fired internally with an interval of 60s (but shot locations were not logged, so these shots won't be used for OBS data). Turning took ~50 minutes.

July 30, 2010 (Fri)

At ~1:30 a.m. local, we turned around DD and headed toward D (beginning line MGL1004_RL_DD). At ~8:20 a.m. local, we started to shoot along D-C (line MGL1004_RL_D), another 2-D refraction line. Sea conditions remained good, and guns were working fine.

Steinhaus told us that fishing gear was observed in the area bounded by waypoints E, DD, and D. Because they could get entangled with a streamer, we will need to watch out for them during MCS profiling. At 10:20 a.m. local, we had a man-overboard drill.

Around noon local, MMO John Nicholas collapsed in the galley, and shortly after, it was ordered that all science gear be recovered. Despite intensive emergency medical care by the ship crew, which lasted for over two hours, John did not come back and officially pronounced dead at ~1:45 p.m. local. At 3 p.m. local, a meeting for all hands was convened in the galley, and the captain informed us that we were now heading to Yokohama, Japan. ETA is 10 a.m. local Monday. All other details are not known at this moment.

July 31, 2010 (Sat)

Transit to Yokohama continued initially at ~10-11 knots. Ship speed later decreased down to ~7 knots because of winds and contrary currents. ETA is now delayed one day (10 a.m. local Tuesday; Wednesday in Japan time). The clock is retarded by one hour at midnight (now in GMT-13).

August 1, 2010 (Sun)

Transit to Yokohama continued. Underway geophysical data were continuously collected during this transit. At midnight, the clock was retarded by one hour, and we skipped a day, so we'll be on August 3 (Tuesday) tomorrow. That is, $\text{GMT-13-1+24} = \text{GMT+10}$ (cf. Japan is in GMT+9).

August 2, 2010 (Mon) [August 3, 2011 (Tue)]

Transit continued, and we entered the Japanese EEZ at 8:20 a.m. local. Geophysical data collection was shutdown. To prepare for tomorrow's docking, watchstanders cleaned the main lab, and watch standing was put on hold. The clock was retarded once more at midnight, and we're now in GMT+9 (JST).

August 3, 2010 (Tue) [August 4, 2012 (Wed)]

Robert Steinhaus informed us of NSF decisions: (1) the cruise can continue with 4 MMOs, and (2) Langseth has to be back to Honolulu by September 14th, i.e., we were granted 7-day extension, with a caveat that we need to stop the survey and start a return transit if the fuel goes below 90,000 gallons, which allows the ship to have 40,000 gallons back at Honolulu (the minimum amount of fuel needed to stabilize the ship against flipping over in case of accidents). Refueling at Yokohama turned out to take at least 3 days, so we need to move on with this fuel constraint. There would be no investigation on the death cause of John Nicolas at Yokohama, so we may be able to depart for the survey area tonight. A briefing on the cruise plan was given in the main lab at 11:45 a.m. local. No one would be allowed to get off the ship. The ship was docked at ~2 a.m. local and departed for the survey area on 7 a.m. local.

August 4, 2010 (Wed) [August 5, 2012 (Thu)]

Return to Shatsky Rise continued at ~11 knots. We moved out of the Japanese EEZ at ~9 a.m. local, and started multibeam, Knudsen, and magnetometer data collection. The clock was advanced by one hour at midnight (we're now in GMT+10).

August 5, 2010 (Thu)

Transit continued at ~10.5 knots. The clock was advanced by one hour at midnight (now in GMT-13).

August 6, 2010 (Fri)

Transit continued at ~11 knots. We had a remarkably calm sea in the morning. The clock was advanced by one hour at midnight (now in GMT-12).

August 7, 2010 (Sat)

Transit continued at 9-10 knots. The sea state became considerably worse compared to yesterday. Guns were being deployed at ~6 p.m. local, and the speed was lowered to 4.5 knots. The deployment was completed by 8:20 p.m. local, with everything working in order. Internal firing interval was set to its maximum of 60 seconds, so shots from this short transit could be exploited from OBS data. At 11:13 p.m. local, we were finally back to the line D-C (line MGL1004_RL_D) and started to shoot on distance (with 162 m interval). We passed the waypoint (where we stopped shooting on July 30) just over midnight.

August 8, 2010 (Sun)

At 00:10 a.m. local, we had the FGSP of MGL1004_RL_DR (reshoot of line D). At 4:30 p.m. local, we completed RL_DR and started line MGL1004_RL_C. Taking into account the 7-day extension from NSF, we were behind the original schedule by ~30 minutes; i.e., we used up all of the extra contingency earned prior to the medical emergency. The 36-gun array has been in order so far. Sea state was fair, with 7-8 foot high waves. Steinhaus informed us that streamer deployment would take only 12 hours because his team fixed it as much as possible on board to minimize the deployment time.

August 9, 2010 (Mon)

At ~00:30 a.m. local, we turned from line MGL1004_RL_C to MGL1004_RL_CC. Around ~5:30 a.m. local, due to gun troubles, we shifted to a 35-gun array with the total of 6500 cubic inch. The smallest of the remaining spares is 180 cubic inch, so we had to go with this 35-gun array, not to exceed the 6600 cubic inch limit. Sea state returned to a reasonable one. Around ~7 a.m. local, line MGL1004_RL_CC was completed, and we turned to line MGL1004_RL_EA. The towed magnetometer was found to get entangled with the line of gun string #1, and was retrieved during the turn from RL_CC to RL_EA. It would be deployed again when the weather gets calm. The turn to RL_EA took approximately 1.5 hour.

August 10, 2010 (Tue)

Around ~9 a.m., line MGL1004_RL_EA was completed, i.e., the gun-only shooting component was completed successfully. Guns were retrieved within an hour, followed by streamer deployment starting at ~10 a.m. local. Weather has been good since yesterday; there were no whitecaps seen during the streamer deployment. Gun string 1 was deployed at ~6:30 p.m. local and started firing. The streamer deployment was completed at ~7 p.m. local, and gun deployment was done at ~10:30 p.m. local. The towed magnetometer was deployed at ~9:30 p.m. local. FGSP (1008) of MCS reflection line MGL1004_ML_A was obtained at 10:54 p.m. local. The average streamer tension

should be around 3200 pounds, and the present currents allowed us to use the speed over ground of ~5.2 knots.

August 11, 2010 (Wed)

We continued shooting over line MGL1004_ML_A under good weather conditions, at a speed of ~5 knots. Around 3:30 p.m. local, the recording system crashed, resulting in the loss of shot gathers for ~1.7 km. Given its relatively low impact for CMP gathers, we decided to proceed without reshooting.

August 12, 2010 (Thu)

Shooting over line MGL1004_ML_A was completed successfully at 6:45 p.m. local. There was no gun problem during this line. Weather was still good. During the turn to ML_B, gun strings #1 and #2 were given preventive maintenance. The turn was completed within 3 hours, and shooting over line MGL1004_ML_B started at ~10 p.m. local. The speed over ground had to be 3.5-4 knots because of currents (speed through water should not exceed 5.5 knots (for guns) and steamer tension should be below 3500 pounds).

August 13, 2010 (Fri)

At 21:19 GMT (10:19 a.m. local), a magnitude 7.2 earthquake took place in the Mariana Island region. The epicentral distance to Shatsky Rise is ~40 degrees. (cf. Magnitude 7.2 Ecuador earthquake on August 12 has an epicentral distance of ~180 degrees.)

Shooting over line MGL1004_ML_B continued, and the speed increased slightly (to ~4.3 knots) around 4 p.m. local; we probably passed over strong currents. Floyd made a poster plot for the near trace image of line ML_A (with the GMT routine psseg), which exhibits intriguing signs of fault scarps, moats, and dipping reflectors near the Tamu Massif top.

August 14, 2010 (Sat)

Weather continued to be good throughout the day. Shooting over line MGL1004_ML_B was completed successfully at ~8 p.m. local. During the turn to line MGL1004_ML_7, gun strings #3 and #4 were given preventive maintenance. The turn was completed in a little over 3 hours, and shooting over line MGL1004_ML_7 started at ~11:30 p.m. local.

August 15, 2010 (Sun)

Weather started to pick up (~4m seas), but we were still able to shoot at ~4.5 knots over line MGL1004_ML_7. The towed magnetometer was pulled up at ~12 noon because of rough weather.

Around ~2 p.m. local, the captain told us to halt the scientific operation because the ship needed to go to Yokohama, Japan to deal with a medical problem of a ship crew member.

August 16, 2010 (Mon)

Transit to Yokohama continued. Seas got better, and the ship speed recovered from ~7 knots to ~11-12 knots during the morning. The clock was retarded by one hour midnight, and we moved to GMT-13.

August 17, 2010 (Tue)

Transit to Yokohama continued with the speed of ~12.5 knots. We had a fire and boat drill at 10:20AM local.

While talking with Dave Martinson, Korenaga was informed that the shot times according to Langseth's acquisition system correspond to the timing of the peak energy, not of the leading edge, the difference between which would be anywhere from 12 to 18 ms. This fact should be taken into account when reading traveltime information from OBS data; the first thing to do is to compare the waveforms of direct waves with those of crustal phases, to see how attenuation affects the time difference between the leading edge and the peak energy.

August 18, 2010 (Wed)

Around 4 a.m. local, we entered Japanese EEZ, so underway geophysical data recording was shut down. Transit to Yokohama continued smoothly.

August 19, 2010 (Thu)

Around 7:15 a.m. local and around the entrance to Tokyo Bay, Mike the Cook was safely transferred to a Japanese vessel "Amagi-maru" for hospitalization (and we got a supply of fresh food as well), and we initiated return to the survey area. Transit speed has been ~11-12 knots.

August 20, 2010 (Fri)

Around 5 a.m. local, we left Japanese EEZ. Transit speed has been ~11 knots.

Sager found out from Steinhaus that we have been towing the magnetometer only at 150 m from the vessel (to avoid entanglement with other lines). This is a bit too short to avoid the magnetic field of the vessel given its size, so we may need to conduct some calibration by figure eights.

The clock was advanced by an hour midnight, so we're now in GMT-12.

August 21, 2010 (Sat)

Transit continued with the speed of ~11-12 knots. Weather has been good. According to Steinhaus, we would be able to deploy streamer at ~1 p.m. local tomorrow, with the current transit speed.

August 22, 2010 (Sun)

Transit speed has been ~10-11 knots. Streamer deployment began at ~1:20 p.m. local and was completed at ~4:20 p.m. Bird #18 displayed a loss of depth control, probably because it picked up some floating debris, resulting in the loss of depth control. By adjusting the neighboring birds, Steinhaus and Martinson tried to bring that part of streamer within the spec (9+-1m) with some success. The situation was not ideal, however, so pending the captain's approval, we may try to send an FRC (fast rescue craft a.k.a. workboat) to fix the bird tomorrow. Gun deployment started at 4:50 p.m. and was completed by 7:30 p.m. Test MCS profiling (MGL1004_TEST) initiated at 7:40 p.m. just above the line 7 (in a reverse direction). We started shooting over line MGL1004_ML_7R (the continuation of line MGL1004_ML_7) at 10:50 p.m. local. We passed over the point where we stopped previously at 11:20 p.m., so it took 7 days and 9 hours to resume what we were doing. Weather has been good in the last few days, and seas were calm.

By analyzing the beginning section of line MGL1004_ML_A, Floyd identified the probable Moho reflection, the two-way traveltime of which suggests the crustal thickness of ~10 km, thicker than normal oceanic crust. This further motivates us to put a westward extension to ML_A to find the actual extent of Shatsky Rise.

August 23, 2010 (Mon)

Shooting over the line MGL1004_ML_7R continued smoothly with a speed of ~5 knots. Around 1 a.m. local, gun #8 in string3 was turned off due to persistent timing error, and the total gun

volume became 6540 cubic inch. The bird #18 issue was not so grave to take the risk of the (potentially dangerous) operation of a workboat, so we decided to keep it as is. Weather was wonderful today, and line MGL1004_ML_7R was completed by 3:30 p.m. local, and during the turn to the next line (ML_6), gun strings 3 and 4 were given repair and preventive maintenance. The turn took 3 hours 40 minutes, and shooting over line MGL1004_ML_6 started at ~7:10 p.m. local (FGSP was obtained at ~8:10 p.m.). The ship speed was ~5 knots.

August 24, 2010 (Tue)

Shooting over line MGL1004_ML_6 was completed at 2:54 p.m. local. An inside turn to the next line (ML_5) started a little earlier (2:52 p.m.) and was completed within 7 minutes. Shooting over line MGL1004_ML_5 began at 2:55 p.m. The speed has been around 5 knots throughout the day; the sea condition was nearly perfect.

August 25, 2010 (Wed)

During the latter half of line MGL1004_ML_5, gun string 2 started to malfunction intermittently (about 1 out of 10 shots on average). The total volume was reduced down to 5710 cubic inch when the failure took place. As we would be at the end of line in a few hours and the effect of randomly reduced gun volume with that frequency would be minor in CDP gathers, we decided to continue shooting as is. Around 7:10 a.m. local, 3 guns in string 3 completely died, so three spares were brought up. Only two of them worked fine, and the total volume became 6460 cubic inch. At 8:30 a.m. local, line MGL1004_ML_5 was completed. During the turn to the next line (ML_C), gun strings 1 and 2 were given repair and maintenance. Line MGL1004_ML_C started around 1 p.m.

Around 5:30 p.m. local, after crossing OBS B2, the gun power was reduced down to one 60 cubic inch due to the sighting of seven whales. To fill the gap, we made a turn during which gun string 4 was given repair. This turn took 4 hours (but we were also able to fix the guns). The ship speed has been ~ 5 knots. Reshoot was called line MGL1004_ML_CR.

August 26, 2010 (Thu)

We had an amazingly calm ocean. Shooting over line MGL1004_ML_CR was completed at ~2:30 p.m. local, and during a turn to the next line (ML_D2), gun strings 1 & 2 were given repair and maintenance. It took ~7 hours to repair the string 2 (Hose Bundle #2 was replaced), which had been suffering from the intermittent firing issue. FGSP of line MGL1004_ML_D2 was obtained at 11:37 p.m. local.

August 27, 2010 (Fri)

We crossed over the way point D2 at ~00:45 a.m. local. The ship speed has been around 4.5-5 knots. All guns were firing perfectly; string 2's intermittent firing problem seemed to have been fixed by the replacement of Hose Bundle #2. We had pouring rain in the morning for a few hours, but it cleared up afterward.

August 28, 2010 (Sat)

Around 3 a.m. local, line MGL1004_ML_D2 was completed, and during a turn to the next line (ML_B)2, gun strings 3 and 4 were given maintenance; the nose piece of string 4 was replaced. Shooting over the last MCS line MGL1004_ML_B2 started at 7:30 a.m. local, which will be terminated by 6:30 a.m. tomorrow to be ready for OBS recovery.

August 29, 2010 (Sun)

At 6:15 a.m. local, line MGL1004_ML_B2 was terminated at 34°24'19.956N, 154°39'54.261E (ML_B2 is 192 km long, which is 30 km less than originally planned). This completed the MCS component of

this cruise. The total length of MCS lines amounts to 2022 km. The retrieval of seismic gears was completed by ~9:30 a.m. local, and we turned to the OBS A1 site. ETA was set to 10 p.m. local. We arrived at the OBS A1 site at 8:40 p.m. local, marking the start of the OBS recovery operation. The first instrument was recovered successfully at 10:50 p.m. Seas were calmer than the daytime.

August 30, 2010 (Mon)

It was realized that picking up OBS in exactly a reverse order of deployment would follow the already mapped tracks (of course!) and would not yield any new underway geophysics data, so the order of going from the long transect to the short one was modified. The OBS recovery operation continues smoothly. All instruments except one were released during the first burn cycle; only OBS A7 required the second cycle. Seas have been 1-3 m. By the end of the day, the total of 9 OBS (up to A9) were recovered.

August 31, 2010 (Tue)

Seas have been about 1-2 m, helping the OBS recovery operation. We have recovered up to OBS B1 (i.e., 19 OBSs in total) by the end of the day.

September 1, 2010 (Wed)

Seas were ~2m throughout the day, and the recovery operation continued to run smoothly, recovering up to OBS A19; only two more to go.

September 2, 2010 (Thu)

The OBS recovery operation was completed successfully at 3:30 a.m. local. All instruments except one needed just one release command. The magnetometer was deployed then, and we started multibeam mapping on the southern flank of the Tamu Massif, which would continue for the next 48 hours (i.e., until the remaining contingency time is used up). Seas are only 1-2 m, and the ship speed has been 10-11 knots.

September 3, 2010 (Fri)

During one of turns for multibeam mapping, we conducted a figure-eight loop (from 2:23 a.m. to 3:26 a.m. local) to see the effect of ship's magnetization on data collected by a towed magnetometer. Seas have been 1-2 m, and the weather was spectacular. Around 7 p.m. local, we exited the survey area and started transit to Honolulu. Peter Lemmond started to cut out SEG Y files from OBS data, and an initial look appeared very promising.

September 4, 2010 (Sat)

Transit to Honolulu continued with a speed of ~11 knots. Lemmond completed the making of OBS seg y files for all refraction and reflection shots. The total size of the files is close to 300 GB, and copying them over the wireless network takes about a day.

At ~06:45 p.m. local, the Knudsen SBP Failed. It was noticed that there was a loud noise coming from the rack mount unit and large arcs could be seen inside the case. The power was secured and the unit was opened to investigate. It was found that the second (of 3) 3.5 kHz High Power Transmitter Backplane boards had a large area of discoloration and a hole burned in the board.

September 5, 2010 (Sun)

Transit continued with the speed of ~11 knots.

September 6, 2010 (Mon)

Transit continued at ~11 knots. Weather has been very good. We had a "Happy Labor Day" BBQ dinner on deck. The clock was advanced at midnight, and we're now in GMT-11.

September 7, 2010 (Tue)

Transit speed slowed down to ~10 knots, as trade winds started to act against us with our decreasing latitude.

September 8, 2010 (Wed)

Transit speed has been around 10 knots, as wind speed is consistently higher than 20 knots.

September 9, 2011 (Thu)

Transit speed has gone below 10 knots, though weather has been nice. At 11:45 a.m. local, Steinhaus convened a science party meeting, in which he informed port call procedures. ETA at the UH dock was given to be 8 a.m. to 12noon on September 13. Immigration and custom clearance will then follow. Custom clearance on baggage will take place later, so all personal belongings should be left on the vessel when going out for dinner, etc.

September 10, 2011 (Fri)

Transit continued with windy but still sunny weather. The clock was advanced by an hour at the midnight, and we're now in GMT-10 (same as Honolulu).

September 11-13, 2011 (Sat-Mon)

We took a group picture on the sun deck in the morning of 11th. Around 10 a.m. local on September 13, the ship arrived at the UH dock, marking the end of MGL1004.

Introduction and Background

Cruise MGL1004, on the R/V *Marcus G. Langseth*, was a geophysical cruise to study the Shatsky Rise oceanic plateau (Fig. 1). Oceanic plateaus are large, volcanic mountains whose origins are poorly understood, so the main objective of the cruise was to learn about the structure and tectonics of the plateau for clues about its formation and evolution. The primary focus of MGL1004 was deep penetration seismic studies. Part of the program was to shoot two seismic refraction lines across the summit of the main volcano (Tamu Massif) using OBS as receivers and the large airgun arrays of the *Langseth* as a sound source. The other aspect of seismic study was the collection of multichannel seismic (MCS) lines across the plateau to image acoustic basement and sub-basement reflectors for indications of plateau structure. In addition, other underway geophysical data were collected, including 3.5 kHz echo-sounder profiles, 12 kHz multibeam bathymetry data, magnetic field data, and gravity data. All of the different data types will be used in various studies to better characterize the geophysical signature of the plateau.

Scientific Background: Oceanic Plateau Formation

Oceanic plateaus are among the most prominent features of the Earth's ocean basins, yet their origins remain uncertain. Knowing how and why oceanic plateaus form is important because these giant basaltic mountains represent a large flux of magma from the mantle - thus they reflect an important aspect of mantle dynamics - and because they are a significant source of volcanism that may not be explained by plate tectonics. The most popular explanation is the plume head hypothesis [Richards et al., 1989; Duncan and Richards, 1991; Coffin and Eldholm, 1994], which calls for rapid plateau construction by high-degree melting associated with the upwelling of a large blob of hot mantle (the plume head) from a thermal boundary layer (usually at the core-mantle boundary). Rapid flood basalt eruptions may have briefly exceeded the output of the entire mid-ocean ridge system, and gasses released by plateau volcanism may have caused significant perturbations of ocean chemistry and climate [Coffin and Eldholm, 1994; Eldholm and Coffin, 2000]. Furthermore, because oceanic plateaus were formed widely during the Mesozoic whereas Cenozoic plumes appear to have had much less output, there may be a fundamental episodicity for large-scale upwelling that indicates different modes of mantle behavior [Stein and Hoffman, 1994].

The plume head hypothesis was developed in part to explain the ocean's largest plateaus, Kerguelen Plateau (KP) and Ontong Java Plateau (OJP). Geochronologic data imply that both formed mainly during a brief interval of time within the Cretaceous [Coffin and Eldholm, 1994; Tarduno et al., 1991; Mahoney et al., 1993]. However, recent ODP legs cored KP [Coffin et al., 2000] and OJP [Mahoney et al., 2001], revealing complications that do not fit a *simple* plume head model. The bulk of OJP, for example, apparently never reached sea level, contrary to the expectation from buoyant plume head uplift [e.g., Korenaga, 2005]. Current LIP research includes efforts to resolve these complications with modifications to the plume model and development of alternative models.

It would be simplistic to presume that all plateaus are created by the same mechanism and a number of complications to the simple plume head have been proposed. For example, some plateaus may have been produced by chemical as well as thermal anomalies. Chemical anomalies have been suggested to result in plume geometries that are more complex than the simple thermal plume head model [e.g., Farnetani and Samuel, 2005; Lin and van Keken, 2006a; 2006b] and this may help explain some observed complications. A few flood basalt provinces (Parana, Deccan, and OJP) are underlain by low velocity anomalies in the mantle [VanDecar et al., 1995; Kennett and Widiyantoro, 1999; Richardson et al., 2000], but the usual interpretation, which is that the low

velocity anomaly is hotter mantle, has recently been called into question. The low velocity anomaly beneath OJP, for example, is also characterized by *lower-than-normal* attenuation [Gomer and Okal, 2003], which is impossible to explain simply by thermal effects. Finally, in addition to the plume head hypothesis, there have been several alternatives proposed to explain oceanic plateau magmatism from shallow sources that result from cracking of the lithosphere and chemical heterogeneities [e.g., Anderson, 2000, Foulger and Natland, 2003; Foulger, 2007].

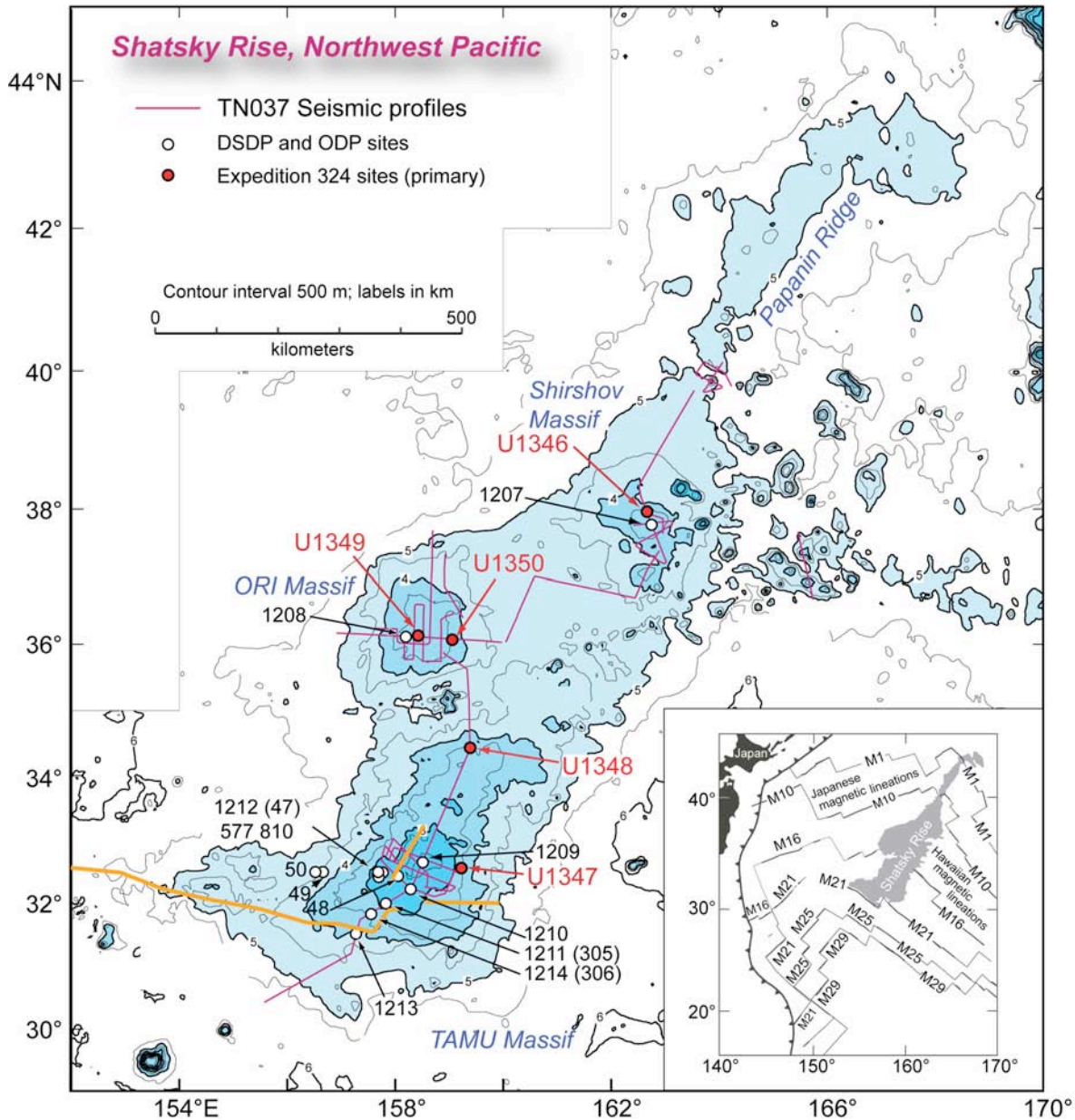


Figure 1. Location map for Shatsky Rise, northwest Pacific Ocean. Blue highlighted area shows the rise shallower than 5 km depth. Red filled circles show locations of sites drilled during IODP Expedition 324; other scientific ocean drilling sites are shown as open circles. Number labels are site designations. Red line is cruise track from TN037 site survey cruise (1994), which collected digital seismic profiles. Orange lines are seismic refraction lines from Den et al. (1969) and Gettrust (1980). Bathymetry contours at 500-m intervals. Inset shows location relative to Japan.

Ocean Drilling Program (ODP) sampling in the 1990s and recent IODP sampling of Shatsky Rise (http://publications.iodp.org/preliminary_report/324/index.html; Expedition 324 Scientists., 2010) provided a significant increase of plateau igneous rock samples over previous Deep Sea Drilling Project (DSDP) coring. These samples yielded new results from geochronologic, geochemical, and isotopic studies that led to new ideas about plateaus. A recent, widely-attended IODP workshop on Large Igneous Province drilling (Neal et al., 2008), reiterated the importance of studying and sampling oceanic plateaus. Nevertheless, ocean plateaus are sparsely surveyed and sampled, so the debate over their origin is currently stalled and significant progress awaits a new generation of observational data.

Origin of Shatsky Rise

The plume head model can explain many characteristics of Shatsky Rise. Age constraints imply that emplacement rates for Tamu Massif, the oldest and largest edifice, were similar to flood basalts [Sager and Han, 1993]. Furthermore, Tamu Massif volume implies that the magma must have come from a large partial melt fraction of a thick section of upper mantle [Sager, 2005]. Evidence of uplift, as expected from a plume head, comes from shallow water fossils dredged from Tamu Massif, implying the volcano summit was subaerial [Sager et al., 1999]. In addition, after the initial rapid volcanic pulse, volcanism waned with time, implying a transition from plume head to tail [Sager et al., 1999]. A plume may also explain the odd kinematics of the triple junction during the ~20 Myr that the entire rise formed. Rather than drift according to geometric kinematics, the junction followed the trend of the rise, perhaps because heat and uplift kept the ridges over the plume [Nakanishi et al., 1999].

In contrast, other observations are not readily explained by the plume hypothesis. One problem is that basalt samples from Tamu and Ori Massifs have geochemical and isotopic signatures that are not very different from mid-ocean ridge basalts [Mahoney et al., 2005]. Another nagging point is the 30° reorientation of the Pacific-Farallon ridge synchronous with Tamu Massif formation [Sager et al., 1988]. If plate motion is driven mainly by subduction [e.g., Lithgow-Bertelloni and Richards, 1998], it is unclear how a plume could cause plate direction change acting on the trailing boundary. Additionally, a plume head surfacing close to a triple junction is highly fortuitous [Sager, 2005] if plume activity and plate motions are independent [e.g., Eldholm and Coffin, 2000]. Given these coincidences, it seems implausible that the triple junction reorganization and the creation of Shatsky Rise resulted from unrelated processes, as implied by the simple plume head hypothesis. Moreover, similar coincidences seem to have occurred with other Pacific plateaus (Hess Rise, Manihiki Plateau, Magellan Plateau, Mid-Pacific Mountains), which also formed near triple junction tracks [Sager, 2005]. Such correlations imply a link between plateaus and triple junctions.

Can ridge tectonics alone lead to massive plateau eruptions? A possibility is the fertile mantle hypothesis [e.g., Anderson et al., 1992; Anderson, 1995; Smith and Lewis, 1999; Korenaga, 2005], which suggests that the asthenosphere is heterogeneous and that some portions have lower melting points that can produce volcanism with triggers from plate tectonics (e.g., cracks in the plate; stress reorientation; stress concentration). Another possibility is that a broad region of mantle beneath the western Pacific was somehow unusual. Plate-tectonic backtracking places present-day north Pacific LIPs near the volcano-rich South Pacific Superswell [e.g., McNutt and Fisher, 1987; Larson et al., 1992]. Although the nature of the Superswell is debated [e.g., Stein and Abbott, 1991], many think that the asthenosphere beneath that region is anomalously warm and a magma source for many small seamount chains [e.g., Courtillot et al., 2003]. Anomalous

geochemistry from Superswell rocks also suggests that a compositional anomaly in the upper mantle may also play a role [Janney et al., 2000]. Shatsky Rise, other plateaus, and many seamount chains in the northwest Pacific may be Jurassic and Early Cretaceous products of this anomalous region [McNutt et al., 1990; Tatsumi et al., 1998; Koppers et al., 2003]. The upper mantle is unlikely to be completely isochemical and isothermal, so these speculations are plausible, but they have been poorly tested by geophysical and geochemical observations largely because data for oceanic plateaus are too sparse to be definitive.

Why Study Shatsky Rise?

Among large oceanic plateaus, Shatsky Rise is unique because of a combination of factors that make it “just right” for studies of oceanic plateau origin. First of all, it is a giant LIP with an area of $\sim 4.8 \times 10^5$ km², about the same size as California [Sager et al., 1999], so it is probably representative of large plateaus. Furthermore, if it is linked with Hess Rise [Bercovici and Mahoney, 1994], the magmatic output may be twice as great. It was formed at the right time, during the late Jurassic and Early Cretaceous when the magnetic field was reversing and magnetic anomalies were recorded in ocean crust to show the locations of spreading ridges [Nakanishi et al., 1999]. That is how we know that Shatsky Rise formed at a triple junction and it allows us to reconstruct the tectonic history of the rise and ridges through magnetic anomalies. Many large oceanic plateaus formed during the Cretaceous Quiet Period when the magnetic field did not reverse, so such tectonic models are difficult. Shatsky Rise also has a convenient tectonic setting. It formed at a triple junction and was heavily modified by spreading and rifting. This association leads to questions about the nature of the connection between the plateau and the triple junction and spreading ridges. Spreading was also relatively rapid and the rise apparently formed such that volcanism was spread laterally, rather than stacked vertically, so that the history of the rise is more easily interpreted. In addition, sediments on Shatsky Rise flanks are generally thin, so the morphology of the rise, which can be measured by bathymetry, is a direct reflection of its structure and evolution. Finally, Shatsky Rise was formed at a rapidly-spreading RRR triple junction, so it formed on lithosphere that was thin and should have had minimal influence on melt generation and migration. Indeed, the thin lithosphere of the on-ridge setting makes Shatsky Rise ideal for using geochemical and geophysical data to test whether the source was thermally or chemically anomalous.

No other oceanic plateaus share this fortunate coincidence of right parameters. OJP, for example, is simply too large to map out its detailed 3-D crustal structure with reasonable acquisition cost. Furthermore, OJP was emplaced mainly at the beginning of the Cretaceous Quiet Period [Tarduno et al., 1991], so no magnetic reversals record the locations of spreading ridges and their relationship to the plateau. Thus, debate over the role of spreading ridges in OJP evolution [e.g., Kroenke et al., 2004] is difficult to resolve.

Other large plateaus have similar problems. Most large, mid-ocean plateaus were formed wholly or mostly during the Cretaceous Quiet Period (e.g., Kerguelen Plateau, Manihiki Plateau, Hess Rise [Coffin et al., 2000; Pringle and Dalrymple, 1993; Taylor, 2006]). Many have been linked to spreading ridge tectonics [e.g., Larson et al., 2002; Sager, 2005], but the link is difficult to prove without spreading ridge locations recorded in the surrounding crust. KP may not even be wholly oceanic; it formed near continental margins as Gondwana rifted apart [Royer et al., 1991] and ODP drilling recovered continental material from the plateau [Coffin et al., 2000]. Of the great plateaus, only Shatsky Rise has a tectonic history that can be readily deciphered.

Testing Plume and Ridge Models

How can geophysical data distinguish between competing models for the formation of oceanic plateaus? Currently this is a question of considerable debate. In general, crustal structure and properties that suggest a surplus of heat and large degree of partial melt imply a plume (though some plumes may be thermochemical) whereas lesser temperatures favor a ridge explanation. For example, a hot plume head should lead to higher crustal velocities owing to greater MgO content of magmas (see Fig. 2). In contrast, a lower temperature chemical anomaly would be expected to yield lesser crustal velocities than normal due to lower MgO and higher silica contents.

One possible seismic diagnostic is the correlation between crustal thickness and velocity. If positive, a thermal origin is favored, but if negative, a chemical origin is likely (Fig. 3). Precise interpretation of absolute crustal velocity in terms of chemical composition is difficult owing to complications from alteration and porosity [e.g., Korenaga et al., 2002], but a negative correlation between thickness and velocity cannot be explained by these complications because they are essentially low-pressure effects that are likely to be subdued in thicker crust. In order to reverse the correlation from positive to negative by such secondary processes, one must invoke the implausible explanation that thicker and deeper crust is more severely altered than thinner crust (note that anelastic effects are insignificant for the old, cold crust considered here). This type of negative correlation has already been reported at several places such as the Galapagos volcanic province [Sallares et al., 2003, 2005]. If a positive correlation is found instead, a thermal origin is likely because higher melting temperatures lead to igneous rocks with higher MgO content [e.g., Kelemen and Holbrook, 1995]. In either case, integration with geochemical information obtained by drilling will allow us to understand the meaning of crustal seismic structure with more confidence. There can be a range of thermochemical models with varying contributions of thermal and chemical anomalies. In order to estimate their relative importance, we will need to combine the proposed geophysical study with drilling data. Also fertile mantle is usually intrinsically denser, so upwelling requires either viscous drag due to plate tectonics and/or a thermal anomaly [Korenaga, 2005]. Interpretation with geodynamical modeling should help us to evaluate the trade-off between the two kinds of anomalies in a dynamically consistent manner. A new generation of observational data acquired through the proposed project, therefore, will provide strong motivation as well as justification to build a more sophisticated, unifying geodynamical model for the formation of oceanic plateaus.

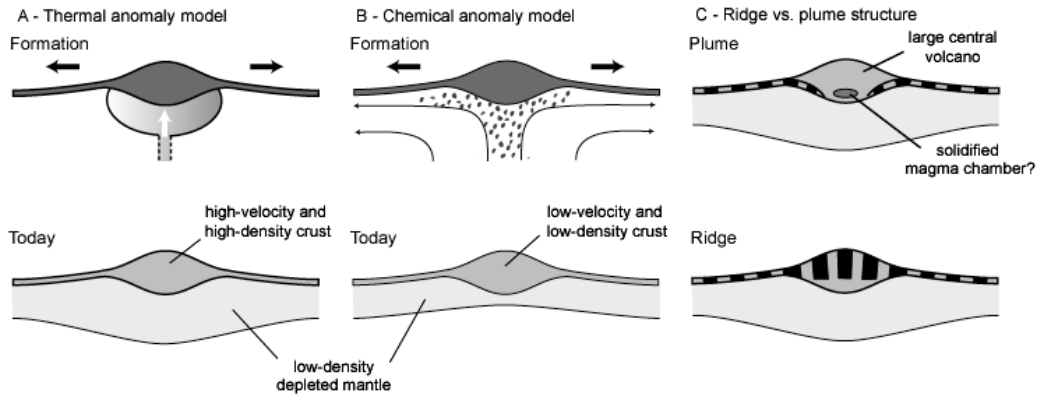


Figure 2. Cartoon depicting differences in plateau velocity and structure resulting from plume vs. ridge formation mechanisms. (A) Thermal anomaly (e.g., plume head impact) results in thick igneous crust, which is characterized by high seismic velocity and density, mainly due to increased MgO content. (B) Chemical anomaly (e.g., mantle embedded with fragments of recycled oceanic crust) is passively dragged up by plate motion. Crustal velocity and density are expected to be similar to or lower than normal due to lower MgO and higher SiO₂ contents. Most igneous products originate from the melting of recycled crustal components, so the thickness of depleted mantle does not correlate with crustal thickness, The locus of magmatism is controlled by (and thus correlated with) the tectonic evolution of the TJ. (C) Comparison of structure formed by plume head (top) and ridge (bottom). A plume head eruption forms large volcanoes with uniform or complex magnetization, depending on whether formed during a period with magnetic reversals. A central volcano may preserve both mass and magnetization anomalies caused by a solidified magma chamber. Edifices formed by ridge volcanism will contain linear magnetic anomalies.

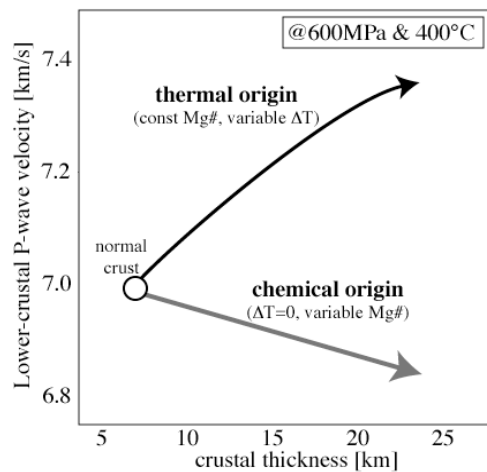


Figure 3. Covariation between crustal thickness and lower-crustal P-wave velocity corrected for reference pressure 600 MPa and temperature 400°C (based on Korenaga et al. [2002] and Sallares et al. [2005]). When thick crust is produced by anomalously hot mantle, positive correlation occurs because higher degree of melting yields magma with higher olivine content. Thick crust can also be created by melting of fertile (Low Mg#) mantle, resulting in a negative correlation. The effect of active upwelling would reduce the extent of positive correlation, but it is likely to be limited for fast spreading, especially when dehydration stiffening is taken into account [Ito et al., 1999; Braun et al., 2000].

MCS, Magnetic, gravity, and bathymetric data have an important role to play in testing plateau formation processes by showing volcano physical structure, faulting, and magnetic isochrons, which are related to eruption style and history. The plume head end-member hypothesis implies massive, rapid eruptions. At Shatsky Rise, the main volcanic edifices are subcircular in plan with central summits, implying eruptions formed large central volcanoes. If rapid, such an eruption would form irregular magnetic anomalies or a single polarity anomaly if erupted during a single magnetic polarity period (Fig. 2) [e.g., Sager and Han, 1993]. Large, extinct, central volcanoes also typically have solidified magma chambers, which are represented by high-density mafic rocks [e.g., Zucca et al., 1982; Kellogg et al., 1987]. In contrast, a LIP formed mainly by ridge processes should contain linear fault structures and magnetic anomalies formed at the ridge, as is the case for Iceland [Ryan, 1990] (note: Iceland is thought to have formed by a plume beneath a ridge - but not by a plume head - so it has not overwhelmed the Mid-Atlantic Ridge and can be viewed as an example fitting into the ridge-process side of plateau end-member models). In addition, ridge-related eruptions would be unlikely to preserve a solidified magma chamber, but if one were isolated, by a ridge jump, for example, it would appear linear. MCS and bathymetry data will be useful in determining where ridge-related rifting, which typically results in rift-parallel faults, has occurred. From existing bathymetry and magnetics [Sager et al., 1999; Nakanishi et al., 1999], we think that the NE and NW flanks of Tamu Massif and the south flank of Ori Massif show linear faults and magnetic anomalies, as opposed to smooth, unrifted SE and SE flanks without clear magnetic lineations. Thus we think that Shatsky Rise initially formed a large volcano that was rifted and dissected at its center. The morphology of the basin between Tamu and Ori massifs has the appearance of an abandoned rift basin and the two massifs may have formed together.

High quality, deep penetration MCS data will also be crucial for determining the structure and layering of the Shatsky Rise edifice, which reflect its origin and construction. For example, at the edges of the rise, it should be possible to determine whether rise volcanism occurred on top of pre-existing ocean crust or whether the rise volcanism was formed at the ridge by augmented crustal formation. At the rise summits, we should be able to determine the structure of the volcano, whether it is one large edifice, or a combination of several. Although these results are not absolutely diagnostic of either plume or non-plume volcanism, they are important for interpretation of drilling results.

Prior Research on Shatsky Rise

By the late 1960s, it was known that Shatsky Rise is ancient because Early Cretaceous sediments were cored from its summit (Ewing et al., 1966). Although seismic refraction experiments have not yet imaged the Moho beneath the high parts of the plateau, they have revealed anomalously thick crust with a similar velocity structure to normal oceanic crust but several times thicker (Den et al., 1969; Gettrust et al., 1980). Seismic profiling showed that the tops of the rise edifices hold thick piles of pelagic sediments (up to 1.2 km), whereas sediments on the rise flanks are thin or absent in places (Ewing et al., 1966; Ludwig and Houtz, 1979; Neprochnov et al., 1984; Sliter and Brown, 1993).

Several Deep Sea Drilling Project (DSDP), Ocean Drilling Program (ODP), and Integrated Ocean Drilling Program (IODP) cruises have cored Shatsky Rise over a span of >30 years (Fig. 1). In succession, DSDP Legs 6 (Sites 47–50), 32 (Sites 305 and 306), and 86 (Site 577) as well as ODP Legs 132 (Site 810) and 198 (Sites 1209–1214) cored atop the highest, southern massif of the rise (Tamu Massif). Many of the holes had only shallow penetration. Drilling during Leg 32 probed deep into the sedimentary cap, recovering Berriasian (earliest Cretaceous) sediments ~50 m above the expected level of basement at Site 306. This finding was significant because it implied that Tamu

Massif formed during latest Jurassic or earliest Cretaceous time. Coring during ODP Leg 198 recovered sediments from all three of the Shatsky Rise massifs (Shipboard Scientific Party, 2002a), including Ori Massif (Site 1208) and Shirshov Massif (Site 1207). At both sites, only the upper part of the sedimentary section was cored, reaching Late Cretaceous sediments. Igneous basement has been cored only twice. Recently, IODP Expedition 324 cored at five sites (U1346-U1350), with two each on Tamu and Ori massifs and one site on Shirshov Massif (Expedition 324 Scientists, 2010). The target of this drilling expedition was coring of igneous basement, which was reached at four of the sites (U1346, U1347, U1349, U1350). Prior to Expedition 324, igneous rocks were recovered at two sites. During Leg 6, drilling stopped at the top of supposed basement at Site 50, recovering only a few pebbles of basalt, perhaps from a basal conglomerate (Fischer, Heezen, et al., 1971). At Site 1213 on the southwest flank of Tamu Massif, a 46 m section of slightly altered basaltic flows or sills intruding earliest Berriasian sediments (Shipboard Scientific Party, 2002b) was cored. These basalts produced the first reliable radiometric date for Shatsky Rise, as well as valuable chemical and Nd-Pb-Sr isotopic data (Mahoney et al., 2005).

Magnetic lineations mapped in the northwest Pacific revealed that Shatsky Rise sits at the confluence of two lineation sets, the northeast-trending Japanese lineations and the northwest-trending Hawaiian lineations (Figure 1; Larson and Chase, 1972; Hilde et al., 1976). This circumstance indicates that the plateau formed at a triple junction separating the Pacific, Farallon, and Izanagi plates (Larson and Chase, 1972). Subsequent studies revealed that the triple junction jumped repeatedly during the time it occupied the location of the rise and that it must have been geometrically unstable to follow the path of the rise (Sager et al., 1988, 1999; Nakanishi et al., 1999). Furthermore, age constraints (Cretaceous sediments and the Site 1213 radiometric date), seismic stratigraphy, and isostatic compensation all indicate that the age of the rise is near that of the adjacent seafloor (Sager et al., 1999), implying that the triple junction and rise formation are linked. Current thought is that a plume head is the link—a source of heat, uplift, and volcanism that both created the rise and captured the triple junction (Sager et al., 1988, 1999). Magnetic data were also instrumental in supporting the idea that Shatsky Rise formed from a plume head. Sager and Han (1993) postulated that the rise formed rapidly, based on modeling of the magnetic anomaly over Tamu Massif. They noted that the magnetic anomaly implies a mainly reversed polarity, in turn implying that most of the edifice may have formed during a single interval of reversed polarity. With simple calculations using the massif volume and an estimate of the length of the single polarity period, the authors inferred that the massif formed with an eruption rate similar to those of several large flood basalts ($\sim 1.8 \text{ km}^3/\text{y}$).

More recent analyses have refined and expanded these conclusions. Paleomagnetic analysis of Site 1213 basalt samples gives inclination values that are most consistent with a reversed magnetic polarity (Tominaga et al., 2005). Furthermore, the mean $^{40}\text{Ar}/^{39}\text{Ar}$ age from two basalt samples is $144.6 \pm 0.8 \text{ Ma}$ (2σ) (Mahoney et al., 2005), a value indistinguishable from the age of the Jurassic/Cretaceous boundary (145.5 Ma) and which correlates with magnetic Anomaly M19 in the Gradstein et al. (2004) timescale. This result limits the formation of much of the Tamu Massif to between Anomalies M21 and M19, a period of 1.5 m.y. If Tamu Massif formed during a single polarity interval, it is likely either M20 or M19, with durations of 0.4 and 0.75 m.y., respectively. Assuming the volume of the massif between Anomalies M21 and M19 formed in 1.5 to 0.4 m.y. (and making the conservative assumption that it formed on existing 7 km thick crust) implies volcanic emplacement at rates of 1.2 to 4.6 km^3/y (Sager, 2005). Again, such values are in the range of estimates for several large continental flood basalts (e.g., Richards et al., 1989; Johnston and Thorkelson, 2000). Although these estimates are intriguing, they were made by very indirect means and require confirmation from radiometric ages of igneous basement samples, particularly from other locations on the rise.

Initial Survey Plan

The original survey plan called for the cruise to be divided into two parts: (1) OBS refraction lines and (2) MCS reflection profiling (Fig. 4). The former included deploying, shooting to the OBS with the airgun array, and recovery of the OBS. The latter included MCS reflection profiling along the OBS seismic lines for imaging purposes as well as lines elsewhere. The rest of the MCS lines were designed to reveal layering and structure of Tamu and Ori massifs and to run over five ODP and IODP drill sites (1213, U1347-U1350).

The MCS profiles were situated to give transects across and along the axis of Tamu Massif, to cross Ori Massif, and to cross the basin between the two (Helios Basin of Sager et al. [1999]). In addition, the lines were situated to cross as many of the IODP drillsites from Expedition 324 as possible (Fig. 4). The OBS refraction lines divide the MCS profiles into two sets, those to the north and those to the south. The initial plan was to shoot all of the MCS lines contiguously in order to save operations time from deploying and recovering seismic gear.

In the initial plan, the work elements were laid out in the following order.

1. Deploy 28 OBS along lines A-B and C-D, starting at point A and ending at point B.
2. Shoot along the OBS lines for refraction at a 70-second interval, with the airguns at 12 m depth. This long shot interval was chosen to allow shot noise to disperse between seismic traces for clearer records. Shooting was to begin at B and then progress to points E, DD, D, E, C, CC, E, and then to A. The lines E to DD, DD to D, E to CC, and CC to C were configured to keep from repeating lines E-D and E-C and to give extra data illuminating the lateral structure of Tamu Massif.
3. At point A, the plan was to deploy the streamer and reconfigure the airguns to a shallower depth (9 m), and begin shooting MCS reflection profiles. Shots were to be placed on distance, with 20 m between shots. According to plan, the first profile would be A to B, followed by B to 1, 1 to 3, 3 to 4, 4 to C, C to 6, 6 to 7, and 7 to B. At this point, MCS profiling would be finished and the gear recovered.
4. Recover OBS, beginning at point B. The recovery path would be from B to E, transit to point D, D to C, transit back to point E, and recover E to A.
5. After finishing the recovery of OBS, the ship was to be at point A and any remaining contingency time would be used in a survey of the nearby area using the multibeam echosounder and other underway geophysical instruments.

The initial plan called for 11 days of OBS operations, 16 days of MCS profiling, and 20 days of transit to and from Honolulu. Approximately 5 days of contingency time was built into the plan to allow for mechanical failures, gaps to be filled, or weather delays.

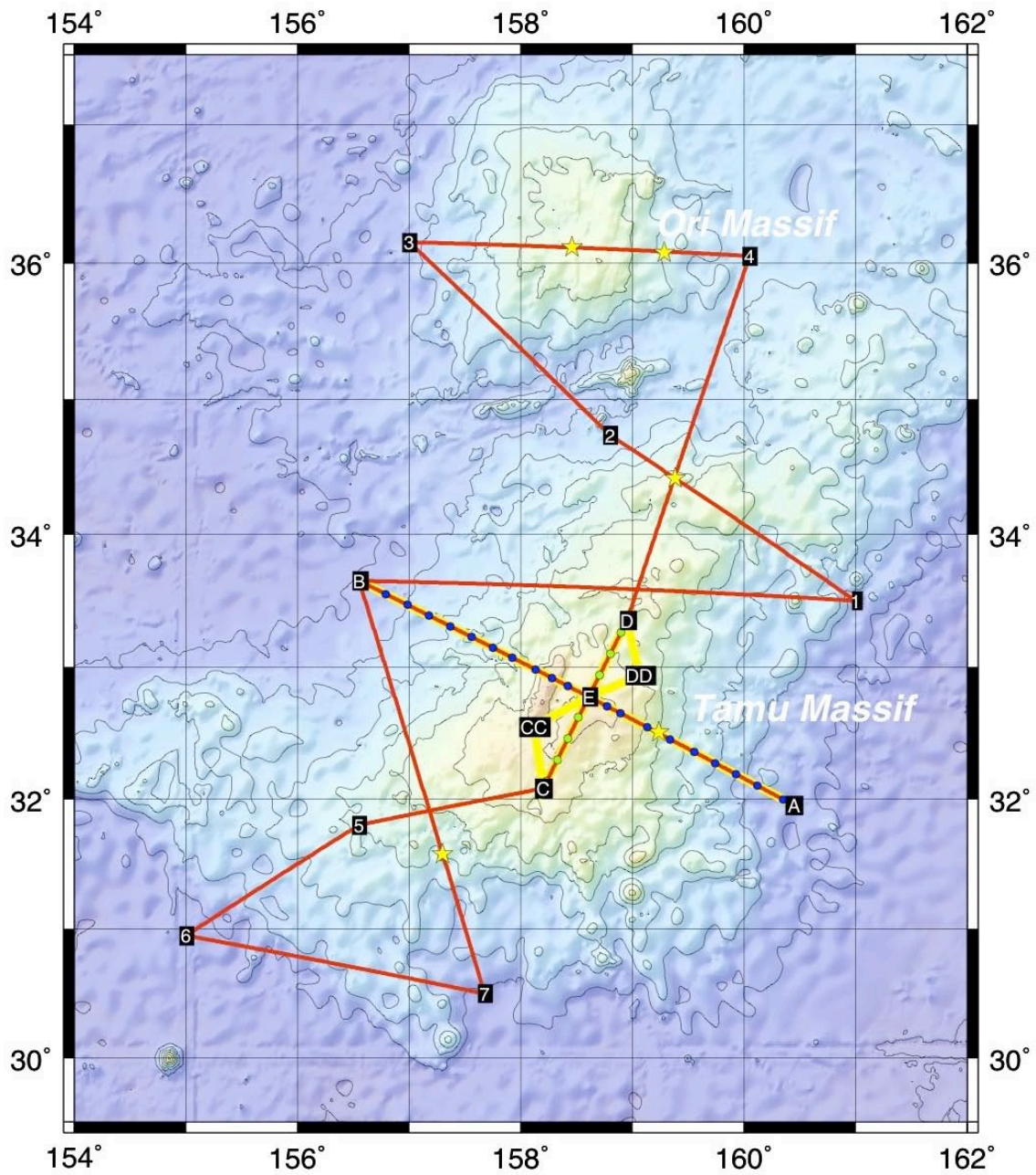


Figure 4. Map showing the initial survey plan, with OBS refraction lines (yellow), MCS reflection lines (red), OBS locations (blue and green circles), and IODP Sites (stars).

Operation Details

Navigation

MGL1004 cruise navigation data were provided by four different DGPS (differential Global Positioning System) satellite receivers: CNav 3050, Seapath 200, Cnav 2000, and PosMV. All four DGPS systems are integrated into the Spectra navigation system with CNav 3050 as primary (weighted heaviest in the final position solution). Spectra resolves a position to the NRP (navigation reference point). The NRP for MGL1004 is the center of frame 0 at the water line, 4.2 m forward of the stern. Serial (NMEA) data from all four DGPS systems are logged to the LDEO logger system. The position referenced in serial data is the position of the respective DGPS antenna location. Most of these antennas are on the MMO tower and are therefore not coincident with the NRP.

The source and streamer are positioned with a combination of RGPS (Posnet system), acoustic links (SIPS), and depth controller (bird) compasses. The Spectra navigation system resolves a position based on the range and bearing of the Posnet GPS unit on each of the source sub-arrays, as well as the tail bouy at the end of the streamer. The positioning of the source is augmented by acoustic ranging between the sub-arrays and the head of the streamer, with the streamer shape modeled on the 21 compass headings provided by the Digicourse birds attached to the streamer. Streamer depth comes from pressure sensors in the birds.

The OBSIP shot files give the vessel position at the NRP. Source position is referenced to the center of the source.

Seismic Refraction Shooting Operations

For the OBS refraction survey, we used the 6,600 cu. in. array with 36 airguns and four spares. For refraction shooting, the airgun shots were made at a distance interval of 162 m, to have a randomized time interval of 70 ± 2 ms. The airguns were positioned at a water depth of 12 m to enhance the low-frequency components of the signal. The source location relative to the ship's navigation reference point has been corrected in the P190 source navigation files and does not need to be relocated for the tomographic inversion.

Multichannel Seismic Shooting Operations

Acquisition Geometry Information: (see Figure 5 for graphic presentation)

Gun Volume: 6,600 cu. in.

Number of Guns: 36 (4 spares)

Source Depth: 9.0 m

Shot Interval: 50.0 m (~20 sec, shot on distance)

Receiver Depth: 9.0 m

Receiver Group Interval: 12.5 m

Number of Channels: 468

Sample Rate: 2 ms

Record Length: 16 s

Low-Cut: 2 Hz

High-Cut: 206 Hz

Tape Format: SEG-D

Distance from Antenna to Center of Source: 193.70 m

Distance from Center of Source to First Channel: 172.0 m

Distance from Center of Source to Last Channel: 6004.5 m

Distance from First Channel to Last Channel: 5837.5 m (= (468-1)*12.5m)

Nominal Fold: 58 (= (468 * 12.5) / (2 * 50) = 58.5)

Nominal CDP Bin: 6.25 m

We acquired 2,022 km of multichannel seismic reflection data along eight lines, including an extra 'bonus' segment (line B2) acquired in the last day of shooting. The 6,600 cu. in., 36 airgun array was shot on distance with a 50 m (~20 s) shot spacing. With 12.5 m between hydrophone groups and a 50 m shot spacing, the common midpoint (CMP) fold is 58 with a spacing of 6.25 m. Other than time lost due to medical emergencies (once before MCS operations began and once in the middle of line 7), we ran into few technical interruptions during the MCS acquisition operations despite having only one working air compressor. One recording failure occurred on the first day in the middle of line A (Reel 0007), which we did not reshoot because the lost data was less than one half of the streamer length, so the fold of the CMPs did not fall to zero. Airguns were serviced during line changes, which minimized lost data acquisition time for maintenance. During the shooting of line 7R, trash became tangled in the streamer from bird 17 to 19 (~ channels 37 to 106) and remained there for the rest of the MCS survey. The entangled item, which was later determined to be a piece of plastic drain pipe, pulled the streamer down to ~ 11 m instead of 9.0 m on bird 18. Only once did we stop shooting operations due to a marine mammal sighting (seven passing sperm whales), which caused us to turn around and reshoot the missing segment on line C.

The distance from the center of source to the first streamer group was recorded incorrectly on the observer logs (variously reporting 193 m and 167 m). The final official offset from the center of the source to the first channel for MCS operations is 172 m. The brute stacked and time migrated lines

used 193 m for lines A and B and 167 m for the remainder of the lines, so the offsets are all incorrect by 5 to 21 m. This does not change the images significantly, but will need to be corrected post-cruise.

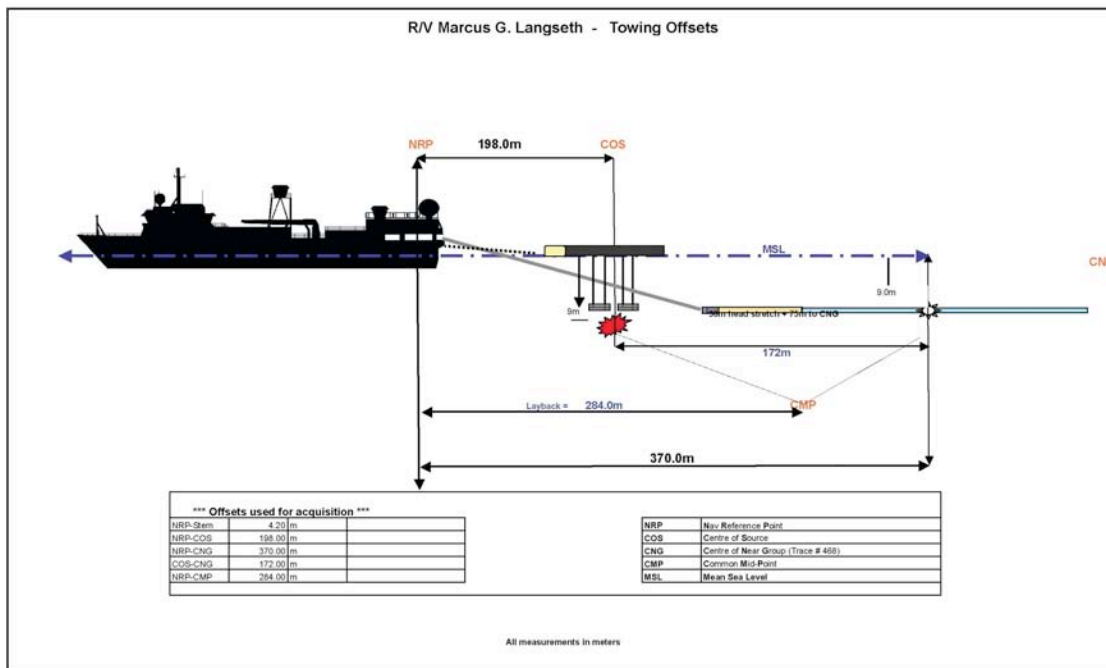
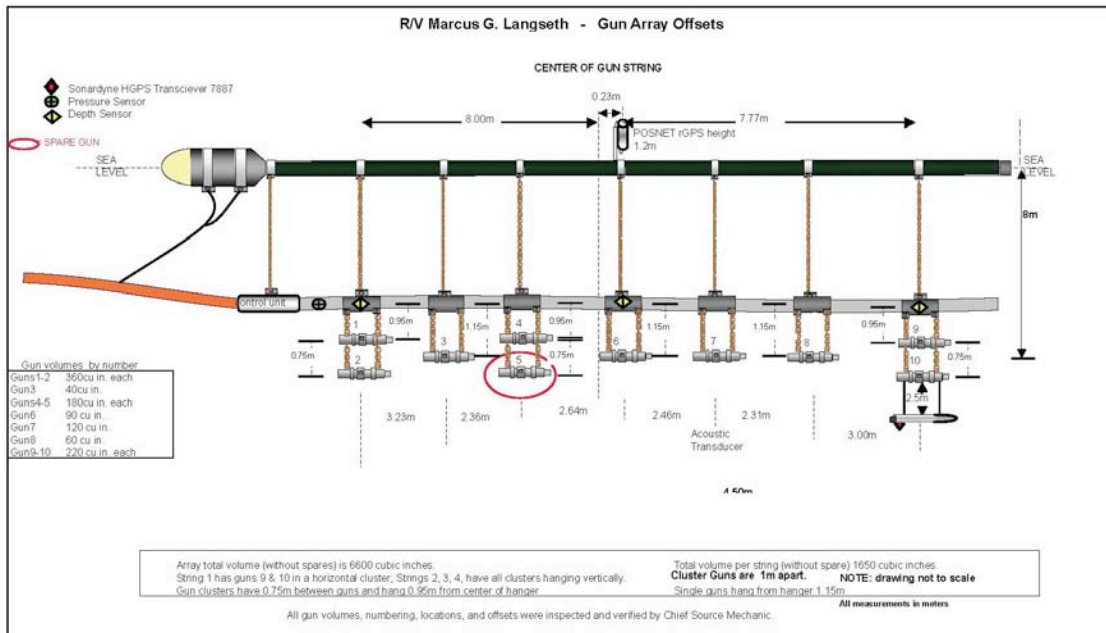


Figure 5. Diagram of source and receiver geometry for MCS operations, MGL1004.

Ocean Bottom Seismometer Operations

WHOI D2 – Deployment

Twenty-eight WHOI D2 instruments were deployed during this experiment. Prior to each deployment, the following procedure was used:

1. Anchor weight is attached to the release link, and burn wire cable is connected.
2. Instrument status is checked, operational parameters are verified, and battery and internal pressure values checked.
3. The internal Seascan clock is set using a precision GPS-based clock, and the offset between each clock is recorded.
4. An acoustic test is made to verify functionality, the release mechanism is tested, and operation of recovery aids (radio and flashers) is observed.

The deployment involves the communication among the OBS team, the main lab, and the bridge, and the overall procedure was the following:

1. About an hour before a deployment site, the OBS team starts to prepare an instrument in the van. Adjust instrument's clock with GPS (which may take some time).
2. The bridge gives the team 15-, 10-, and 5-minute warning as we approach the site.
3. At 15 minutes prior to the site, two gunners (for winch and A-frame operations) and one watchstander (as a helper) go out to the deck (with hard helmets and life jackets). The A-frame operator is charged with radio communication.
4. Ask the engine room to turn off the fan on the deck.
5. The OBS team sets up the instrument for A-frame for deployment.
6. The ship approaches to the site at 1 knots (~0.5m/s), and when crossing ~50m off the site, the bridge informs the deck to go. Watchstander in the lab marks the time ("on site"). The OBS team then initiates deployment, which usually takes 100 seconds (so we'd hit the site almost exactly).
7. When the release is accomplished, the A-frame operator calls a mark on the radio. Another watchstander in the main lab then freezes the navigation display (by hitting the middle mouse button) and logs data, time, and location ("instrument away").
8. At the same time, science officer secures multibeam and Knudsen (not to interfere with acoustic communication in the next step).
9. In the dry lab, the OBS team communicates with the instrument, and after verifying that it is actually sinking (up to 100-200 m depth), the acoustic communication is disabled. Watchstander marks time for "instrument good".
10. The team calls the main lab to resume transit to the next site. The lab tells the bridge to go, and science officer resumes multibeam and Knudsen operation. The watchstander notes time for "in transit". The fan on the deck can be turned on.
11. The watchstander makes four entries in the E-log: "on site", "instrument away" (with latitude, longitude, and depth), "instrument good", and "in transit".

Deployment operations began on 27 July 2010 at 03:50 GMT, and were completed on 28 July 2010 at 23:30 GMT.

WHOI D2 – Recovery

All twenty-eight WHOI D2 instruments deployed were successfully recovered. The following procedure was used for each recovery:

1. Upon arrival at the deployment site, an acoustic signal was sent to the OBS to “enable” communications. The watchstander logs time for “OBS Recover: On site”. EM122 and Knudsen are secured so they do not interfere with the OBS communication.
2. The range to each instrument was obtained, as a check on the depth and location of the instrument on the seafloor.
3. A coded acoustic signal was sent, to begin the instrument release sequence. The release sequence (also referred to as the “burn”) lasts 15 minutes. Periodic acoustic signals are sent by the instrument during this time to confirm the release sequence is functioning. Watchstander logs time for “OBS Recover: Release command”.
4. When the release sequence completes, the range to each instrument is checked again, in order to verify that the OBS is no longer on the seafloor and is ascending through the water column.
5. WHOI D2 instruments rise at approximately 70 meters per minute. During this experiment, the necessary rise times ranged from 30 to 80 minutes, due to the range of depths used for deployment sites.
6. After each instrument was sighted on the surface (either by radio signal, flashing lights, or direct visual observation), the Langseth was maneuvered into position such that the OBS floated along the starboard side of the ship. Watchstander logs time for “OBS Recover: Sighted”.
7. When each instrument was close enough to the ship, a recovery line was attached and the OBS hoisted out of the water and onto the deck. When the instrument is hooked, the time and position of the event is be logged (“OBS Recover: Hooked”). EM122 and Knudsen operation is then resumed.
8. After the instrument is secured in the OBS van, the team let the bridge know that we can start transit to the next site. Time for “OBS Recover: Secured” is logged.

After recovery, it is necessary to “de-brief” each OBS. The following procedure was used for each instrument:

1. The OBS was secured in the WHOI OBSIP van and connected to power and the communication network.
2. The instrument is taken out of “recovery mode” and put into normal operational status.
3. The basic functions of the instrument (battery level, internal pressure, etc) are checked.
4. The offset between the internal Seascan clock and the precision GPS-based clock is measured and recorded.
5. The deployment data is downloaded from the internal hard drive to PC hard drive in the WHOI Van.

Deployment operations began on 30 August 2010 at 08:40 GMT, and were completed on 2 September 2010 at 15:40 GMT.

Underway Geophysics

Multibeam Bathymetry

Multibeam bathymetry data were collected during the MGL1004 cruise using the R/V Marcus G. Langseth's hull-mounted Simrad-Kongsberg EM122 echo-sounder. The vessel is fitted with a $0.5^\circ \times 1.0^\circ$ degree array, that forms up to 432 beams per sonar ping in a swath arc 140° wide. Throughout the duration of the cruise, the instrument was operated in dual ping mode, generating two pulses per cycle, which doubles the sampling density and allows for more reliable ping-editing during processing.

Towed magnetometer

Total magnetic field data were measured during cruise MGL1004 using a Geometrics G-882 cesium vapor magnetometer. The magnetometer was towed 150 m astern from the starboard side of the aft main deck rail. Measurements were recorded every second along with time. These data were then merged with navigation at one second intervals.

The towing layback of 150 m is too short to completely avoid interference by the magnetic anomaly of the ship. The short layback is a necessity to keep the magnetometer cable and sensor from tangling with the airgun arrays, which are ~ 30 m farther astern. Because of the layback, we did calibration turns in an area of Tamu Massif where the magnetic field gradient was expected to be small. The calibration maneuver was in the shape of a "figure-8", with the ship turning first to one side, making a complete 360° turn, and then doing the same in the opposite direction. The figure-8 was done from 1423-1526 UT on 3 September. The raw data show ~ 100 nT peak-to-peak anomaly from the effect of the ship. In post-cruise processing, this effect must be removed (e.g., Bullard and Mason, 1961; Buchanan et al., 1996) and the data must be corrected for the current International Geomagnetic Reference Field (IGRF).

Gravimeter

Gravity data were measured by a Bell BGM-3 gravimeter (Bell and Watts, 1986) located in the Langseth main lab. Raw data were recorded at 1-second intervals by the shipboard data logging system. Absolute gravity tie measurements were made before and after the cruise using a portable Worden gravimeter to tie the dock next to the ship with the gravity station located at the Army Museum in Waikiki, Oahu, Hawaii. Gravity data require post-cruise processing including filtering, Eötvös effect, drift correction, and tie to the absolute gravity network.

Fluxgate magnetometer

A Bartington 3-axis magnetic field sensor was set up on the roof of the winch booth, and it was connected to Spectramag-6 six-channel spectrum analyzer, which was placed inside the winch booth. The spectrum analyzer fed data into Dell laptop via USB, and Spectramag-6 software was run on the laptop to record 3-component magnetic data at a sampling rate of 5 Hz. This fluxgate magnetometer system was brought onboard by Korenaga and is not part of the Langseth's scientific instrumentation.

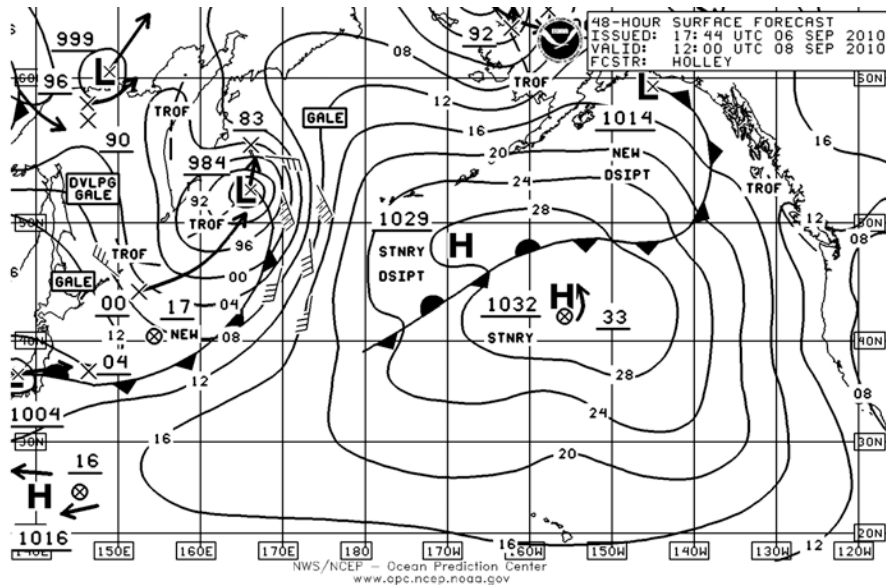
These magnetic data will be merged with ship's attitude data (heading, roll, and pitch), which are stored in the POS/MV navigation data, to calibrate for the effects of ship's own magnetic field using the method of Korenaga (1995).

Weather Information

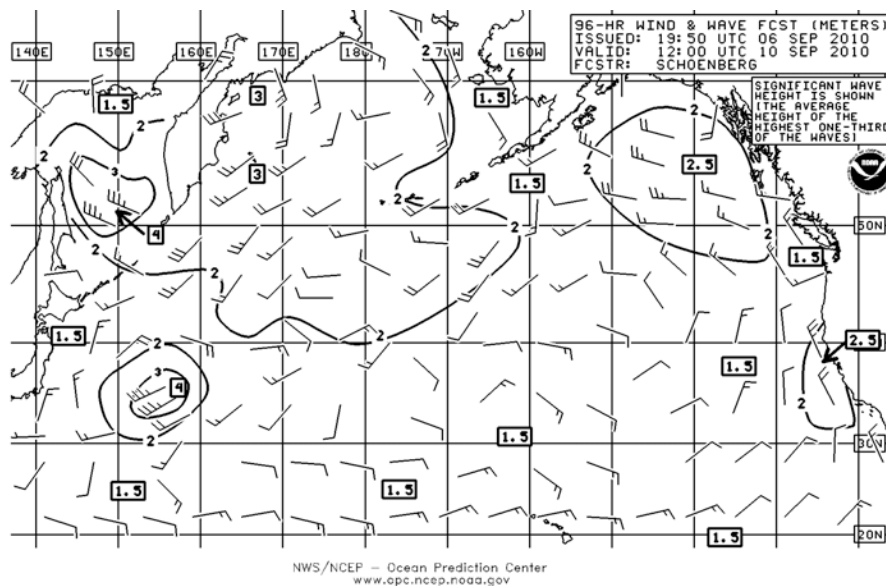
The Chief Science Officer posted daily 48-hour and 96-hour forecasts for atmospheric pressure as well as wind and wave heights, by downloading information from the Ocean Prediction Center of the National Weather Service at NOAA (<http://www.opc.ncep.noaa.gov/>). He also used the following military weather sites: <https://www.fnmoc.navy.mil/public/> and <http://www.usno.navy.mil/ITWC>.

Sample forecast images are shown below:

* 48-hour surface forecast



* 96-hour wind and wave forecast



Shipboard Computing Environment

All members of the science party brought their own laptop onboard, and because the Internet connection was available through the Highseas Net on *Langseth*, important announcements were often made by emails. There were two wireless LANs, "Langseth" and "MGL-Admin", through which we can access the cruise web site (containing E-log, data formats, Facebook for crew members, software manuals, etc) as well as the file server "fserve". A public folder on fserve was very useful for file exchange among the science party. "MGL-Admin" allows the PIs to connect to the Internet as well after the following routing command "% route -nv add -net 192.168 -interface en1 -host 192.128.0.0 -netmask 255.255.0.0". Two HP laser printers (one color and one B/W) and one HP plotter were also available through the LANs, and they were used to print out various plots of MCS and OBS data. The computing environment in the main lab was well maintained and organized.

For shipboard data processing, TAMU's Linux PC (Dell-Optiplex 745 with CentOS) "carina" was used primarily for MCS data processing using ProMAX. The main lab has a better computing resource, "proc1", which is a Redhat Linux cluster with 16 CPUs, 24GB memory, and 4TB internal hard drive, but because the version of ProMAX installed on proc1 was higher than that on carina, we decided to do ProMAX processing solely on carina to avoid any inconvenience due to version difference during post-cruise data processing. The proc1 server was used only for making GMT figures of near-trace and brute stack images. Chris Paul's PC laptop was used for multibeam data processing, and Korenaga's MacBook Pro was used for OBS data processing.

Shipboard Data Processing

Multichannel Seismic Profiles

On R/V Marcus Langseth cruise MGL1004, we created near-trace seismic sections and full-fold, time-migrated stacks using ProMAX. We used GMT to create annotated plots in black and white and color on both the large format HP plotter and the 8.5" x 11" HP laser printer. This section describes the main processing steps for creating near-trace plots, setting up the geometry, processing the data through time migration, and creating plots with GMT. Refer to the outline for details on the specific ProMAX flows and processing parameters.

1: Creating Near Real-Time Seismic Plots with ProMAX and GMT

The server and Atlantek plotter that we expected to use to create real-time plots with SIOseis were not operational during MGL1004. We therefore developed a procedure for creating near-trace seismic profiles from the shot gathers with ProMAX, GMT, and the HP DesignJet 800ps plotter. ProMAX was used to select the near channel (468) from each shot gather, apply a bandpass filter, and output each seismic section in SEG Y format. ProMAX application SEG D Input was used to load the near channel for each shot. Because of a limitation (possibly a bug) in ProMAX, only one tape of shots could be loaded at a time, so multiple SEG D Input / Disk Data Output steps were created to load all of the tapes for each line in a single flow. A separate Disk Data Input/Output sequence combined the traces from each tape into a single file using the Append option in Disk Data Output. The data were then output to disk in IEEE Real format using SEG Y Output.

2: ProMAX Processing Procedure

2.1 Geometry Setup

The most critical procedure to complete during onboard processing is navigation and geometry setup. This allowed us to take advantage of having all of the navigation data and related acquisition information at hand (watchstander logs, fresh memories, etc.), which is important for taking account of recording failures, ship turns, and other issues during initial geometry setup. Trace editing was also completed onboard, during which noisy traces are removed or filtered for noise bursts. We found that the number of bad channels averaged ~5% of the total number of channels for each line.

For 2D processing, we assumed that the multichannel seismic reflection streamer is always directly behind the boat, 180° from the sailing direction. Christopher Paul (TAMU) contributed a Python script (p190_shot_dist_xend.py) that calculates the total distance from the first shot based on the shot locations in the P190 navigation files. These values were used as the X axis in the ProMAX source pattern spreadsheet. The Y offset was assumed to be zero. .

2.2 Decon, Velocity Analysis, Radon Filter, Inside NMO Mute, Stack, Time Migration

Onboard processing steps on MGL1004 included bandpass filtering, deconvolution, inside NMO mute, stack, and time migration. Processes that require detailed picking of the seafloor reflection or multiple passes of velocity analysis were not universally applied during onboard processing, except for one or two lines of interest. Radon filtering, for example, requires two or more passes of velocity analysis and approximately doubles the CPU processing time to stack the data, but it was found to be very useful for helping us to identify primary reflections and avoid stacking multiply reflected arrivals. An initial velocity analysis was performed using a wide 2,000 CMP interval to create moved out gathers for Radon filtering, and then a shorter CMP interval with Radon applied was used for velocity analysis. Initial velocity picks err toward lower velocities prior to Radon filtering to avoid accidental removal of overcorrected primary reflections. A predictive deconvolution filter was designed to compress the wavelet before NMO correction. Post-NMO, a mute was applied to attenuate water bottom multiple energy with picks at every 500 to 1,000 CMPs depending on the topography. Finally, time migration was applied. We tested migration velocities based on the stacking velocities, but found that time migration at the water velocity (1,500 m/s) worked best to avoid over-migrating interbed and water bottom multiples.

2.3 Suggested Post-Cruise Processing

Suggested post-cruise data processing steps include time-variant and multi-window bandpass filtering and deconvolution, detailed velocity analysis particularly for specific horizons of interest, Radon and F-K filtering for multiple removal (possibly using multiple, time variant windows), and depth migration using an accurate velocity model.

3: Printing SEGY Seismic Data with GMT

We used GMT to create annotated PostScript plots from the SEGY data. The seismic profiles can be plotted as both variable area black and white images (plotsegy.gmt) and color gridded seismic images (segy2grd.gmt with seis.cpt). A custom plot size is needed to plot the seismic sections on the large HP DesignJet 800ps plotter. The command "gmtset PAPER_MEDIA=Custom_1728x3650" sets the paper size, where the width (1728) and length (3650) are in units of pixels.

Multibeam Bathymetry

Bathymetry data were processed using MB-System swath sonar bathymetry software, version 5.13b. This version of the software has a known issue when processing data from current generation Simrad sonars, the EM-122 being such an instrument, which makes it currently impossible to recalculate beam ray paths after applying new sound velocity profiles. Accordingly, due diligence was paid to the operating sound velocity profile used during acquisition, and it was updated with a new eXpendable Bathymetric Thermograph probe (XBT) cast daily.

Bathymetry data were ping edited using MB-System. Erroneous soundings were recognized as outliers by departure from a smooth depth profile and deleted from the dataset prior to gridding of the data. Swath widths during the cruise reliably ranged from 3 to 4.8 times water depth and so gridding resolution was calculated (by dividing swath width by total number of beams per ping) at 50 meters. This value ensures at least one beam in each gridding bin for all depths of the survey, both on site at Shatsky Rise as well as in abyssal depths on the transits to and from the survey site. The current standard for scientific bathymetric surveys is 100 meter resolution, and previous surveys on Shatsky Rise, conducted in 1994, were done at 150 meter resolution, so this is a significant increase in resolution for this survey.

Throughout the duration of the MGL1004 cruise, processed bathymetry data were gridded at the end of each Julian Day (UTC) and merged with previous swath bathymetry (from the 1994 survey) and 1 arc-minute resolution estimated bathymetry from satellite altimetry (Smith and Sandwell, 1997) to generate daily plots of the bathymetry surveyed.

At the completion of the cruise, the total pool of bathymetry data collected will be gridded into three major regions: The Pacific Basin covered by the transits between Hawaii and Shatsky Rise, The Pacific Basin covered by the transits between Japan and Shatsky Rise, and Shatsky Rise proper. These three grids will be made available to the cruise participants and will be uploaded to the Marine Geophysical Database maintained by Lamont-Dougherty Earth Observatory, where they will be available to the cruise participants via the internet immediately, and to the general public after the expiration of the two-year post-cruise moratorium.

Sound Velocity Profiles (SVPs) were generated during the course of MGL1004 by the use of Sippican XBTs at an interval of one every 24 hours. At transit speeds, T-7 model XBTs were used, collecting water column temperature profiles to a depth of 760 m. At slower survey speeds, T-5 model XBTs were used to collect profiles up to 5000 m, and one occasion, a C-5 eXpendable Conductivity Temperature Depth (XCTD) probe was used to collect its full suite of water column information to a depth of 1300 m. The temperature profiles collected by these probes, when used with the current seawater salinity (measured by the ship's thermosalinograph system), were used to calculate SVPs that were then loaded into the Seafloor Information System (SIS) acquisition software that is used with the Simrad EM-122 multibeam system. The SIS software compares these SVPs with surface water sound velocity probe values measured from the thermosalinograph system in the multibeam array housing to ensure that the calculated SVP values are within the expected range. If the SVP matches the measured probe values, then SIS applies that profile to the beam depth calculations for each beam in each sonar pulse. At any time that the SVP values were more than three meters per second different than the probe reading, a warning light was turned on in the software, and plans were made to take a new XBT cast to update the SVP in SIS.

Initial Ocean Bottom Seismometer Data Processing

Processing of the data collected by each WHOI D2 instrument is best done after all instruments have been recovered and their individual data downloaded. The following procedures are used for each instrument:

1. Data for the entire deployment is copied from the PC hard drive in the WHOI van to a hard drive attached to a Mac OS X based system in the processing lab. Total data recorded by each D2 ranged from 2.1 GB to 2.9 GB. This variation is due to the length of actual deployment and the efficiency of data compression.
2. Data is split into individual channel files on a per day basis. These files (day files per channel) are then managed by an Antelope-based database system. (Antelope is a commercial, seismic processing software system, see <http://www.brtt.com> for details).
3. Salient details about each deployment are assembled into a number of program parameter files. These entries consist of such data as instrument location, deployment dates and duration, instrument identifier, and so forth. This information is then incorporated into the Antelope database for each deployment.
4. The clock offset between the Seascan internal clock and GPS-based time are tabularized and verified. When complete, the day files per channel data are "clock corrected," using Antelope software. This insures that all data is referenced at the correct UTC time.
5. Shot instance files were obtained from the Langseth navigation team. These files contain the date and time of each shot, along with the corresponding ship and sound source location, shot number, and water depth.
6. SEG-Y Files were made for each instrument with both OBS ("RL") lines and MCS ("ML") lines. These are produced using the time and position from the shot files, then extracting the waveform data from the Antelope database with a trace length of 70 seconds, sampled at 200 samples per second. The location of the instrument itself is estimated from its corresponding deployment position and multibeam sonar derived depth.
7. Completed SEG-Y files were copied to the Langseth public file server (\\fserve\mg11004\public\SEG_Y), per request of the Chief Scientist, for dissemination.

Ocean Bottom Seismometer SEG-Y Data Processing

Initial quality check was done by Korenaga's segytool as follows:

1. Decompose each SEG-Y file into four components with `segycut`.
2. Apply velocity reduction with `segycut`.
3. Apply bandpass filter of 5-20 Hz by `segycut`.
4. Apply predictive deconvolution with the filter duration of 0.6 s and the delay of 0.15 s with `segycut`.
5. Convert to ASCII data by `segycut` to be plotted with GMT's `pswiggle`.

The hydrophone component was found to be consistently of high quality (see Appendix: OBS Data Quality), but the geophone components were of variable quality. Data with a shot interval of 70 s are minimally influenced by previous shot noise, though they may be improved by further applying some kind of a coherency filter. The present implementation of `segycut` is still rather premature, and further testing need to be done. The development of a better coherency filter is also essential to make the best use of OBS data for 20-s interval MCS shots, which are important for 3-D crustal tomography but suffer considerably from previous shot noise.

The post-cruise data processing must start from relocating the instruments using the direct wave arrivals and the multibeam bathymetry. Offsets between the instruments and the shots will then be recalculated with the WGS-84 ellipsoid using the formula of Vincenty (1975) (note: GMT uses a spherical approximation when calculating the shortest distance between two points, which may not be accurate enough for our long refraction line A-B). Each refraction and reflection lines will be extracted from the WHOI SEGY files with an increasing order of shot-receiver distance, as up to a few lines are bundled in a single SEGY file.

Survey Outcome and Assessment

The map below (Fig. 6) summarizes what was originally planned for and what was actually achieved during MGL1004. The original plan was to (1) deploy all OBSs (shown as circles) starting from A and ending at B, (2) gun-only shooting with 70-s interval over B-E-DD-D-C-CC-E-A (yellow lines), (3) MCS profiling over A-B-1-2-3-4-D-C-5-6-7-B (red lines), and (4) recover all OBSs starting from B and ending at A. These seismic lines were designed to cross five drilling sites (stars). By starting and ending at waypoint A, this plan minimizes the transit time between Honolulu and the survey area.

The first medical diversion took place during the gun-only shooting over the segment D-C. When we proceeded to MCS profiling later, we decided to shoot the southern part first upon the recommendation of the chief science officer. There was always a risk of losing the compressor, and the unfavorable sea state in the northern part also motivated the decision. The MCS shooting order was then A-B-7-6-5-C-D-4-3-2-1-B.

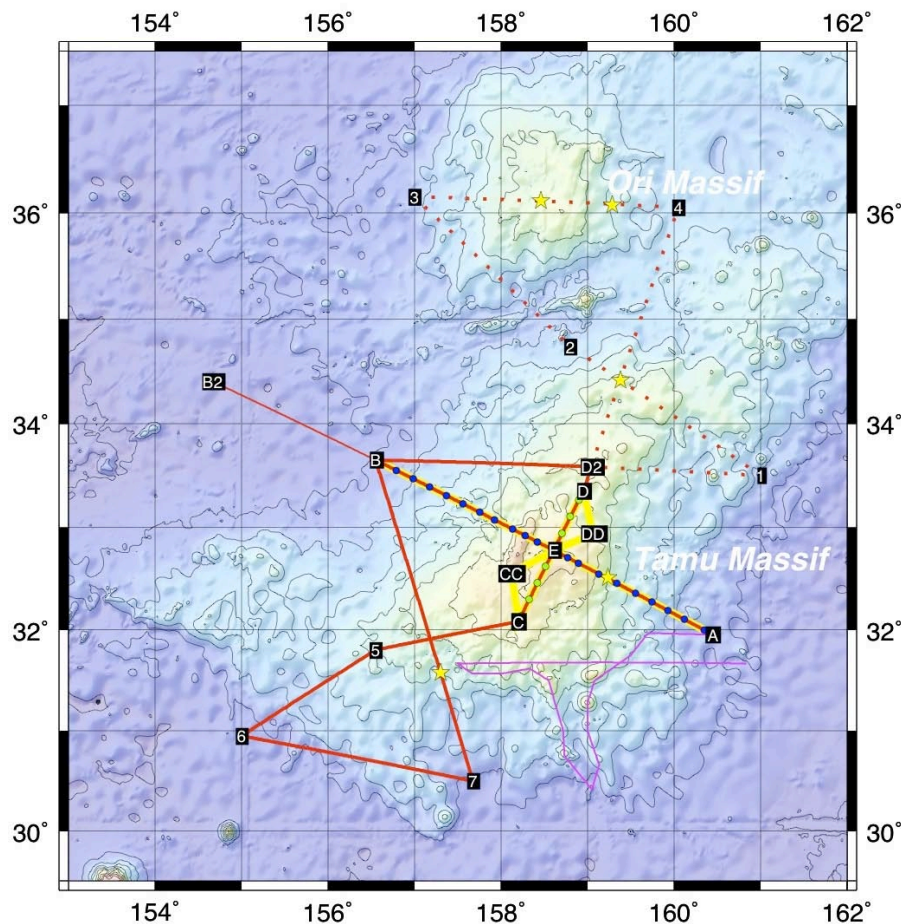


Figure 6. Work completed on cruise MGL1004. Heavy lines show those completed during the cruise. Dotted lines represent those not completed. Note that the MCS seismic line between points A and B was extended into the abyssal plain to point B2. The light purple line shows the ship track during which extra contingency time was used for bathymetric mapping after the recovery of OBS.

The second medical diversion then took place during the transect 7-6. At this time, there was no hope of completing all of MCS profiling, and because another cruise was granted by NSF to compensate the loss of science days, we decided to focus on the southern part, and the MCS shooting plan became A-B-7-6-5-C-D-D2-B. As this shooting went fairly smoothly, we were able to shoot an extra transect B-B2 (thin red line), which turned out to yield critical data. After transiting to B, we recovered all OBSs as originally planned, and used remaining contingency to collect extra multibeam data along peculiar volcanic features on the southeastern flank of the Tamu Massif (purple lines). The unfinished MCS lines (dotted red lines) are planned for completion in 2012.

As this cruise was disrupted so severely by medical diversions, which we do not normally take into account as contingency, a simple comparison between the original schedule and the actual timeline is not very useful to evaluate the survey plan. In Table 1, therefore, we compare the actual timeline with the part of the original schedule corresponding to the southern part. The total cruise duration assumed in this calculation is 43 days (i.e., original 52 days - 16 days of medical diversions + 7 days of NSF extension). Cruise waypoints are given in Table 2.

Lessons learned from this comparison may be summarized as:

- Contingency for OBS deployment can be minimal (e.g., a few hours total, instead of half an hour for each instrument).
- LDEO's timing guideline for MCS operations was reasonable. We gained about a day in total, but it is because we were lucky to have minor gun problems only.
- We gained more than a day from OBS recovery, thanks to the efficiency of the WHOI OBS team and also to good weather. Having sufficient contingency cushion was still felt important to reduce stress to the recovery operation.
- The shooting operation benefitted from low biological productivity in the survey area. We lost only 4 hours in total, for an encounter with a pod of whales during the MCS line C-D.

Table 1. Operation time summary.

Plan				Actual				
	duration	elapsed			elapsed		diff.	
Task	(hour)	(hour)	(day)	duration	(hour)	(day)	(hour)	note
Honolulu-A	232	232	9.7	226.0	226	9.4	6.0	(*3)
OBS deployment(*1)	71	303	12.6	44.0	270	11.3	27.0	
deply guns	7	310	12.9	3.0	273	11.4	4.0	
gun-only shooting B-E-DD-D	37	347	14.5	39.5	312.5	13.0	-2.5	
gun maintenance	4	351	14.6	0.0	312.5	13.0	4.0	(*4)
gun-only shooting D-C-CC-E-A	55	406	16.9	62.4	374.9	15.6	-7.4	
retrieve guns	2	408	17.0	1.0	375.9	15.7	1.0	
deploy streamer	24	432	18.0	9.0	384.9	16.0	15.0	
deploy guns	2	434	18.1	3.5	388.4	16.2	-1.5	
MCS shooting A-B	49	483	20.1	44.4	432.8	18.0	4.6	
gun maintenance	4	487	20.3	3.3	436.1	18.2	0.7	
MCS shooting B-7	44	531	22.1	46.1	482.2	20.1	-2.1	
gun maintenance	4	535	22.3	3.3	485.5	20.2	0.7	
MCS shooting 6-5-C	40	575	24.0	36.3	521.8	21.7	3.7	
gun maintenance	4	579	24.1	4.7	526.5	21.9	-0.7	
MCS shooting C-D-D2	22	601	25.0	25.2	551.7	23.0	-3.2	(*5)
gun maintenance	4	605	25.2	10.4	562.1	23.4	-6.4	
MCS shooting D2-B	27	632	26.3	26.3	588.4	24.5	0.7	
gun maintenance	4	636	26.5	4.5	592.9	24.7	-0.5	
MCS shooting B-B2	27	663	27.6	22.8	615.7	25.7	4.2	
retrive guns	2	665	27.7	0.8	616.5	25.7	1.2	
retrive streamer	8	673	28.0	2.3	618.8	25.8	5.7	
OBS recovery(*2)	109	782	32.6	79.0	697.8	29.1	30.0	
A-Honolulu	232	1014	42.3	232.0	929.8	38.7	0.0	
Contingency	19	1033	43.0	78.0	1007.82	42.0		(*6)

Transit speed: 10 knots
 Shooting speed: 4.5 knots

Shooting net difference: -2.0 hours
 MCS gear-related operations net difference: 23.2 hours

(*1) Transit speed between OBS sites is assumed to be 8 knots, and each deployment takes 30 minutes. Another 30 minutes of contingency is added for each instrument.

(*2) Transit speed between OBS sites is assumed to be 8 knots. Rise speed is 70m/min, each recovery takes 1 hour, and another 30 minutes of contingency is added for each instrument.

(*3) This includes 8.5 hour delay in departure (assuming 8AM departure being normal).

(*4) Chief Sci. Officer recommended to keep shooting.

(*5) includes an turn due to MMO sighting

(*6) 39 hours of MCS shooting (B-B2) before OBS recovery, which includes gun maintenance and transit back to B, and 39 hours of multibeam mapping after OBS recovery.

Table 2. List of cruise waypoints.

Shooting waypoints			OBS waypoints		
	latitude	longitude		latitude	longitude
A	31.950000	160.450000	OBSA1	33.630037	156.598396
B	33.650000	156.550000	OBSA2	33.549996	156.791757
B2	34.405540	154.665070	OBSA3	33.469655	156.984760
C	32.080000	158.200000	OBSA4	33.389015	157.177404
D	33.350000	158.950000	OBSA5	33.308079	157.369690
D2	33.585700	159.043000	OBSA6	33.226847	157.561620
E	32.775000	158.610000	OBSA7	33.145320	157.753192
DD	32.937700	159.064000	OBSA8	33.071696	157.925302
CC	32.551700	158.120000	OBSA9	32.981391	158.135268
1	33.500000	161.000000	OBSA10	32.919618	158.278180
2	34.735000	158.800000	OBSA11	32.857683	158.420893
3	36.150000	157.000000	OBSA12	32.774851	158.610866
4	36.050000	160.050000	OBSA13	32.704219	158.772065
5	31.800000	156.550000	OBSA14	32.650067	158.895162
6	30.950000	155.000000	OBSA15	32.545592	159.131468
7	30.500000	157.675000	OBSA16	32.453289	159.338963
			OBSA17	32.356427	159.555434
			OBSA18	32.271900	159.743292
			OBSA19	32.187095	159.930800
			OBSA20	32.102014	160.117959
			OBSA21	31.995276	160.351416
			OBSB1	32.136471	158.232846
			OBSB2	32.297769	158.326915
			OBSB3	32.458998	158.421320
			OBSB4	32.620155	158.516063
			OBSB5	32.942256	158.706578
			OBSB6	33.103197	158.802356
			OBSB7	33.264065	158.898485
Additional multibeam waypoints					
	latitude	longitude			
M1	31.967000	159.700000			
M2	31.750000	159.500000			
M3	31.500000	159.083000			
M4	31.283000	159.000000			
M5	31.000000	159.000000			
M6	30.667000	159.133000			
M7	30.417000	159.050000			
M8	30.750000	158.733000			
M9	31.000000	158.717000			
M10	31.500000	158.550000			
M11	31.617000	158.333000			
M12	31.567000	158.000000			
M13	31.567000	157.667000			
M14	31.667000	157.500000			
M15	31.667000	160.833000			

Preliminary Data Review

Multichannel Seismic Profiles

Lines A, B2. Lines A and B2 are a crossing of the summit of Tamu Massif and an extension into abyssal seafloor to the northwest, respectively. Line B2 was added once it was realized that even though Line A extended to seafloor >5200 m in depth, the edge of the massif had not been reached. The combined line shows Tamu Massif as a huge volcanic construct with two summits and low flank slopes far into the adjacent abyssal plains. At the distal ends of the flanks, the slope of acoustic basement is a fraction of a degree.

The near-trace plot (Fig. 7), shows thin sediments on the flanks of Tamu Massif, generally 0.1-0.2 sec two-way traveltime (twtt) in thickness. At the summit, in the basin between peaks is filled with ~1.0 sec twtt of sediment. The line crosses four cones on the east side of the volcano and two escarpments, 0.2 and 0.4 sec twtt high, on the west flank. The igneous basement is easily recognized and although mostly continuous, it has a slightly rough texture that distinguishes it from smoother sediment layers. The western summit ridge (Toronto Ridge of Sager et al., [1999]) appears even taller in the seismic profile because its buried extent is visible. The ridge appears to be formed in a hole as the acoustic basement on its west side appears to drop sharply toward the ridge. The eastern ridge is buried and has gentler slopes. Its summit is broken with offsets indicating faulting. This ridge probably represents a volcanic rift zone. Its width and continuity with the east and west flanks suggests that it was the main source of Tamu Massif eruptions. In contrast, Toronto ridge appears to be a later feature built on top of the wider volcano.

In a profile that has been stacked and migrated, interbasement reflectors are visible up to 2-3 sec twtt below the top igneous surface. Reflectors dip outward from the center of the volcano at places and have a form similar to that of sedimentary delta foreset beds (Fig. 8). Apparently, these dipping reflectors indicate layers of prograding lava flow lobes.

Line B2 extends into deep water at the distal end of the Tamu Massif flank. It shows sloping volcanic basement on its southeast side that is continuous with Line A and buried by a thin layer of sediments, approximately 0.2-0.25 sec twtt in thickness. At about the middle of the line, basement mounds are seen and the downward slope from Tamu Massif ends, implying that this is the end of Shatsky Rise volcanics. The northwest end of the line appears to show abyssal plan crust.

In the stacked and migrated profile, a deep set of reflections is seen beginning at ~10.0 sec twtt on the northwest end of the line. Its surface undulates, but it is nearly continuous and stretches across the line and is 10.5 sec twtt in depth at the join with Line A (Fig. 9). On Line A, we can see this same reflector continue to deepen beneath Tamu Massif. From the depth and character of the reflector, we think that this is the Moho.

Line B. (Fig. 10) Line B has an appearance similar to Lines A, B2 because it also crosses perpendicular to the backbone of the Tamu Massif. On this line, we also see thin sediments on the flanks of Tamu Massif, 0.1-0.25 sec twtt, and thick sediments at the summit. The summit at Line B is deeper than at Line A, because the latter crosses down the flank from the summit, and the sediments are thick, but not as much as on Line A. On line B, we also see a large scarp on the lower flank. This one has a height of 0.9 sec twtt and it has a small cone at its top. Both the scarp and the cone are prominent in multibeam bathymetry. Basement character in the near-trace plot is similar to Line A.

As with Line A, the stacked and migrated version of Line B shows reflectors up to 2-3 sec twtt below the surface of the igneous basement. These reflectors have significant dips in places and generally the pattern is outward from the center, however, on this line there are overlapping piles that suggest stacking patterns.

Line B also shows a deep reflector on the east side of Tamu Massif that has a similar appearance to that seen on Lines A and B2 to the west of the volcano. The depth of this reflector appears to be 9.0 seconds at the southeast end of the line.

Line 7. Line 7 crosses a low part of Tamu Massif that stick out to the southeast of the main volcano and has a trend parallel to magnetic lineation M21 [Nakanishi et al., 1999]. The near trace plot (Fig. 11) shows a low mound with a four to five cones on top with heights of 0.5-1.5 sec twtt. The low mound is broad and has a height of ~1.0 sec twtt. Interestingly, the steeper cones at its summit also occur at its edges. The seismic data show thin sediments over the adjacent abyssal plains (0.2-0.3 sec twtt) and a slightly thicker sedimentary layer on top of the volcanic mound (0.4 sec twtt).

Stacked and migrated data do not reveal much structure at this location. We can see reflectors ~0.5 sec twtt below the top of igneous basement.

Line 6. Line six is the deepest of three lines (Lines 7, 6, and C) that make up a transect from the base of the Tamu slope up the axis of the volcano to its summit. The near-trace plot (Fig. 12) shows sediments up to 0.3 sec twtt in thickness near the base of slope and that thickness increases upslope to 0.4 sec twtt. Along this profile, we see two zones of higher volcanic slope and the lower of the two may be an escarpment, but the morphology is not as clear as with other lines. As with Line 7, the stacked and migrated version of Line 6 does not show much sub-basement detail. Reflectors are seen to ~0.5 sec twtt below the top of the igneous pile, but details are not as abundant or clear.

Line 5. Line 5 climbs up the southwest flank of Tamu Massif. The near-trace plot (Fig. 13) shows that sediments continue to thicken upslope from 0.4 to 0.9 sec twtt. Igneous basement is well resolved and has a character similar to that seen on Lines A and B. An interesting mound occurs at the seafloor near the middle of this line. There seems to be no root to the mound through the sediments, so it is either an erosional remnant of surface sediments or a late volcanic cone that penetrated through the sediments. Stacked and migrated data show intra-basement reflectors up to ~0.5 sec twtt below the top of the igneous pile. These sub-basement reflectors show a pattern of flows truncated by the igneous surface. It appears that the flow fronts retreat upslope with time. In sedimentary settings, this pattern would be called "offlap".

Line C. Line C crosses the summit of Tamu Massif through the middle of the sediment basin. Naturally, this means that the sediments are thick. The near-trace plot (Fig. 14) shows sediments up to ~1.0 sec twtt in thickness with sculpting and multiple episodes of erosion and deposition on the north side of the summit. The sedimentary section in the summit basin shows two buried mounds, each several hundred meters in height. Igneous basement is easily recognized and many sub-basement reflectors are seen. On the stacked and migrated version of this line, inter-basement reflectors are seen 2.0-2.5 sec twtt below the igneous surface. These reflectors are relatively flat lying and conformable to the igneous basement surface. However, we do see more variety to the structure around the buried cones that may be from their disruption of lava flows.

Line D2. Line D2 extends from the north side of the Tamu Massif summit down the west flank to connect with Lines A and B2. The near-trace plot (Fig. 15) shows sediments that are thick near the

summit (~0.5 sec twtt) and thin downslope to ~0.15 sec twtt at the base of slope. The sediments are also thinned and cut on the western flank by the canyon erosion. An escarpment on the lower slope is also seen on this line and it connects to that imaged on Line A. The scarp has an offset of 0.2 sec twtt of igneous basement. The stacked and migrated version of the seismic line shows intra-basement reflectors that dip generally downslope and can be traced 2.0-2.5 sec twtt below the basement surface. In places, the slope changes, mimicking the effect of delta foreset beds. At least two different lava deltas are seen on this line.

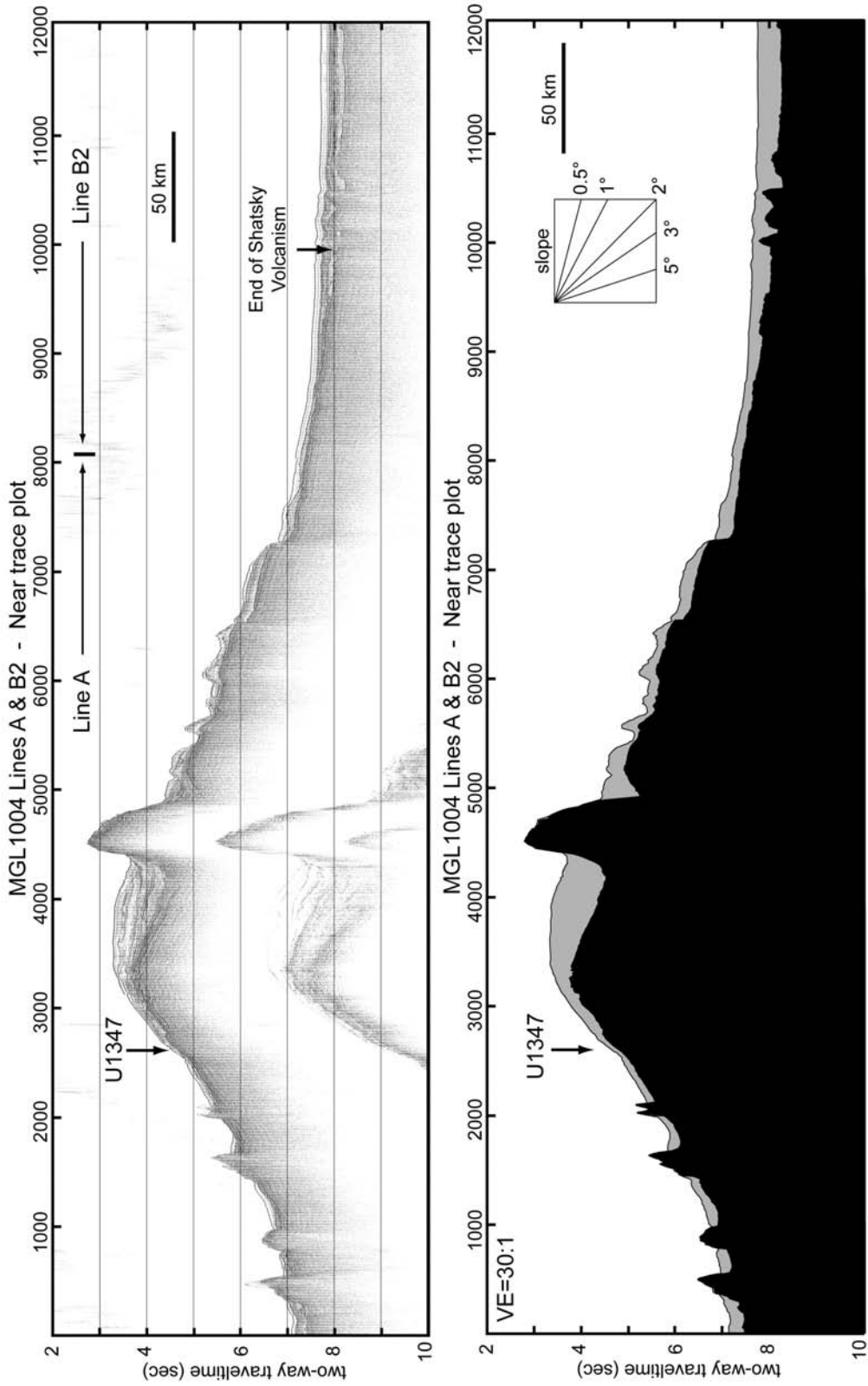


Figure 7. Near-trace plot of seismic line MGL1004_ML_A and interpretation. Black area of interpretation panel shows igneous basement and gray area represents sediment.

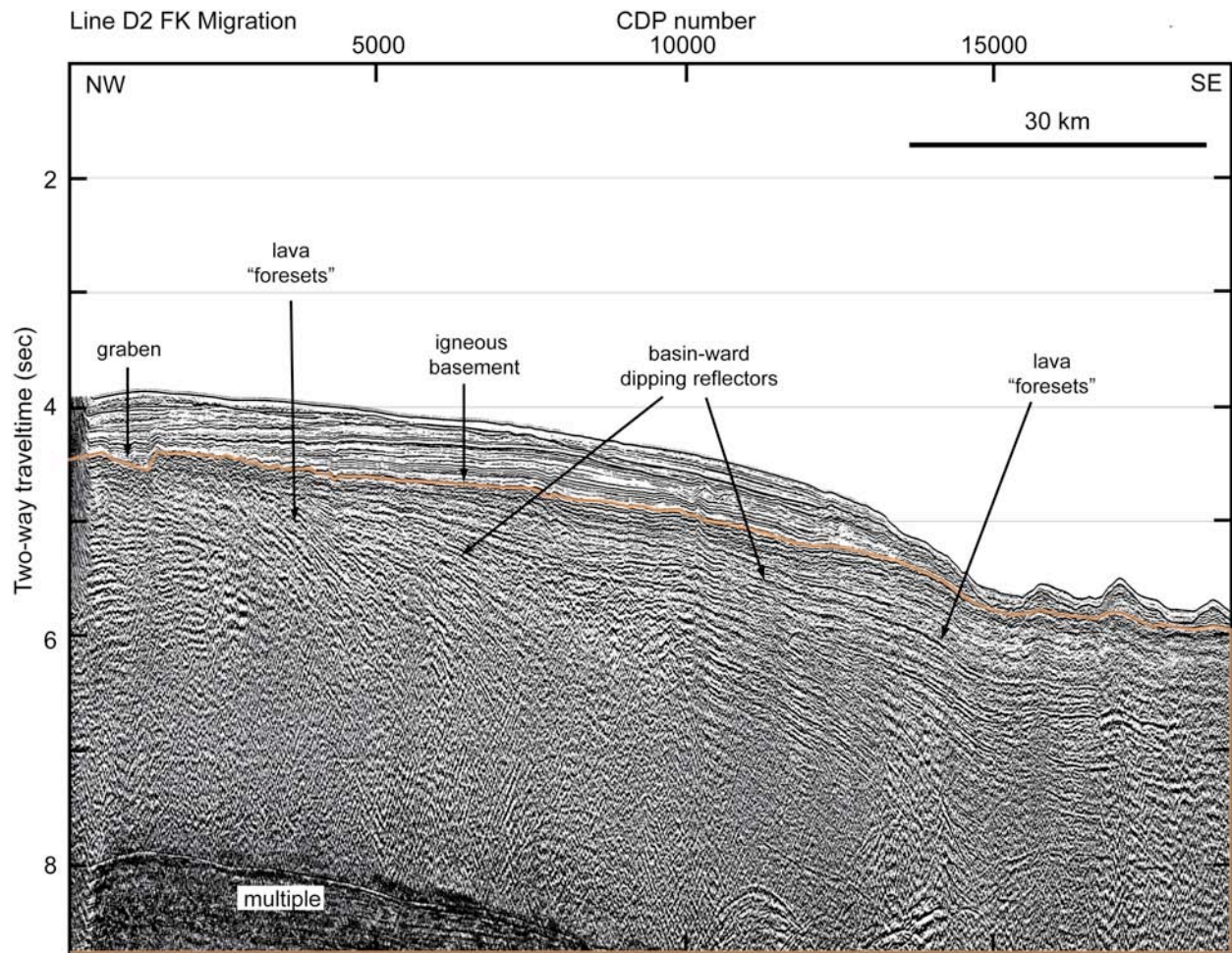


Figure 8. Example of migrated seismic line showing dipping intra-basement reflectors. Dips and onlap geometries of reflectors give “foreset bed” appearance, similar to siliciclastic sediment deltas. Red line highlights igneous basement. This is a portion of Line MGL1004_ML_D2, located on the west side of the Tamu Massif summit. The data have been stacked, filtered, and migrated using FK migration.

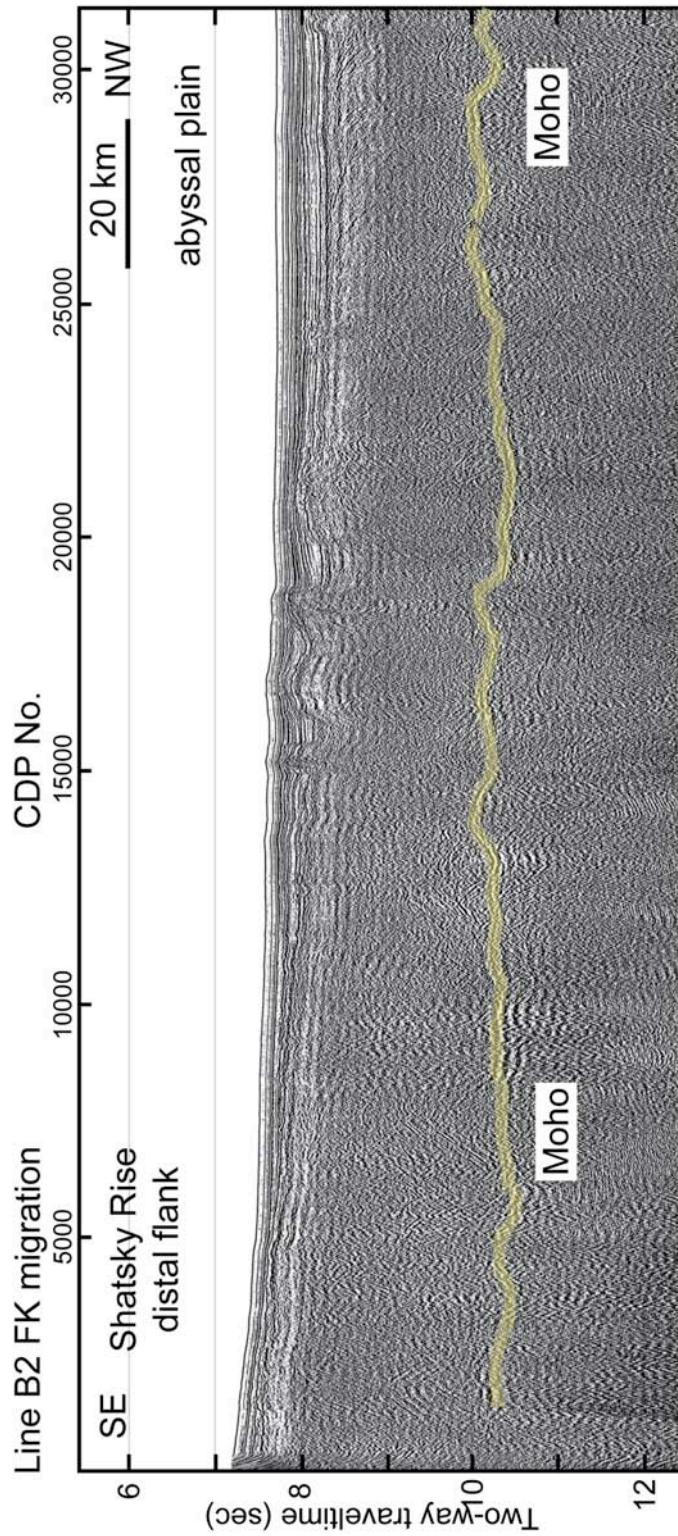


Figure 9. Seismic Line MGL1004_ML_B2, over the abyssal plain west of Tamu Massif. The data show a deep, undulating reflector interpreted as the Moho. The data have been filtered, stacked, and migrated with FK migration.

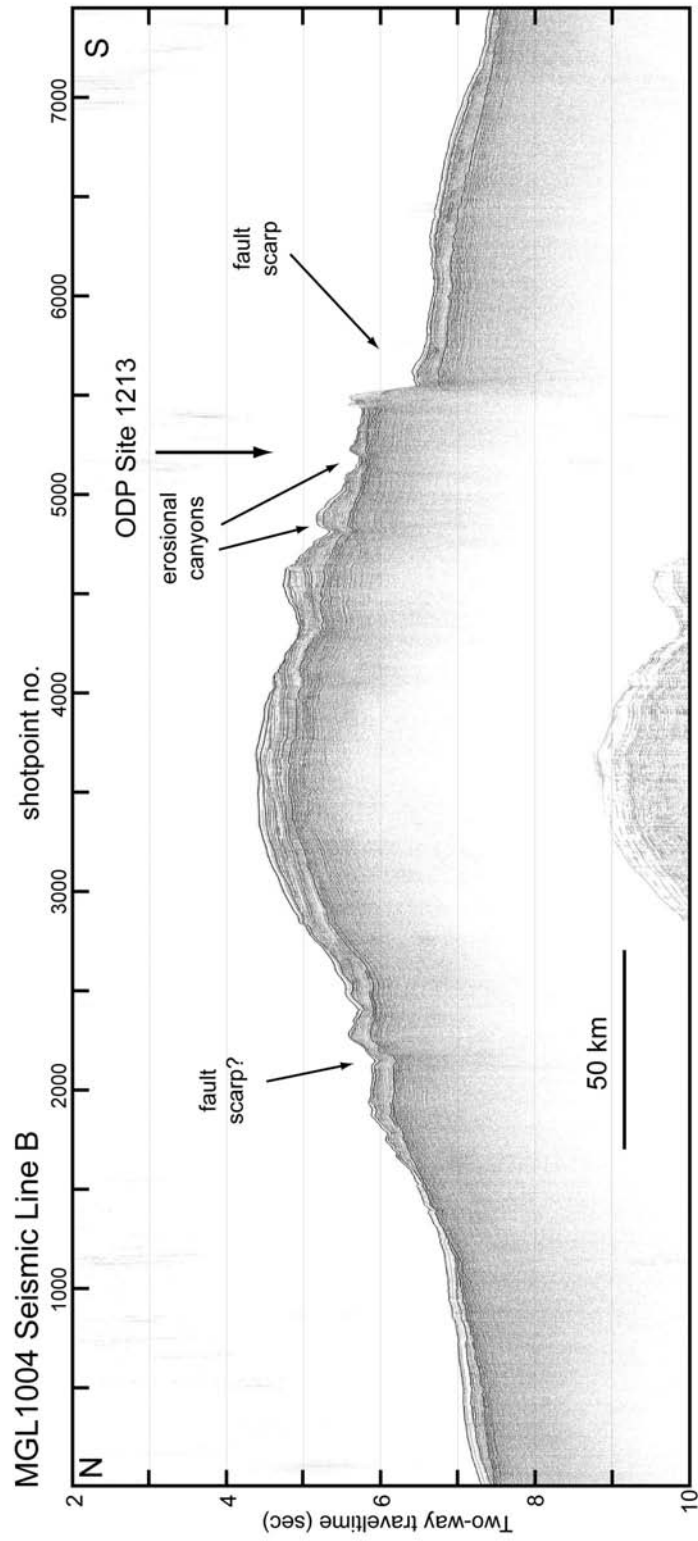


Figure 10. Near-trace plot of seismic Line MGL1004_ML_B, crossing the axis of Tamu Massif to the southwest of the summit.

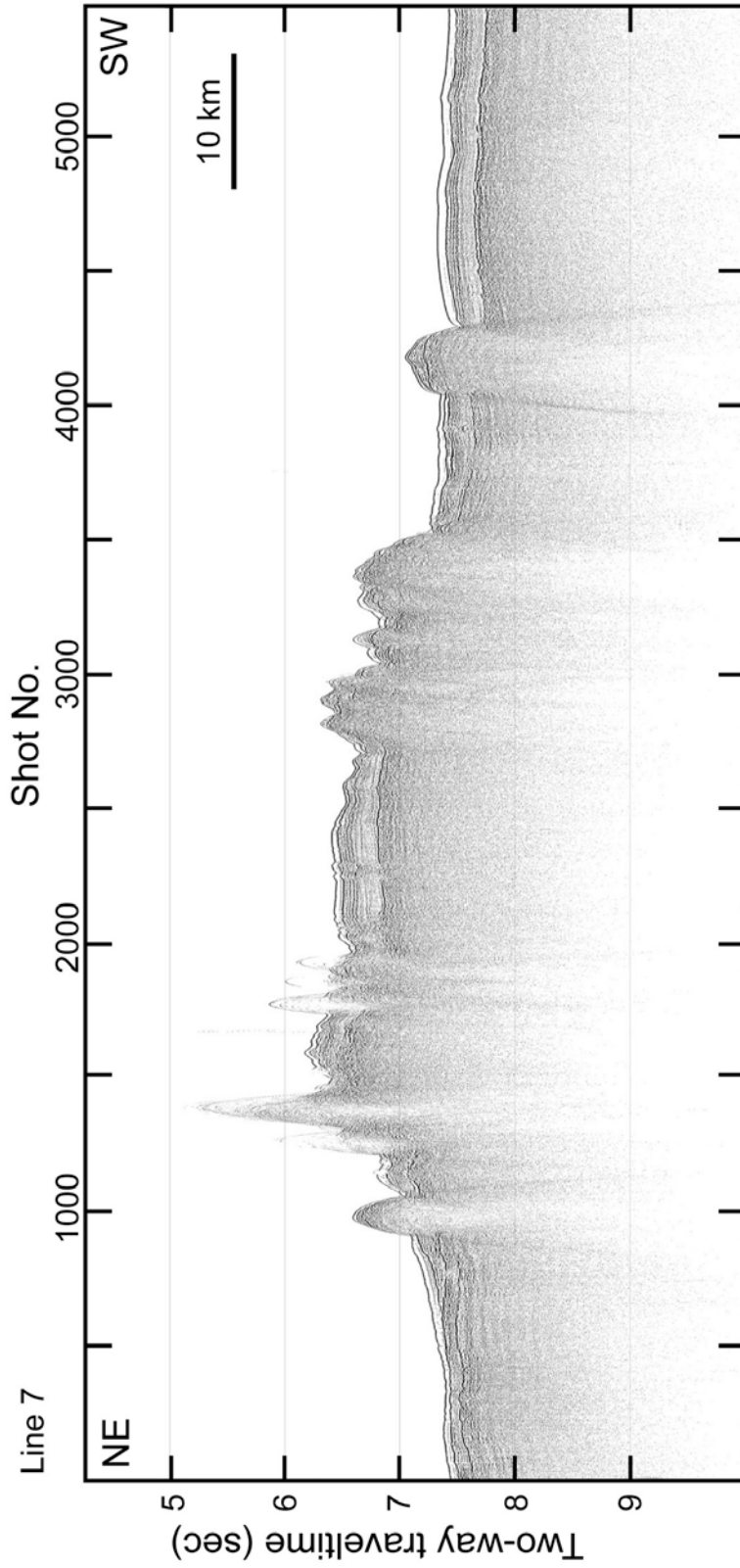


Figure 11. Near-trace plot for seismic Line MGL1004_ML7. The transect crosses a low part of the southern distal flank of Tamu Massif.

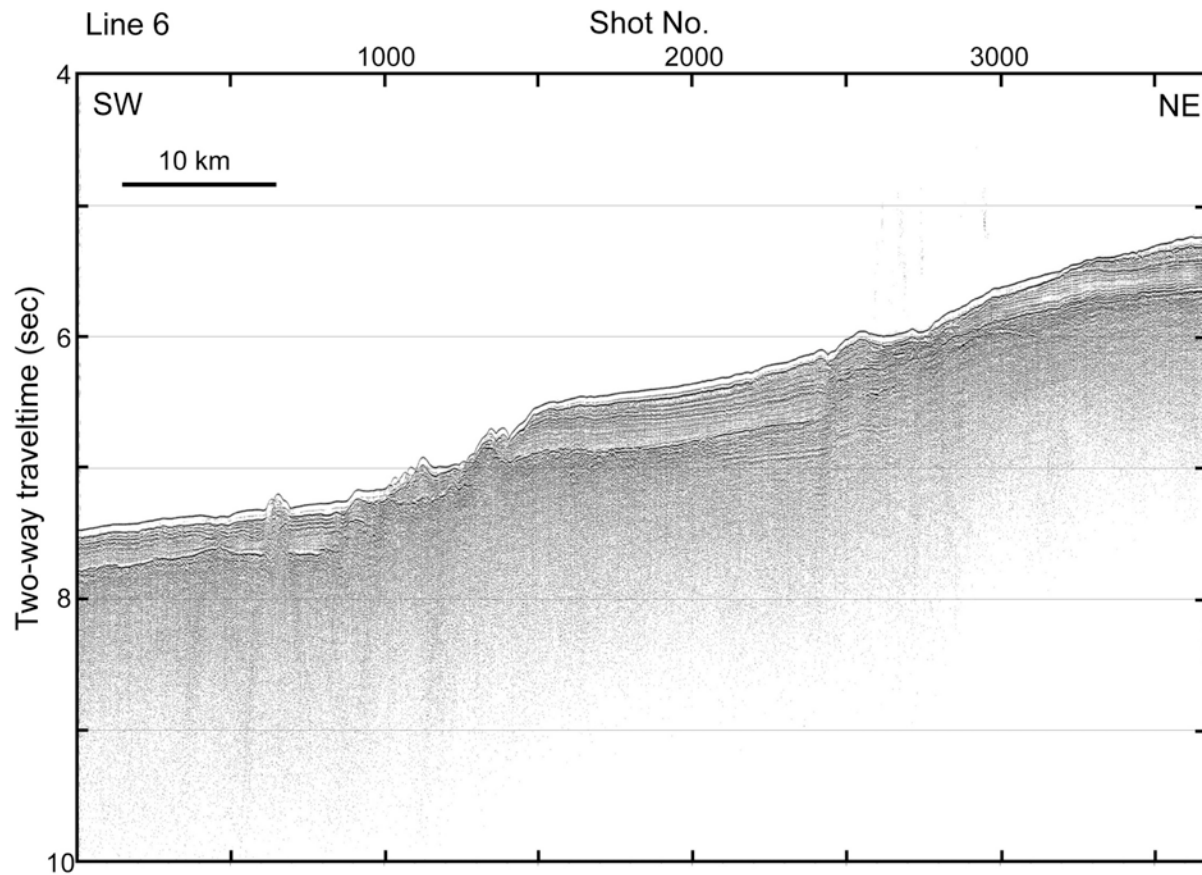


Figure 12. Near-trace plot for seismic Line MGL1004_ML6. The transect crosses from the base of the southwest flank of Tamu Massif to the mid-flank level. It connects with Line MGL1004_ML5.

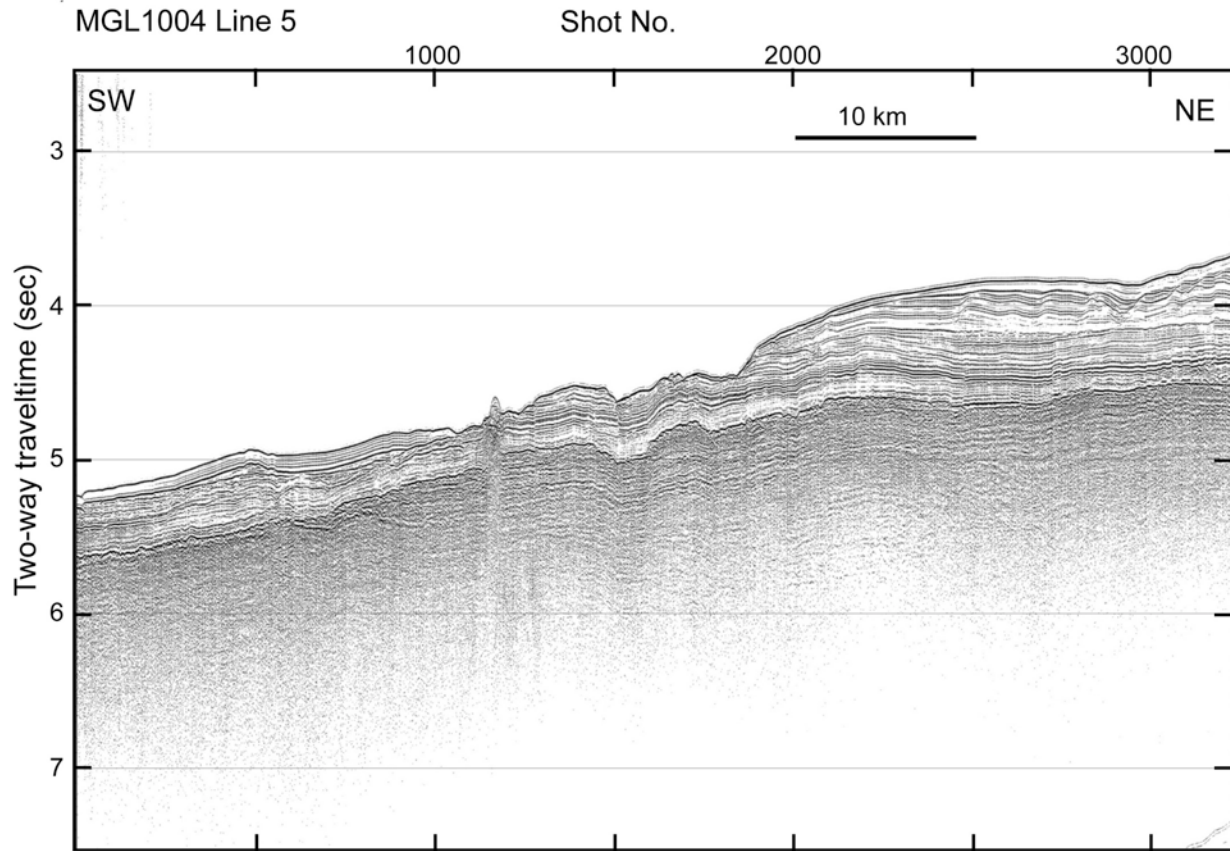


Figure 13. Near trace plot for seismic Line MGL1004_ML5. This seismic line continues the transect up the axis of Tamu Massif. It is contiguous with Lines MGL1004_ML_6 and ML_C.

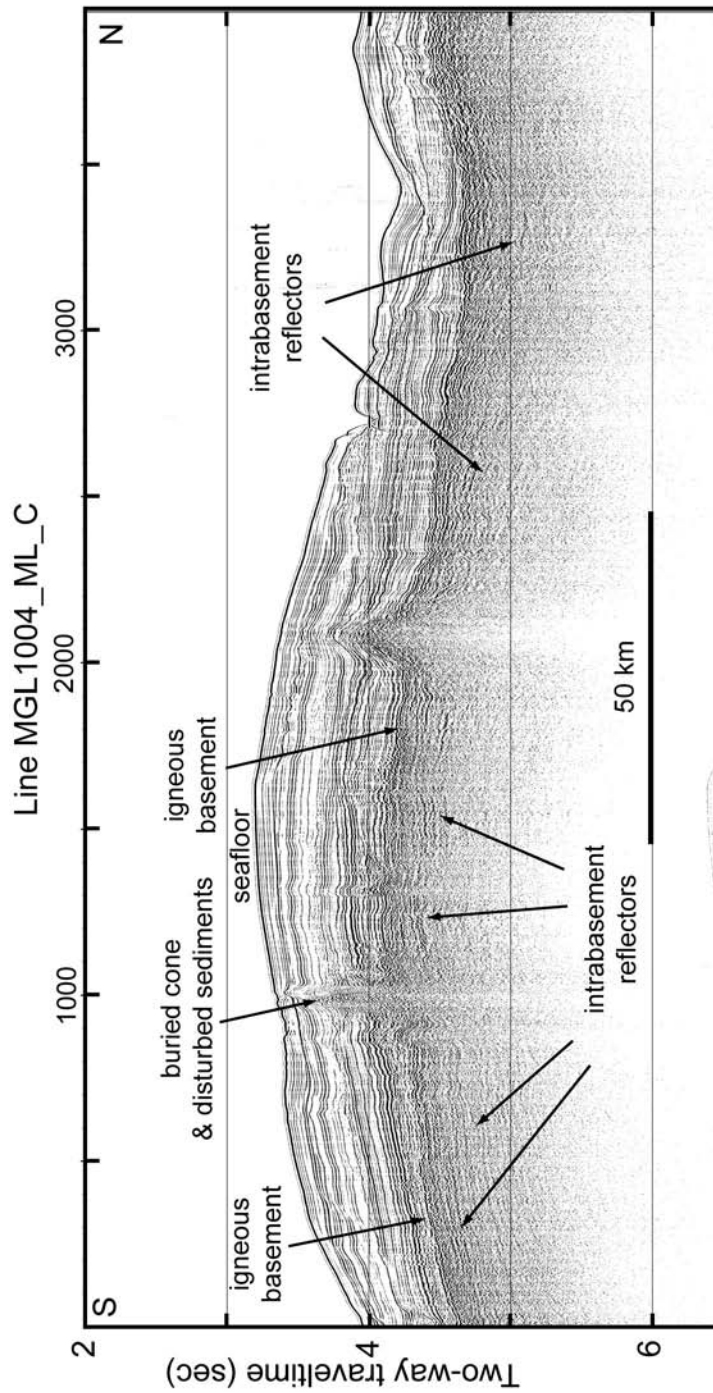


Figure 14. Near trace plot for seismic Line MGL1004_ML_C. This seismic line continues the transect of Lines MGL1004_ML6 and ML5.

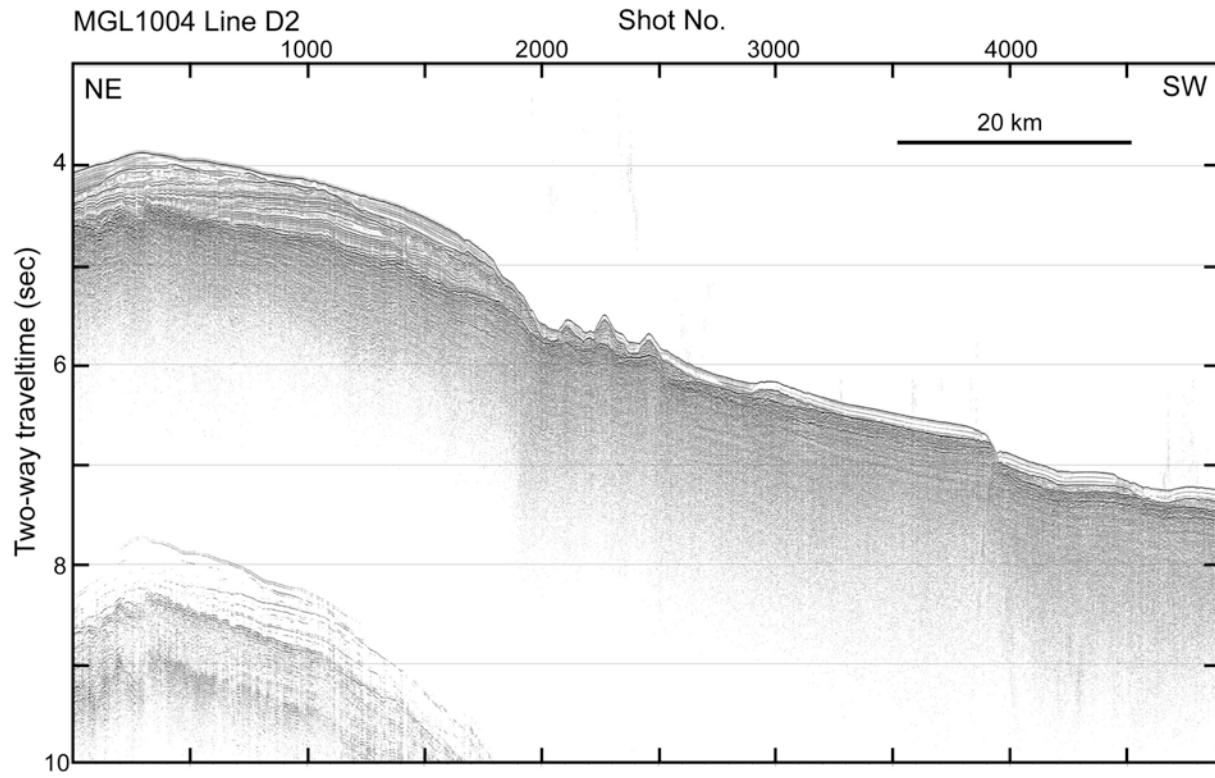


Figure 15. Near trace plot for seismic Line MGL1004_ML_D2. This seismic line runs from the northern summit of Tamu Massif down the western flank.

Ocean Bottom Seismometer Data

Examples of the hydrophone-component data are shown for OBS A4 and A8 (Fig. 16 and 17). The former is located ~70 km from waypoint B and at the depth of ~4600 m. Data with negative offsets correspond to shots above deeper seafloor to the west, and those with positive offsets correspond to shots above shallower seafloor to the east. We expect that crustal thickness gradually increases as bathymetry shallows, and indeed, on the western side (with negative offsets) the convergence of Pg and PmP phases takes place at the source-receiver distance of only ~60 km. On the eastern side, such convergence does not take place even at the distance of 160km, indicating considerable crustal thickening toward the rise axis. Apparent velocity is higher for Pg on the eastern side, but this is mostly due to the changing seafloor depth and does not readily imply faster crustal velocity. OBS A4 data also show a few mid-crustal reflectors, and we need to see if they can be consistently seen by adjacent instruments. If so, we may be able to determine the depths and shapes of these reflectors.

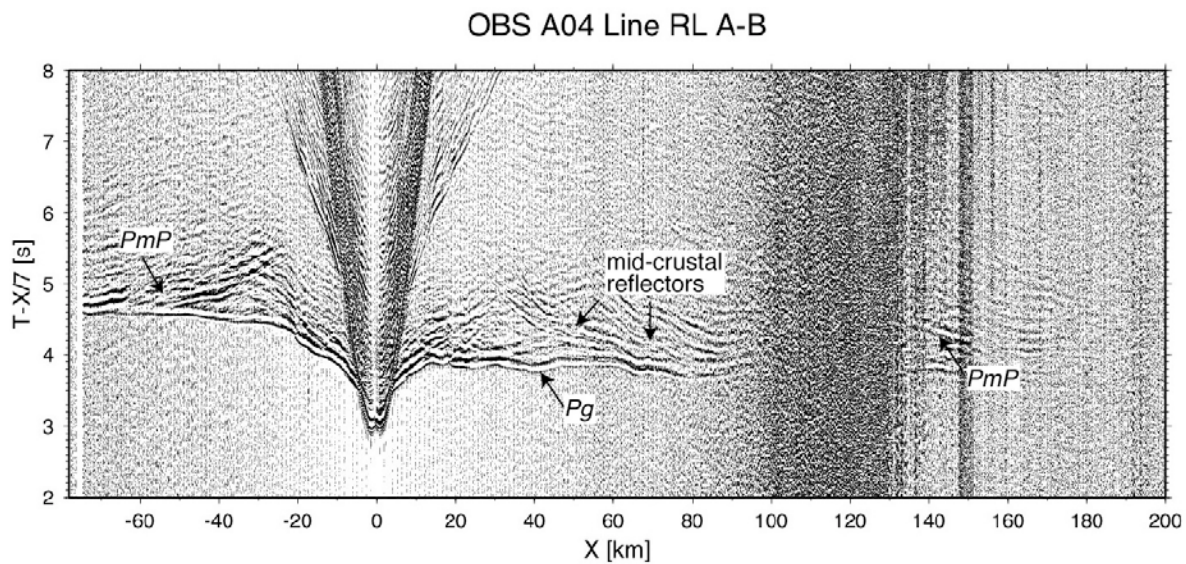


Figure 16. Reduced travel-time plot of hydrophone signals recorded from OBS A4. Shot interval is ~70 sec.

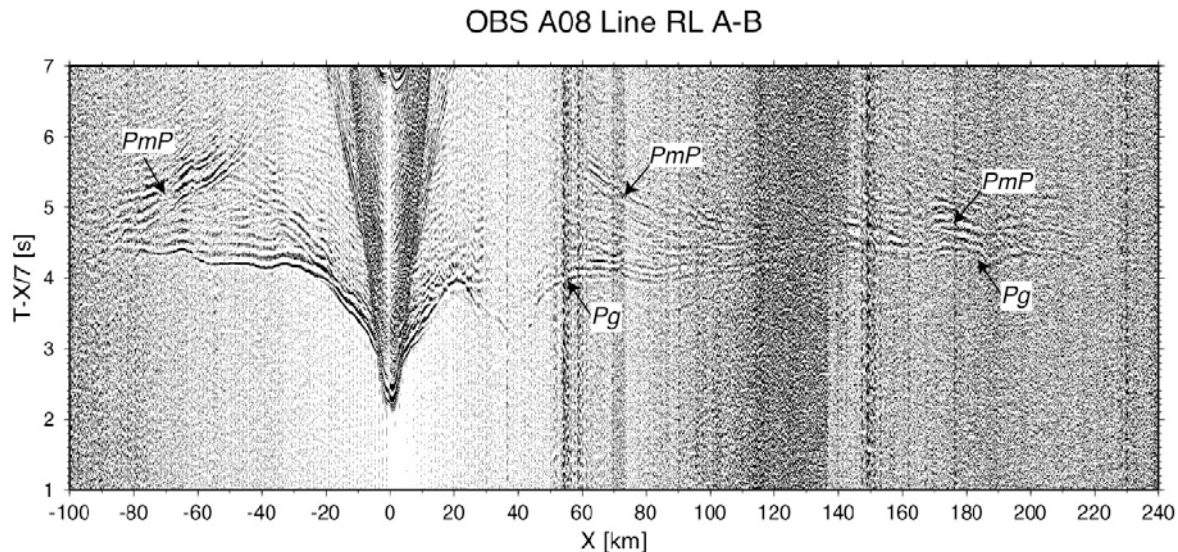


Figure 17. Reduced travel-time plot of hydrophone signals from OBS A8. Shot interval is ~70 sec.

OBS A8 is located ~140 km from the waypoint B or ~70 km from the waypoint E (the crossing point of the two main refraction lines). Instruments like this in the middle of the massif flank are expected to record *PmP* arrivals bounced off the base of the thickest portion of the rise crust, and this instrument shows particular clear *PmP* arrivals from km 60 to km 180. Crustal refraction *Pg* can also be traced up to km 220. The western side of the record (with negative offsets) corresponds to wave propagation through the lower portion of the massif flank, and by comparing the record from OBS A4, the effect of gradual crustal thickening may be recognized. The travel time difference between *Pg* and *PmP* is zero at km -60 for OBS A4, but it grows to 1 s at the same source-receiver distance for OBS A8. This delaying in the *PmP* arrival is a clear sign of thicker crust.

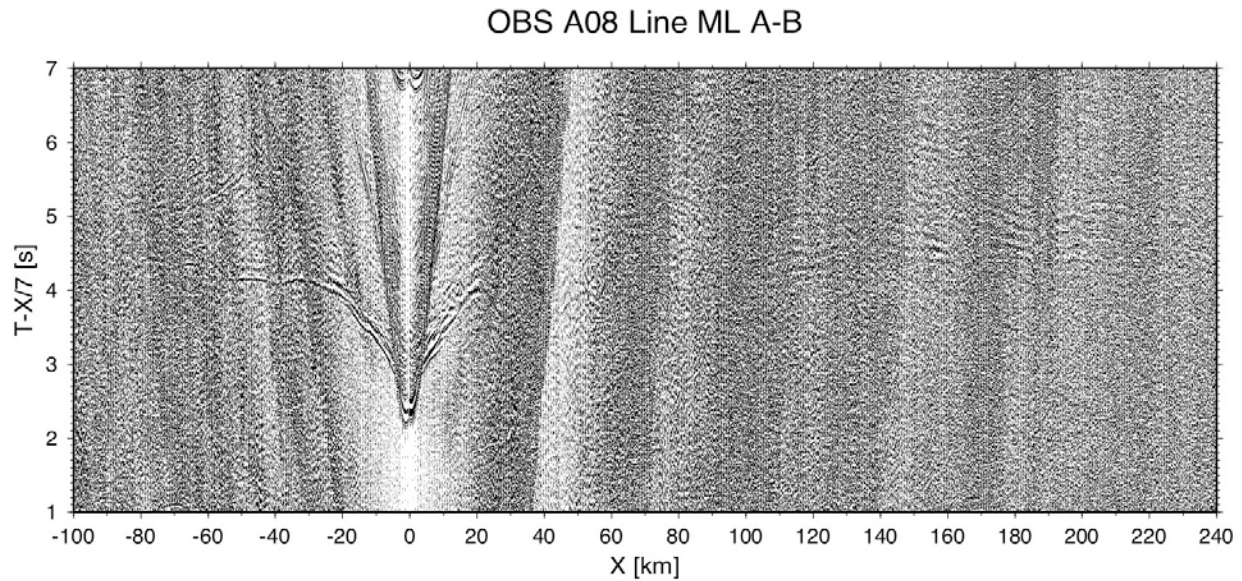


Figure 18. Reduced travel time plot of hydrophone signals from OBS A8 during shooting at ~20 second interval.

For comparison, data from the same instrument (OBS A8) for the same line but with MCS 50-m shot interval (~20 s) are shown above. The effects of previous noise are severe, and it remains to be seen how they can be mitigated by further data processing such as coherency filtering.

Multibeam Bathymetry

The EM122 multibeam echosounder provided detailed bathymetry on a wide swath throughout the cruise, giving insights to geologic processes and structure. For the purposes of discussion, the cruise is divided into three areas: Tamu Massif of Shatsky Rise, the two transits to and from Yokohama, and the transit to the survey area from Honolulu and return.

Tamu Massif. Multibeam data confirm the general shape of this large volcanic edifice, which is mound-like, with slow flank slopes (Fig. 19). The summit of Tamu Massif also displays a rounded, dome-like shape and is the surface of a thick pelagic sediment cap. Multibeam data also show a variety of small geologic features, with some of the more notable being scarps, canyons, sediment slides and erosion, and parasitic volcanic cones.

Scarps have been noted previously (Ito and Clift, 1998; Sager et al., 1999). They typically occur on the middle or lower flanks of Tamu Massif and the sense of movement is the distal side is downdropped. The scarps are typically a few hundred meters in height. Notable scarps occur on the deep flank of the west side of Tamu Massif (Seismic Line ML_A) and on the southeast side at mid-flank level (Seismic Line ML_B). The origins of these scarps is unclear, but Ito and Clift [1998] suggest differential subsidence owing to underplating of the volcano.

Tamu Massif bathymetry displays spectacular evidence of downslope sediment movement. Notable are deep (>100 to several hundred meters), wide (5-10 km) canyons incised into the sediment cover on the upper and lower flanks of the mountain. The largest such features mapped are a series of 2-3 canyons on the west side of Tamu Massif near the summit ridge (Toronto Ridge). Two of these were noted in a previous multibeam survey (Sager et al., 1999), but the new data show that these canyons have other offshoots and that they run down the entire flank to the base of slope. At the base of slope, a broad sediment mound is likely the deposit of sediments that flowed down the canyons. Another nearby canyon runs up the slope a little to the north and appears to connect to sediment failures on the north and east side of Toronto Ridge. Other canyons are seen on the south side of Tamu Massif, including one near ODP Site 1213 that appears to be a major canyon like those on the west side of the mountain. Many smaller canyons appear to cut into the edge of the pelagic cap. In places the cap appears sculpted and eroded with re-entrants that suggest the upper flanks of the cap have failed, causing sediment flows that may have excavated the canyons.

A somewhat surprising feature of Tamu Massif is the large number of small volcanic cones. The largest are ~10-20 km in diameter and the smaller are only a few kilometers across. The greatest abundance of these cones is seen on the south and east flanks of Tamu Massif, including an enigmatic double line of cones that trend SSE from the south flank of the larger edifice. Parasitic cones are not unusual features on large volcanoes, but they typically are found near volcanic rift zones where there is a source of magma. At Tamu Massif they appear more widely distributed, perhaps indicating that the large volcano did not have fixed rift zones.

Honolulu Transit. (Fig. 20) Along the transit tracks to Honolulu, seafloor features related to seafloor spreading and volcanism are seen. In many places along the tracks, angular, linear ridges and troughs are noted, usually with a NW-SE trend. This trend parallels the Hawaiian magnetic lineations (Hilde et al., 1976) and thus these features are probably horsts and grabens formed at the Pacific-Farallon Ridge during the creation of the lithosphere. Such features were once called "abyssal hills" before their tectonic significance was clear. These spreading fabric features are most

notable west 180° in the basin near Shatsky Rise and less so in the shallower abyssal depths close to the Hawaiian Ridge.

Two different kinds of seafloor volcanism were also noted. The bathymetry swath crossed a number of small seamounts en route. Mostly these are isolated, rounded features that indicate a central volcano. They are some of the thousands of such features in the Pacific Basin (Wessel, 2001). In addition, linear volcanic ridges were also noted in several locations. The ship crossed the large Necker Ridge at and a smaller ridge with the same trend a bit farther east. Similar linear ridges were also noted in the vicinity of the Mendocino and Pioneer fracture zones in the area from 167-174° E.

Japan Transit. (Fig. 21) The two trips to Japan gathered paired ingress/egress tracks from Tamu Massif toward Japan along a nearly east-west path at 33.5-34.5°N (northern tracks) and along a SE-NW path from 31-34°N (southern tracks). Both transits cross seamounts of the Geisha group (Sager et al., 1993), with some being large guyots. The northern path crosses the summit of an unnamed guyot at 148°E and the northern flank of Takyo-Daisan Guyot at 145.8°E. The southern path crosses Winterer Guyot and two adjacent smaller seamounts at 148.2°E. Both paths show seafloor spreading fabric lineations in the region from 148°E to the western edge of the survey data. These lineations have a SSW-NNE trend, parallel to the Japanese magnetic lineations (Larson and Chase, 1972; Hilde et al., 1976).

The multibeam bathymetry swaths of the Japan transits also cross an enigmatic feature at 32°N, 152°W. This feature is a rhomboidal hole with two triangular fault blocks. It sits at the location where the Japanese and Hawaiian magnetic lineations intersect west of Shatsky Rise. It thus may have been formed during the tectonic reorganization that began forming Shatsky Rise.

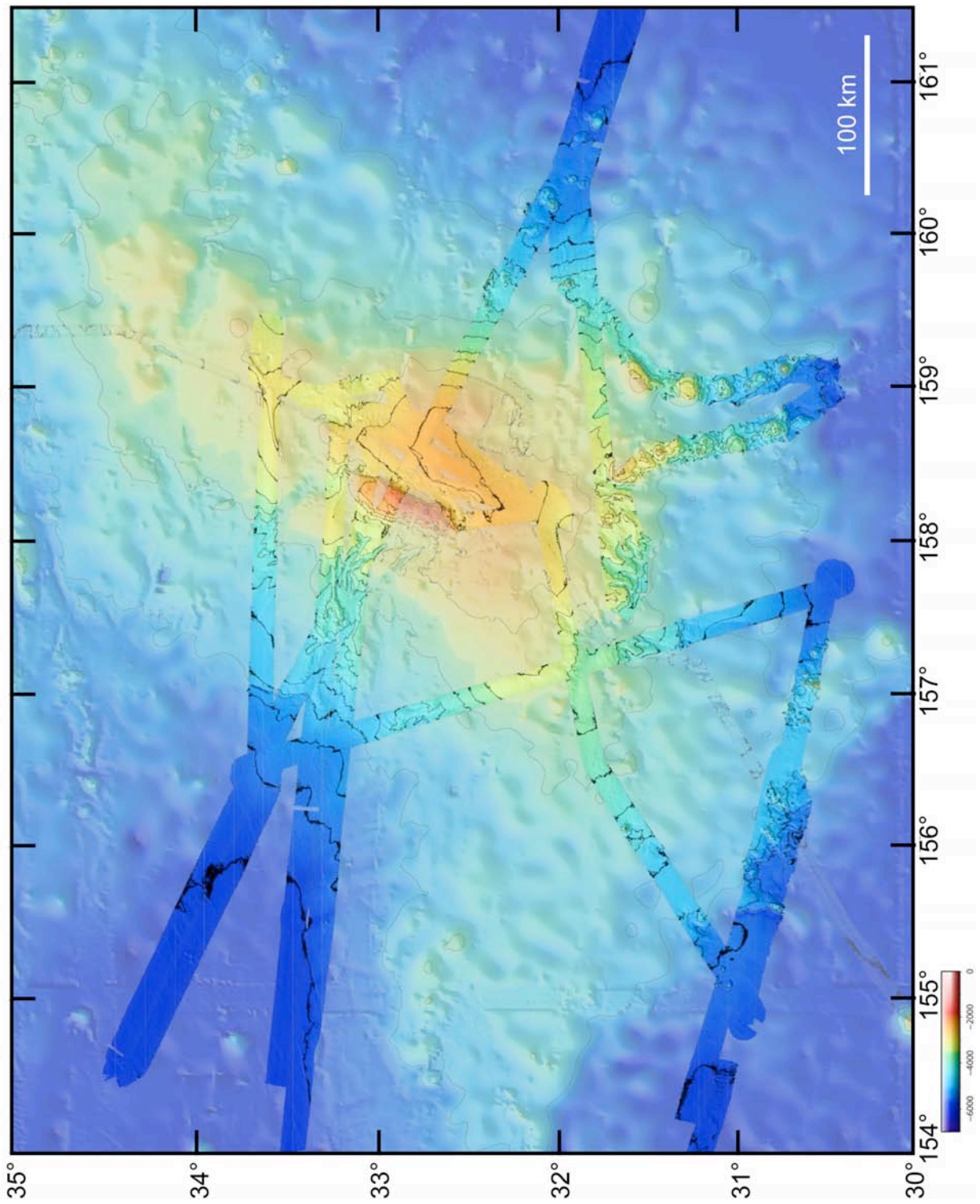


Figure 19. Bathymetry map of Tamu Massif from merged MGL1004 multibeam (bright colors) and satellite altimetry (faded colors) (Smith and Sandwell, 1997) data. Contours at shown at 500-m intervals.

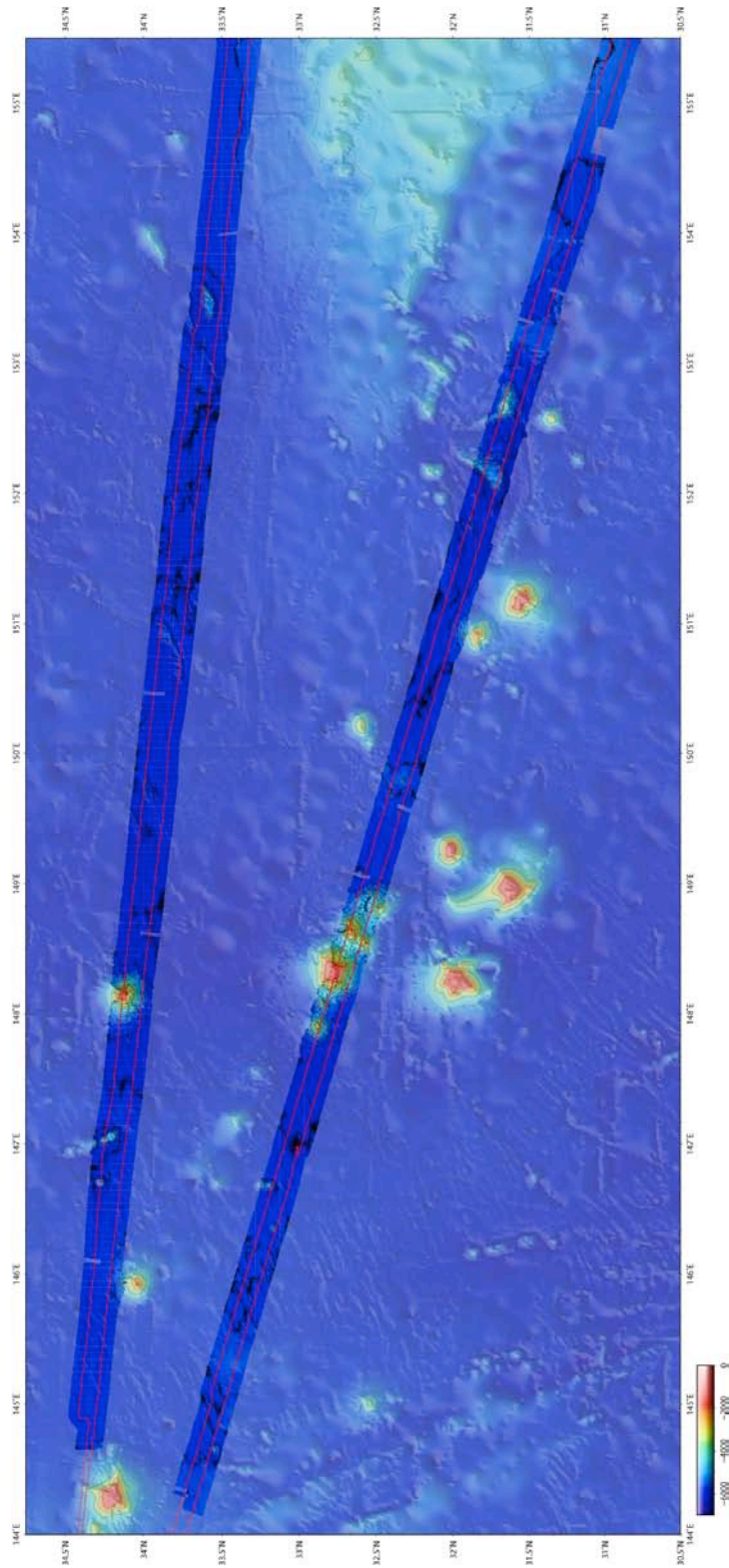


Figure 20. Bathymetry map of the area west of Shatsky Rise covered by the transits to Japan. Bathymetry data are from MGL1004 multibeam data (bright colors) and satellite altimetry (faded colors) (Smith and Sandwell, 1997). Contours are shown at 500-m intervals.

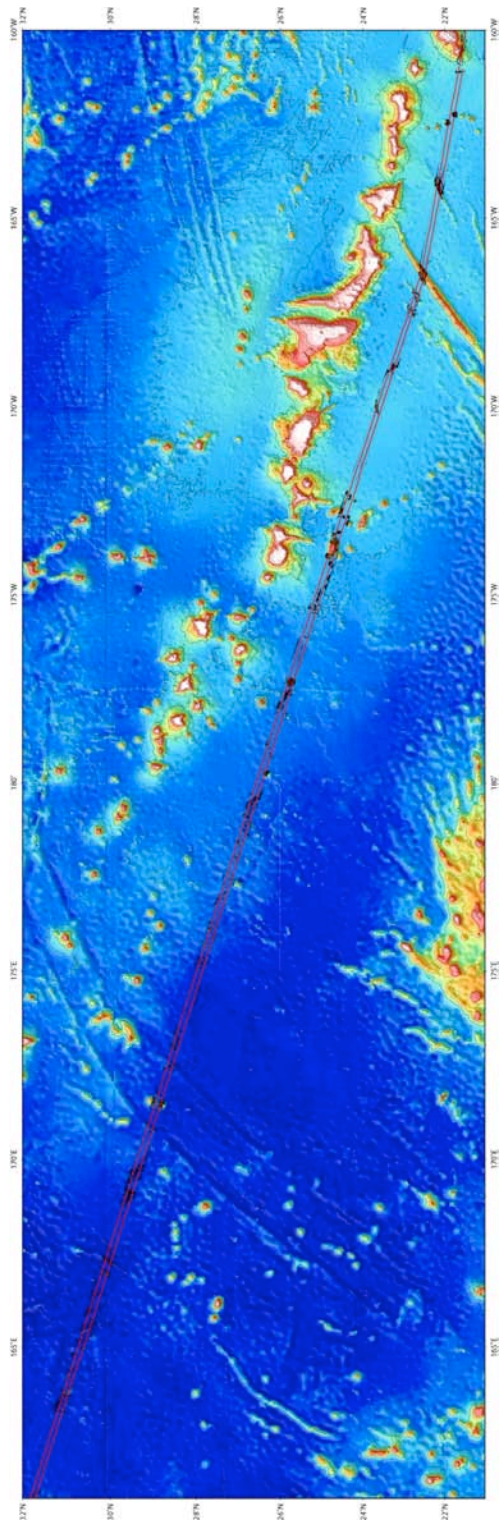


Figure 21. Bathymetry map of the area east of Shatsky Rise covered by the transits to Honolulu. Bathymetry data are from MGL1004 multibeam data (bright colors) and satellite altimetry (faded colors) (Smith and Sandwell, 1997). Contours are shown at 500-m intervals.

Underway Geophysical Data

After merging with navigation data, proton magnetic data were reduced to the total-intensity anomaly, by subtracting the main-field component as predicted by the International Geomagnetic Reference Field (with the 11th generation coefficients). The total-intensity anomaly for most of reflection lines is shown in Fig. 22 (anomaly for line C-D is not shown for the sake of clarity).

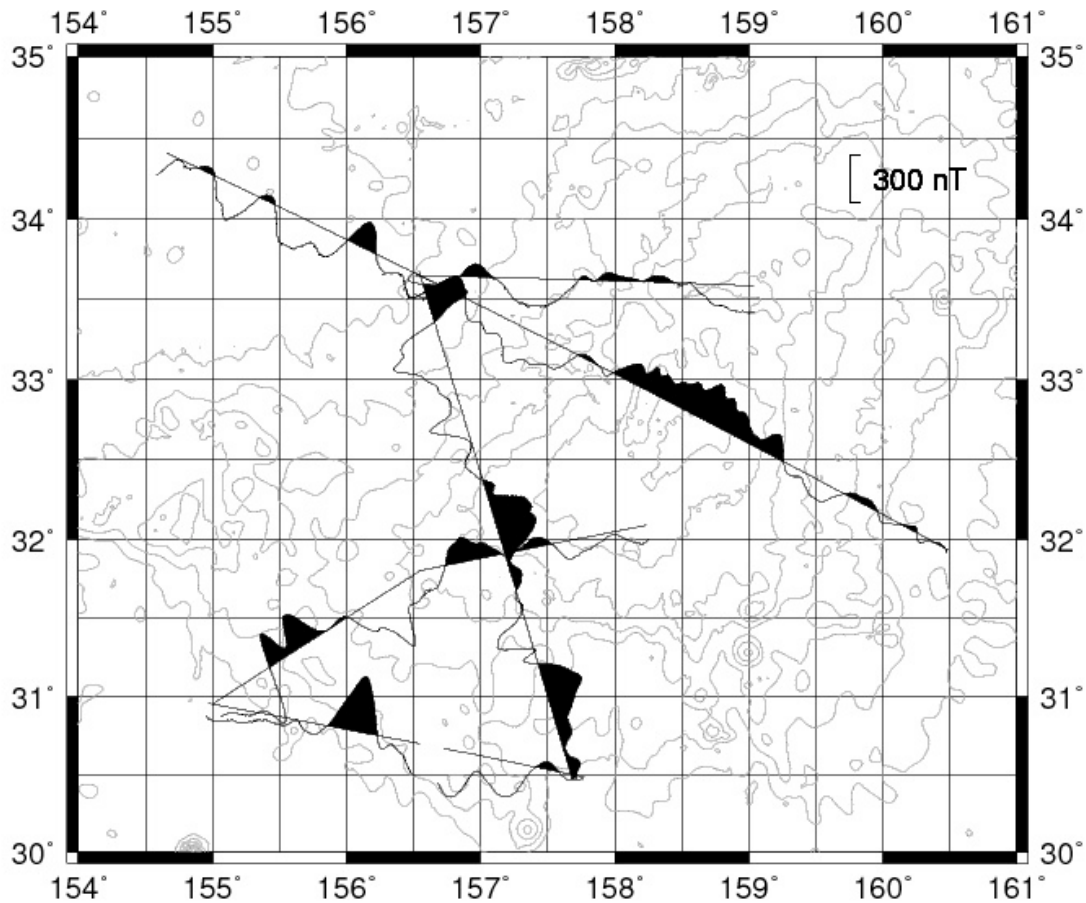


Figure 22. Wiggle plot of magnetic anomalies along MGL1004 ship tracks.

The problem with *Langseth's* magnetic data, which are hard to detect in Fig. 22, is that the proton magnetometer is towed from the ship with an offset of only 150 m. To test the effect of ship's own magnetic field on the towed magnetometer, we conducted a figure-eight operation during the extra multibeam survey we did after the OBS recovery. Data from this operation are shown in Fig. 23.

Figure 8 operation

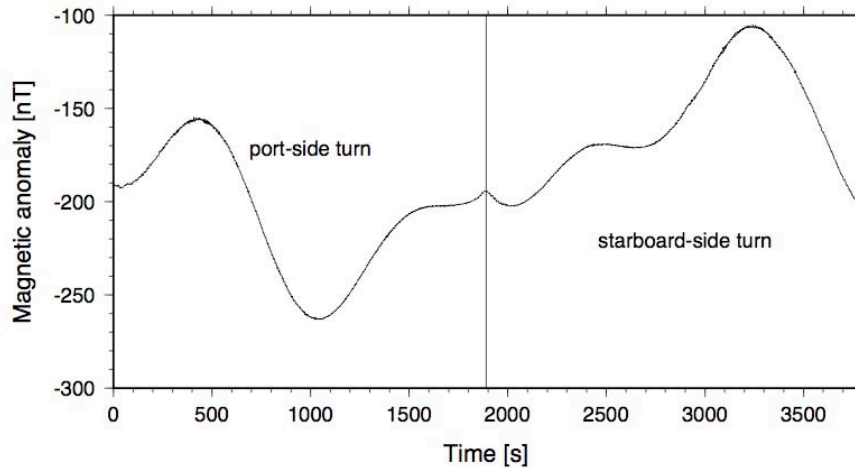


Figure 23. Magnetic anomaly data collected during a “Figure-8” maneuver to calibrate the ship’s effect on magnetic field measurements.

Ship's magnetic field appears to have the amplitude of about ± 50 nT at the location of the magnetometer. Data from the port-side turn are nearly sinusoidal, which is an expected heading dependence, but this sinusoidal behavior was not reproduced during the starboard-side turn. One possible explanation is that the magnetometer was probably on different sides during different turns. We expect it to be on the port side during a port-side turn and vice versa, and ship's magnetic field is unlikely to be symmetrical with respect to ship's major axis. Sager will gather magnetic data from all turns during the survey and try to seek an empirical correction method.

Processed gravity data were not available during the cruise. Pre-cruise and post-cruise gravity ties were made on 17 July 2010 and 14 July 2010, respectively. The ties were made to the J5 gravity station at DeRussey park in Waikiki. The LDEO science officer Anthony Johnson was in charge of post-cruise processing, including drift correction, the Etövös correction, and the calculation of free-air gravity anomaly. *Langseth's* gravity processing is adapted from R/V *Ewing* processing. R/V *Ewing* data was previously tied to the Potsdam system. The *Langseth* processing flow is updated to use the post-Potsdam system.

References

- Anderson, D. L., Lithosphere, asthenosphere, and perisphere, *Rev. Geophys.*, 33, 125-149, 1995.
- Anderson, D. L., The thermal state of the upper mantle; No role for mantle plumes, *Geophys. Res. Lett.*, 27, 3623-3626, doi:10.1029/2000GL011533, 2000.
- Anderson, D. L., T. Tanimoto, and Y.-S. Zhang, Plate tectonics and hotspots: The third dimension, *Science*, 256, 1645-1651, 1992.
- Bell, R. E., and A. B. Watts, Evaluation of the BGM-3 sea gravity meter system onboard *R/V Conrad*, *Geophysics*, 51, 1480-1493, 1986.
- Bercovici, D. and J. Mahoney, Double flood basalts and plume head separation at the 660-kilometer discontinuity, *Science*, 266, 1367-1369, 1994.
- Braun, M. G., G., Hirth, and E. M. Parmentier, The effects of deep damp melting on mantle flow and melt generation beneath mid-ocean ridges, *Earth Planet. Sci. Lett.*, 176, 339-356, 2000.
- Buchanan, S. K., R. A. Scrutton, R. A. Edwards, and R. B. Whitmarsh, Marine magnetic data processing in equatorial regions off Ghana, 125, 123-131, 1996.
- Bullard, E. C., and R. G. Mason, The magnetic field astern of a ship, *Deep-Sea Res.*, 8, 20-27, 1961.
- Coffin, M. F. and O. Eldholm, Large igneous provinces: Crustal structure, dimensions, and external consequences, *Rev. Geophys.*, 32, 1-26, 1994.
- Coffin, M. G., F. A. Frey, P. J. Wallace and shipboard scientific party, Leg 183 summary: Kerguelen-Broken Ridge – a large igneous province, *Proc. ODP, Init. Repts.*, 183, 1-101, 2000.
- Courtillot, V., A. Davaille, J. Besse, and J. Stock, Three distinct types of hotspots in the Earth's mantle, *Earth Planet. Sci. Lett.*, 205, 295-308, 2003.
- Den, N., W. J. Ludwig, S. Murauchi, J. I. Ewing, H. Hotta, N. T. Edgar, T. Yoshii, T. Asanuma, K. Hagiwara, T. Sato, and S. Ando, S., Seismic-refraction measurements in the northwest Pacific Basin. *J. Geophys. Res.*, 74, 1421-1434, 1969.
- Duncan, R. A., and M. A. Richards, Hotspots, mantle plumes, flood basalts, and true polar wander, *Rev. Geophys.*, 29, 31-50, 1991.
- Eldholm, O., and M. F. Coffin, Large igneous provinces and plate tectonics, in *The history and dynamics of global plate motions*, *Geophys. Monogr. Ser. 121*, M. A. Richards, R. G. Gordon, and R. D. van der Hilst (eds.), AGU, Washington, DC, 309-326, 2000.
- Expedition 324 Scientists, Integrated Ocean Drilling Program Expedition 324 Preliminary Report, IODP-MI, 1-115, 2010. http://publications.iodp.org/preliminary_report/324/index.html
- Ewing, M., T. Saito, J. I. Ewing, and L. H. Burckle, 1966. Lower Cretaceous sediments from the Northwest Pacific. *Science*, 152, 751-755, 1966.
- Farnetani, C. G., and H. Samuel, Beyond the thermal plume paradigm, *Geophys. Res. Lett.*, 32, 1-4, L07311, doi:10.1029/2005GL022360, 2005.
- Fischer, A.G., B. C. Heezen, et al., *Init. Repts. DSDP*, v. 6, Washington, DC (U.S. Govt. Printing Office, 1971).
- Foulger, G. R., The “plate” model for the genesis of melting anomalies, in *Plates, Plumes, and Planetary Processes*, G. R. Foulger and D. H. Jurdy (eds.), Spec. Pap. 430, GSA, Boulder, CO, p. 1-28, doi:10.1130/2007.2439(1), 2007.
- Foulger, G. R., and Natland, J. H., Is “hotspot” volcanism a consequence of plate tectonics? *Science*, 300, 921-922.
- Gettrust, J.F., K. Furukawa, and L. W. Kroenke, Crustal structure of the Shatsky Rise from seismic refraction measurements. *J. Geophys. Res.*, 85, 5411-5415, 1980.
- Gomer, B.M., and E.A. Okal, Multiple-ScS probing of the Ontong-Java Plateau, *Phys. Earth Planet. Inter.*, 138, 317-331, 2003.
- Gradstein, F.M., J. G. Ogg, J.G., and A. Smith, *A Geologic Time Scale 2004*, Cambridge Univ. Press, Cambridge, UK, 2004.

- Hilde, T.W.C., N. Isezaki, and J. M. Wageman, J.M., Mesozoic sea-floor spreading in the North Pacific. In *The Geophysics of the Pacific Ocean Basin and its Margins*. Geophys. Monogr. Ser., 19, G. P. Woollard, G. H. Sutton, M. H. Manghnani, and R. Moberly, R. (Eds.), AGU, Washington, DC, 205-226, 1976.
- Ito, G., and P. Clift, Subsidence and growth of Pacific Cretaceous plateaus, *Earth Planet. Sci. Lett.*, 161, 85-100, 1998.
- Ito, G., Y. Shen, G. Hirth, and G. J. Wolfe, Mantle flow, melting, and dehydration of the Iceland mantle plume, *Earth Planet. Sci. Lett.*, 165, 81-96, 1999.
- Janney, P. E., J. D. MacDougall, J. H. Natland, and M. A. Lynch, Geochemical evidence from the Pukapuka volcanic ridge system for a shallow enriched mantle domain beneath the South Pacific Superswell, *Earth Planet. Sci. Lett.*, 181, 47-60, 2000.
- Johnson, S.T., and D. J. Thorkelson, Continental flood basalts: episodic magmatism above long-lived hotspots, *Earth Planet. Sci. Lett.*, 175, 247-256, 2000.
- Kelemen, P. B., and W. S. Holbrook, Origin of thick, high-velocity igneous crust along the U.S. East Coast Margin, *J. Geophys. Res.*, 100, 10,077-10,094, 1995.
- Kellogg, J. N., B. S. Wedgworth, and J. Freymueller, Isostatic compensation and conduit structures of western Pacific seamounts: Results of three-dimensional gravity modeling, in *Seamounts, islands, and atolls*, B. H. Keating, P. Fryer, R. Batiza, and G. W. Boehlert (eds.), Geophys. Monogr. Ser. 43, AGU, Washington, DC, pp. 85-96, 1987.
- Kennett, B.L.N., and S. Widiyantoro, A low seismic wavespeed anomaly beneath northwestern India: a seismic signature of the Deccan plume? *Earth Planet. Sci. Lett.*, 165, 145-155, 1999.
- Koppers, A. A. P., H. Staudigel, M. S. Pringle, and J. R. Wijbrans, Short-lived and discontinuous intraplate volcanism in the South Pacific: Hot spots or extensional volcanism? *Geochem., Geophys., Geosys.*, 4, 1089, doi:10.1029/2003GC000533, 2003.
- Korenaga, J., Comprehensive analysis of marine magnetic vector anomalies, *J. Geophys. Res.*, 365-378, 1995.
- Korenaga, J., Why did not the Ontong Java Plateau form subaerially?, *Earth. Planet. Sci. Lett.*, 234, 385-399, 2005.
- Korenaga, J., P. B. Kelemen, and W. S. Holbrook, Methods for resolving the origin of large igneous provinces from crustal seismology, *J. Geophys. Res.*, 107(B9), 2178, doi:10.1029/2001JB001030, 2002.
- Kroenke, L. W., P. Wessel, and A. Sterling, Motion of the Ontong Java Plateau in the hot-spot frame of reference: 122 Ma-present, in *Origin and evolution of Ontong Java Plateau*, J. G. Fitton, J. J. Mahoney, P. J. Wallace, and A. D. Saunders (Eds.), Geological Society, London, UK, 8-20, 2004.
- Larson, R.L., and C. G. Chase, Late Mesozoic evolution of the western Pacific Ocean, *Geol. Soc. Am. Bull.*, 83, 3627-3644, 1972.
- Larson, R. L., M. B. Steiner, E. Erba, and Y. Lancelot, Paleolatitudes and tectonic reconstructions of the oldest portion of the Pacific plate: A comparative study, *Proc. ODP, Sci. Res.*, 129, 615-631, 1992.
- Lin, S.-C., and P. E. van Keken, Dynamics of thermochemical plumes, 1, Plume formation and entrainment of a dense layer, *Geochem. Geophys. Geosys.*, 7, Q02006, 1-21, doi:10.1029/2005GC001071, 2006a.
- Lin, S.-C., and P. E. van Keken, Dynamics of thermochemical plumes: 2. Complexity of plume structures and its implications for mapping mantle plumes, *Geochem. Geophys. Geosys.*, 7, 1-18, Q03003, doi:10.1029/2005GC001072, 2006b.
- Lithgow-Bertelloni, C., and M. A. Richards, 1998. The dynamics of Cenozoic and Mesozoic plate motions, *Rev. Geophys.*, 36, 27-78, 1998.
- Ludwig, W.J., and R. E. Houtz, *Isopach Map of Sediments in the Pacific Ocean Basin and Marginal Sea Basins*. AAPG Map Ser., 647, 1979.

- Mahoney, J. J., R.A. Duncan, M.L.G. Tejada, and W.W. Sager, Jurassic-Cretaceous boundary age and mid-ocean-ridge-type mantle source for Shatsky Rise, *Geology*, 33, 185-188, 2005.
- Mahoney, J. J., J. G. Fitton, P. J. Wallace, and shipboard scientific party, Leg 192 summary, *Proc. ODP, Init. Repts.*, 192, 1-75, 2001.
- Mahoney, J. J., M. Storey, R. A. Duncan, K. J. Spencer, and M. Pringle, Geochemistry and age of the Ontong Java Plateau, in *The Mesozoic Pacific: Geology, Tectonics, and Volcanism*, M. S. Pringle, W. W. Sager, W. V. Sliter, and S. Stein (eds.), *Geophys. Monogr. Ser. 77*, AGU, Washington, DC, pp. 233-261, 1993.
- McNutt, M. K., and K. M. Fisher, The South Pacific Superswell, in *Seamounts, Islands, and Atolls*, *Geophys. Monogr. 43*, B. H. Keating, P. Fryer, R. Batiza and G. W. Boehlert, (eds.), AGU, Washington, D.C., 25-34, 1987.
- McNutt, M. K., E. L. Winterer, W. W. Sager, J. H. Natland, and G. Ito, The Darwin Rise: A Cretaceous Superswell?, *Geophys. Res. Lett.*, 17, 1101-1104, 1990.
- Nakanishi, M., W. W. Sager, and A. Klaus, Magnetic lineations within Shatsky Rise, northwest Pacific Ocean: Implications for hot spot-triple junction interaction and oceanic plateau formation, *J. Geophys. Res.*, 104, 7539-7556, 1999.
- Neal, C. R., M. F. Coffin, E. Eldholm, C. Farnetani, G. Fitton, S. Ingle, N. Ohkouchi, M. Teichow, S. Self, Y. Tatsumi, L. Vanderkluysen, Scientific drilling of large igneous provinces, *Scientific Drilling*, in press, 2008.
- Neprochnov, Y.P., L. R. Merklin, and L. M. Khankishiyeva, Distribution map of the sedimentary cover on the Shatsky Rise. *Dokl. Akad. Nauk SSSR*, 277, 1204-1207, 1984.
- Pringle, M.S., and G. B. Dalrymple, G.B., Geochronological constraints on possible hotspot origin for Hess Rise and the Wentworth seamount chain, in *The Mesozoic Pacific: Geology, tectonics, and volcanism*, *Geophysical Monograph 77*, M. S. Pringle, W. W. Sager, W. V. Sliter, and S. Stein, (Eds), American Geophysical Union Geophysical Union, Washington, DC, p. 263-277, 1993.
- Richards, M. A., R. A. Duncan, and V. E. Courtillot, Flood basalts and hot-spot tracks: Plume heads and tails, *Science*, 246, 103-107, 1989.
- Richardson, W.P., E.A. Okal, and S. Van der Lee, Rayleigh-wave tomography of the Ontong-Java Plateau, *Phys. Earth Planet. Inter.*, 118, 29-51, 2000.
- Royer, J.-Y., J. W. Peirce, and J. K. Weissel, Tectonic constraints on the hot-spot formation of Ninetyeast Ridge, *Proc. ODP, Sci. Res.*, 121, 763-776, 1991.
- Ryan, M. P., The physical nature of the Icelandic magma transport system, in *Magma Transport and Storage*, M. P. Ryan (Ed.), John Wiley and Sons, Chichester, UK, pp. 175-224, 1990.
- Sager, W. W., What built Shatsky Rise, a plume head or ridge processes, in *Plates, Plumes, and Paradigms*, Special Paper 388, G. R. Foulger, J. H. Natland, D. C. Presnall, and D. L. Anderson (Eds.), *Geol. Soc. Amer.*, Boulder, CO, pp. 721-733, doi:10.1130.2005.2388(41), 2005.
- Sager, W. W., and H.-C. Han, Rapid formation of Shatsky Rise oceanic plateau inferred from its magnetic anomaly, *Nature*, 364, 610-613, 1993.
- Sager, W. W., D. W. Handschumacher, T. W. C. Hilde, and D. R. Bracey, Tectonic evolution of the northern Pacific plate and Pacific-Farallon-Izanagi triple junction in the Late Jurassic and Early Cretaceous (M21-M10), *Tectonophysics*, 155, 345-364, 1988.
- Sager, W. W., J. Kim, A. Klaus, M. Nakanishi, and L. M. Khankishieva, Bathymetry of Shatsky Rise, Northwest Pacific Ocean: Implications for Ocean Plateau Development at a Triple Junction, *J. Geophys. Res.*, 104, 7557-7576, 1999.
- Sallares, V., P. Charvis, E. R. Flueh, and J. Bialas, Seismic structure of Cocos and Malpelo volcanic ridges and implications for hotspot interaction, *J. Geophys. Res.*, 108, 2564, doi:10.1029/2003JB002431, 2003.
- Sallares, V., P. Charvis, E. R. Flueh, J. Bialas, and The SALIERI Scientific Party, Seismic structure of the Carnegie ridge and the nature of the Galapagos hotspot, *Geophys. J. Int.*, 161, 763-788, 2005.

- Sandwell, D. T., and W. H. F. Smith, Global marine gravity from retracked Geosat and ERS-1 altimetry: Ridge segmentation versus spreading rate, *J. Geophys. Res.*, 114, B01411, doi:10.1029/2008JB006008, 2009.
- Shipboard Scientific Party, Leg 198 summary. In Bralower, T.J., Premoli Silva, I., Malone, M.J., et al., *Proc. ODP, Init. Repts.*, v. 198, Ocean Drilling Program, College Station, TX, 1–148, 2002a.
- Shipboard Scientific Party, Site 1213. In Bralower, T.J., Premoli Silva, I., Malone, M.J., et al., *Proc. ODP, Init. Repts.*, v. 198, Ocean Drilling Program, College Station, TX, 1–110, 2002b.
- Sliter, W.V., and G. R. Brown, Shatsky Rise: seismic stratigraphy and sedimentary record of Pacific paleoceanography since the Early Cretaceous, In *Proc. ODP, Sci. Results*, v. 132, Natland, J.H., M. A. Storms, et al. (Eds.), Ocean Drilling Program, College Station, TX, 3–13, 1993.
- Smith, A. D., and C. Lewis, The planet beyond the plume hypothesis, *Earth Sci. Rev.*, 48, 135-182, 1999.
- Smith, W. H. F., and D. T. Sandwell, Global seafloor topography from satellite altimetry and ship depth soundings. *Science*, 277, 1956–1962, 1997.
- Stein, C. A., and D. Abbott, Heat flow constraints on the South Pacific Superswell, *J. Geophys. Res.*, 96, 16,083-16,100, 1991.
- Stein, M., and A. W. Hofmann, Mantle plumes and episodic crustal growth. *Nature*, 372, 63–68, 1994.
- Tarduno, J. A., W. V. Sliter, L. W. Kroenke, M. Leckie, J. J. Mahoney, R. J. Musgrave, M. Storey, and E. L. Winterer, Rapid formation of the Ontong Java Plateau by Aptian mantle plume volcanism, *Science*, 254, 399-403, 1991.
- Tatsumi, Y., H. Shinjoe, H. Ishizuka, W. W. Sager, and A. Klaus, Geochemical evidence for a mid-Cretaceous superplume, *Geology*, 26, 151-154, 1998.
- Taylor, B., The single largest oceanic plateau: Ontong Java-Manihiki-Hikurangi, *Earth Planet. Sci. Lett.*, 241, 372-380, 2006.
- Tominaga, M., W. W. Sager, and J. E. T. Channell, Paleomagnetism of the igneous section, Hole 1213B, Shatsky Rise. In *Proc. ODP., Sci. Results*, v. 198, T. J. Bralower, I. Premoli Silva, and M. J. Malone, (Eds.), Ocean Drilling Program, College Station, TX, 1–15, 2005.
- VanDecar, J. C., D. E. James, and M. Assumpcao, Seismic evidence for a fossil mantle plume beneath South America and implications for plate driving forces, *Nature*, 378, 25-31, 1995.
- Vincenty, T., Direct and inverse solutions of geodesics on the ellipsoid with application of nested equations, *Surv. Rev.*, 12, 88-93, 1975.
- Wessel, P., Global distribution of seamounts inferred from gridded Geosat/ERS-1 altimetry, *J. Geophys. Res.*, 106, 19,431-19,441, 2001.
- Zucca, J. J., D. P. Hill, and R. L. Kovach, Crustal structure of Mauna Loa volcano, Hawaii, from seismic refraction and gravity data, *Bull. Seis. Soc. Amer.*, 72, 1535-1550, 1982.

Appendices

Data List

Navigation:

- fserve/MGL1004/raw/serial/posmv/* (2.5 GB; POS/MV position and orientation data) [Y, T]
- fserve/MGL1004/raw/serial/cnav/* (2GB; CNAV GPS receiver data) [Y, T]
- fserve/MGL1004/raw/serial/seapth/* (1.9GB; Seapath 200 navigation data) [Y, T]

MCS data:

- fserve/segd/MGL1004/* (670GB; raw MCS data in SEG D format) [Y, T]
- TAMU's linux:/media/usbdisk3/mgl1004geom/* (956MB; geometry) [Y, T]
- TAMU's linux:/media/usbdisk3/promax/* (292GB; ProMAX files) [Y, T]
- fserve/processed/shotlogs/* (11MB; shot information) [Y, T]

OBS data:

- fserve/public/SEG Y/* (298GB; raw OBS data in SEG Y format) [Y]
- fserve/processed/obsip_shotlogs/* (5MB; shot information for OBS) [Y]
- fserve/MGL1004/raw/serial/shot1/* (3MG; original shot data) [Y]

Multibeam:

- fserve/MGL1004/raw/multibeam/* (34GB; raw EM122 data) [T]
- fserve/MGL1004/docs/MGL1004_Expendable_Drops.xls [T]
- fserve/MGL1004/raw/XBT/* (4MB; raw XBT data) [T]
- fserve/MGL1004/processed/svp/* (2MB; sound velocity profiles) [T]
- fserve/MGL1004/raw/serial/bath02/* (16MB; EM122 centerbeam data) [Y, T]
- fserve/MGL1004/docs/map/data_produc s/* (4GB; GMT grid files) [Y, T]

Underway geophysics:

- fserve/MGL1004/raw/serial/bath01/* (35MB; Furuno FE700 echosounder data) [Y, T]
- fserve/MGL1004/raw/serial/mag01/* (165MB; Geometrics 882 magnetometer data) [Y, T]
- fserve/MGL1004/processed/maggie_nav/* (138MB; magnetic data merged with navigation) [Y, T]
- fserve/MGL1004/raw/serial/vc01/* (186MB; Bell Aerospace BGM-3 gravimeter) [Y, T]
- fserve/MGL1004/raw/knudsen/* (8.3GB; Knudsen 3.5 kHz data) [Y, T]
- fserve/MGL1004/public/PI-Data/* (750MB; fluxgate magnetometer data) [Y]

Logs:

- fserve/MGL1004/docs/elog/* (E-log) [Y, T]
- fserve/MGL1004/docs/Nav_Logs/* (seismic navigation logs) [Y, T]
- fserve/MGL1004/focs/Observer_Logs/* (seismic acquisition logs) [Y, T]
- fserve/MGL1004/docs/reports/* (30 min log, data reports, etc) [Y,T]

Other useful files:

- fserve/MGL1004/public/formats/* (65KB; data formats for serial data) [Y, T]
- fserve/MGL1004/docs/gravity_tie/* (16MB; gravity tie information) [Y, T]
- fserve/MGL1004/docs/offsets/* (3.5MB; offset information for MCS survey) [Y, T]
- fserve/MGL1004/docs/Operatioins/Daily_Reports/* (16MB; daily reports from Tech-in-charge) [Y, T]
- fserve/MGL1004/docs/map/items_of_interest/* (760MB; plots of interesting bathymetric features) [Y, T]
- fserve/MGL1004/public/ProMAX_plots/* (7.8GB; processed MCS data image) [Y, T]

*Y=Yale, T=TAMU

MCS Logs

LINE	LENGTH (KM)	LOG FGSP	LOG LGSP	PROC FGSP	PROC LGSP	FIRST TAPE	LAST TAPE	FIRST CDP*	LAST CDP	START DAY	END DAY
ML_A	413.9	1008	9287	1008	9287	4	12	519	67203	223	225
ML_B	372.6	916	8368	917	8368	13	18	519	60594	225	227
ML_7&7R	274.1	807	6286	830	6286	19	25	519	44654	225	235
ML_7		807	3374	807	3249	19	21			225	226
ML_7R		3194	6286	3250	6286	1023	1025			233	235
ML_6	179.7	1001	4501	910	4501	1026	1028	520	29738	236	237
ML_5	158.9	1005	4247	1005	4184	1029	1031	520	26416	237	237
ML_C&CR	195.0	887	4766	860	4766	1032	1035	520	32179	238	239
ML_C		887	1625	860	1550	1032	1032			238	238
ML_CR		1550	4766	1551	4766	1033	1035			238	239
ML_D2	234.7	1001	5695	1001	5695	1036	1039	520	38534	239	240
ML_B2	193.4	1001	4865	1001	4865	1040	1043	520	31924	240	241
Total	2022.1										

*Note: First CDP number changed due to change in recorded distance between source and first group from 179 to 167. The correct source-receiver offset is 198 m.

The CDP at the first shot point is set to CDP 1000.

MCS Processing Parameters Outline

Data Storage Locations:

Ship Server:

Main Directory: smb://fserve/cruisedata/MGL1004

Navigation Files (p190): smb://fserve/cruisedata/MGL1004/processed/sprint

SEGD Files: /remote/mgl1004-segd/MGL1004

Python scripts: smb://fserve/cruisedata/MGL1004/public/seisproc

TAMU Computer:

Geometry: /media/usbdisk3/mgl1004geom

ProMAX: /media/usbdisk3/promax

Creating Near Real-Time Plots with ProMAX and GMT

1. Copy SEG-D tapes from ship server to local working directory
 - a. Can run this every few hours as each tape is completed or at the end of the line.
2. Load near trace from each shot (chan 468)
 - a. Note: ProMAX can only handle one tape's worth of shots at a time. So you need to set up multiple SEG-D Input/Disk Data Output pairs for each tape. Then create a flow to combine all of the tapes into one set of gathers.
 - b. SEG-D Input
 - i. Browse for tape folder and select shots

- ii. Primary selection choice: Input ALL
 - iii. Secondary selection choice: Channel
 - iv. Channel selection mode: Include
 - 1. Specify CHANNEL input list: 468/
 - 2. Streamline CHANNEL selection?: No
 - c. Disk Data Output
 - i. File name: nt_tape1
- 3. Combine tapes into one line (sample for combining two tapes into one line)
 - a. Disk Data Input: nt_tape1
 - i. Trace read option: Get All
 - b. Disk Data Output: nt_line_D2
 - i. New, or Existing, File: New
 - c. Disk Data Input: nt_tape2
 - i. Trace read option: Get All
 - d. Disk Data Output: nt_line_D2
 - i. New, or Existing, File: Append
- 4. Output SEG Y Near Trace File
 - a. Disk Data Input: nt_line_D2
 - i. Trace read option: Get All
 - b. Bandpass Filter
 - i. 4-8-60-80
 - c. SEG Y Output
 - i. Type of SEG Y: Standard
 - ii. Type of storage to use: Disk Image
 - iii. Desired trace format: IEEE Real
- 5. GMT File to Create a Wiggle Seismic Plot: plotseg y.gmt
 - a. Use gmtset PAPER_MEDIA=Custom_1728x3650 for the large HP designjet 800 ps plotter in the R/V Marcus Langseth science lab (units: pixels)
- 6. GMT File to Create a Color Gridded Seismic Plot: seg y2grd.gmt
 - a. Color file: seis.cpt

Trace Editing Procedure:

Load first gather from each tape and last gather from last tape and view in Trace Display

Fill out trace edit log: write down bad channel numbers.

Create common channel gathers to see if the bad channels should be deleted completely from the line. Small random bursts can be removed with Spike & Noise Burst Removal.

Flow: SEG D Input

SEG D input - select first and last shot gathers

Bandpass filter - 4-8-60-80

Trace Display - review gathers and header information

P190 Navigation Procedure:

Copy the P190 file from

smb://fserve/cruisedata/MGL1004/processed/Spectra_P190

Edit out any bad shots (usually before FGSP, after LGSP) from P190 file

Run the p190 file through the Python script, p190_shot_dist_xend.py.

> python p190_shot_dist_xend.py MGL0908_2.p190

The output file will be a tab-delimited file:

MGL0908_2_shdist.txt

ProMAX Processing Parameters:

1. Geometry Setup:

1) Purpose: Set up geometry in ProMAX

a) 2D Marine Geometry Spreadsheet

1. Setup:

- a. Select: Matching pattern number in the SIN and PAT spreadsheets
- b. Station Intervals:
 - i. Nominal Receiver Station Interval: 12.5
 - ii. Nominal Source Station Interval: 50.0
 - iii. Nominal Sail Line Azimuth: 90.0
 - iv. Nominal Source Depth: 9.0
 - v. Nominal Receiver Depth: 9.0
- c. Units: Meters
- d. Co-ordinate origin:
 - i. X0: 0.0
 - ii. Y0: 0.0

2. Sources: Shot Pattern Spreadsheet:

- a. Upload the source, station, x, y, and water (H2O) depth from the modified p190 file.
- b. Fill in by hand source depth (9.0), FFID based on log info, and streamer azimuth (270).
- c. *Note: Shot and FFID numbers might not match up along the line such as when a portion of a line needs to be reshot. Hand editing may be required to match the correct Shot and FFID number pairs.
- d. Click Save
- e. Click Exit

3. Patterns: Receiver Pattern Spreadsheet: Fill in by hand the following values

- a. Min Chan: 468 (Closest to vessel)
- b. Max Chan: 1 (Farthest from vessel)
- c. Chan Inc: -1 (Count from min to max chan)
- d. Group Int: 12.5
- e. X Offset: 167.0 (source to first channel)
- f. Y Offset: 0.0
- g. Edit: Nchans: 468
- h. Click Exit

4. Bin: 2D Marine Binning

- a. Assign Midpoints
 - i. Select Matching pattern number in the SIN and PAT spreadsheets
 - ii. Click OK
- b. Binning
 - i. Select: Midpoints, user defined OFB parameter
 1. Source station tie to CMP number: Use first shot number
 2. CMP number tie to source station: 1000
 3. Distance between CMPs: 6.25
 4. Offset bin center increment: 12.5
 5. Minimum offset bin center: 167.0
 6. Maximum offset bin center: 6004.5

7. Check: CMP numbers increase in shooting direction
 8. Check: Receiver numbers increase in shooting direction
 9. Click OK
 - ii. Select: Receivers
 1. Receiver bin width: 12.5
 2. Click OK
 - c. Finalize Database
 - i. Click OK
2. Load SEG-D Data and enter Geometry into Trace Headers
 - 1) Purpose Load SEG-D data into ProMAX and combine with Geometry info in one step.
 - 2) Inline Geom Header Load
 - a) Primary header to match database: SOU_SLOC
3. Shot Display
 - 1) Purpose: Quality Control Shots. Look for bad channels, spikes, etc.
 - 2) Disk Data Input
 - a) Primary Key: Source Index Number
 - b) Secondary Key: Recording Channel Number
4. Trace and noise burst edit
 - 1) Purpose: Remove bad channels, spikes and noise bursts
 - 2) Trace Kill/Delete
 - a) Enter numbers of bad channels determined from shot display
 - 3) Spike & Noise Burst Edit
 - a) Purpose: Test Spike & Noise Burst Edit parameters on known noise bursts
 - b) Review with Trace Display
 - c) Apply to gathers in subsequent flows
5. Deconvolution Test
 - 1) Run on near trace CMP plot or brute stacked section (usually just a small section ~1000 CMPs)
 - 2) Review autocorrelation in trace display
 - 3) Test deconvolution operator length (~100 ms) and prediction distance (~20 ms)
 - 4) Note: See Yilmaz for an in-depth discussion of picking deconvolution parameters.
6. Near Trace CMP Plot
 - 1) Pick basement horizon and other important horizons for use in velocity analysis
 - 2) Choose secondary header to be CHAN
7. Velocity Analysis Precompute
 - 1) Note about Radon filtering: This is applied in the second pass of velocity analysis, not the first. Pick the stacking velocities first, then run Radon analysis and pick a bottom mute. (An easy basic mute is bottom mute at 200 ms P-value (moveout) applied from near 0 ms to T_{max} of data. Refine after second velocity analysis.) With a bottom mute in the Radon transform space, you will mute the primaries and model the multiples, which are then subtracted from the data. On the first round of velocity picking, err toward lower velocities so that you don't accidentally delete primaries with the Radon filter. On the second velocity analysis pass, add the nmo-Radon-reverse nmo sequence on the gathers and refine the velocity picks. Arrivals at higher velocities should become clearer, now that many multiples are removed, and you will likely adjust velocities upward in the deeper section of the CMP gather. You might even find the Moho!
 - 2) Disk Data Input
 - a) Primary Sort Header: CMP
 - b) Secondary Sort Header: Channel

- c) Sort Order: 997-60003(500)[11]:*/
 - 1. For brute stack: large CMP spacing
 - 2. Final stack: small CMP spacing (function of structure)
 - 3) Resample/Desample: 4 ms
 - 4) Disk Data Output
 - a) Dataset: temp
 - 5) 2D Supergather Formation
 - a) Dataset: temp
 - b) Max Fold: 59
 - c) Min center CMP: 1000
 - d) Max center CMP: 60000
 - e) CMP increment: 500
 - f) CMPs to combine: 7
 - 6) Bandpass Filter
 - 7) Spike & Noise Burst Edit
 - 8) Spiking/Predictive Decon
 - 9) NMO (Second pass)
 - a) Direction: Forward
 - 10) Radon Filter (Second pass)
 - a) Number of P-values: 71
 - b) Time gates: 1
 - c) Min P-value of interest: -50
 - d) Max P-value of interest: 800
 - e) Reference offset: 6004.5
 - f) Type of transform: Parabolic
 - g) Pass modeled data or subtract from input: Subtract
 - h) Mute in Radon domain: Yes
 - i) Type of mute: Bottom
 - j) Perform sparse inversion: No
 - k) Reapply TX trace mute after filter: Yes
 - 11) NMO (Second pass)
 - a) Direction: Inverse
 - 12) Velocity Analysis Precompute
 - a) Number of CMPs to sum into gather: 7
 - b) Number of CMPs per stack strip: 11
 - c) Method of computing velocity functions: Constant Velocity
 - 13) Disk Data Output
 - a) Dataset: lineB.velanal.precomp
8. Velocity Analysis for Precomputed Supergathers
- 1) Disk Data Input
 - a) Dataset: line.B.velanal.precomp
 - b) Primary: Supergather Bin Number
 - c) Secondary: None
 - d) Sort order list: */
 - 2) Velocity Analysis
 - a) Is the incoming data precomputed: Yes
 - b) Copy picks to next location: Yes
9. Stack
- 1) Spike & Noise Burst Edit

- 2) Bandpass Filter
 - 3) Deconvolution
 - 4) NMO
 - 5) Radon Filter (Optional)
 - 6) Inside NMO Mute
 - 7) Stack
10. Time Migration
- 1) Memory Stolt F-K Migration
11. Multiple removal options
- 1) F-K filter in CMP domain
 - requires additional velocity analysis
 - 2) Radon filter in CMP domain
 - takes longer to run
 - 3) Inside mute
 - inside traces only
 - 4) Time-variant frequency filter
 - low-pass filter below seafloor multiple applied in addition to above steps

Little Scripts for MCS Processing

Python script for P190 files: p190_shot_dist_xend.py

```
# script to pull the shot location information
# from p190 data files on the MGL1004 cruise
# and calculate distance along line from first point
# shot location is from center of source

import string
import math
import sys
from sys import argv

if len(argv)>1:
    filename = argv [1]
    out = str(filename)
    out_step = out.split(".")
    output = out_step[0]+"_shdist.txt"
    print "shot distances output to: ", output
else:
    print "usage: python p190_shdist.py filename.p190"
    sys.exit(0)

infile = open(filename, 'r')
line_list = infile.readlines()
infile.close()

outfile = open(output, 'w')

count = 0

for i in range(len(line_list)):
    items = list(line_list[i])
    if items[0]=="S":
        count+=1
```

```

    seisid=""; shot_num=""; lat_deg=""; lat_min=""; lat_min=""; lat_sec="";
lng_deg=""
    lng_min=""; lng_sec=""; easting=""; northing=""; depth=""; jd=""; time=""
    dist=0.0; x=0.0; y=0.0; x2=0.0; y2=0.0
    for j in range(1, 10): seisid+=items[j]
    for j in range(21, 25): shot_num+=items[j]
    for j in range(25, 27): lat_deg+=items[j]
    for j in range(27, 29): lat_min+=items[j]
    for j in range(29, 34): lat_sec+=items[j]
    lat_sign=items[34]
    for j in range(35, 38): lng_deg+=items[j]
    for j in range(38, 40): lng_min+=items[j]
    for j in range(40, 45): lng_sec+=items[j]
    lng_sign=items[45]
    for j in range(46, 55): easting+=items[j]
    for j in range(55, 64): northing+=items[j]
    for j in range(64, 70): depth+=items[j]
    for j in range(70, 73): jd+=items[j]
    for j in range(73, 79):
        if items[j]==" ": items[j]="0"
    time=items[73]+items[74]+":"+items[75]+items[76]+":"+items[77]+items[78]
    east_i = float(easting); north_i = float(northing)
    if count==1: east_1=east_i; north_1=north_i
    x = (east_i-east_1); y = (north_i-north_1)
    x2 = x ** 2; y2 = y ** 2
    #at this point, distance is calculated
    fdist = math.sqrt(x2+y2)
    #but printing a floating point number screws the column format up, so we
do this dance:
    ndist = round(fdist, 1); sdist = str(ndist); sdist_parts=sdist.split(".")
    dist_dec=list(sdist_parts[1])
    dist=sdist_parts[0]+ "." +dist_dec[0]
    #surely there's a better way to print a floating point number to 1
decimal place
    #I just wish my programming skills were adequate enough to know it.
    lout1 = shot_num+"\t"+seisid+"\t"+lat_deg+"\t"+lat_min
    lout2 = lat_sec+"\t"+lat_sign+"\t"+lng_deg+"\t"+lng_min+"\t"+lng_sec
    lout3 = lng_sign+"\t"+jd+"\t"+time
    lout4 = depth+"\t0.0\t"+dist
    lout = lout1+"\t"+lout2+"\t"+lout3+"\t"+lout4+"\n"
        outfile.write(lout)
outfile.close()

```

GMT script for plotting black white seismic sections: plotsegy.gmt

```
gmtset PAPER_MEDIA=Custom_1728x2275
```

```
map=ntp_line_D2
```

```
psbasemap -JX72/-50 -R1/4893/2/10 -BNEWS500f100:"Shot Point No.(shot interval
50m)"/1.0g1.0f.1:"TWT(sec)":::"[Shatsky Rise] MGL1004-ML-D2 Near Trace
Plot": -X4 -Y4 -K > $map.ps
```

```
pssegy $map.segy -JX72/-50 -R1/4893/2/10 -V -F0 -D.15 -M67000 -B-.5 -N -O >>
$map.ps
```


GMT script for plotting color seismic sections: segy2grd.gmt

```
gmtset PAPER_MEDIA=Custom_1728x3650
```

```
map=cdp2500_stack_migration5000_line_A
```

```
psbasemap -JX120/-50 -R987/67196/2/10 -BNEWS5000f1000:"CDP No.(CDP interval  
6.25m)"/1.0g1.0f.1:"TWT(sec)":::"[Shatsky Rise] MGL1004-ML-A  
Stack&Migration": -X4 -Y4 -K > test.ps
```

```
seggy2grd $map.segy -G$map.grd -I1/0.004s -R987/67196/2/10 -V -M67000
```

```
grdimage $map.grd -Cseis.cpt -JX120/-50 -R987/67196/2/10 -O -K -V >> test.ps
```

*GMT color map file: seis.cpt was created by "makecpt -Cpolar -T-20/20/1 -Z".

WHOI D2 Seismic Receiver Instrument Description

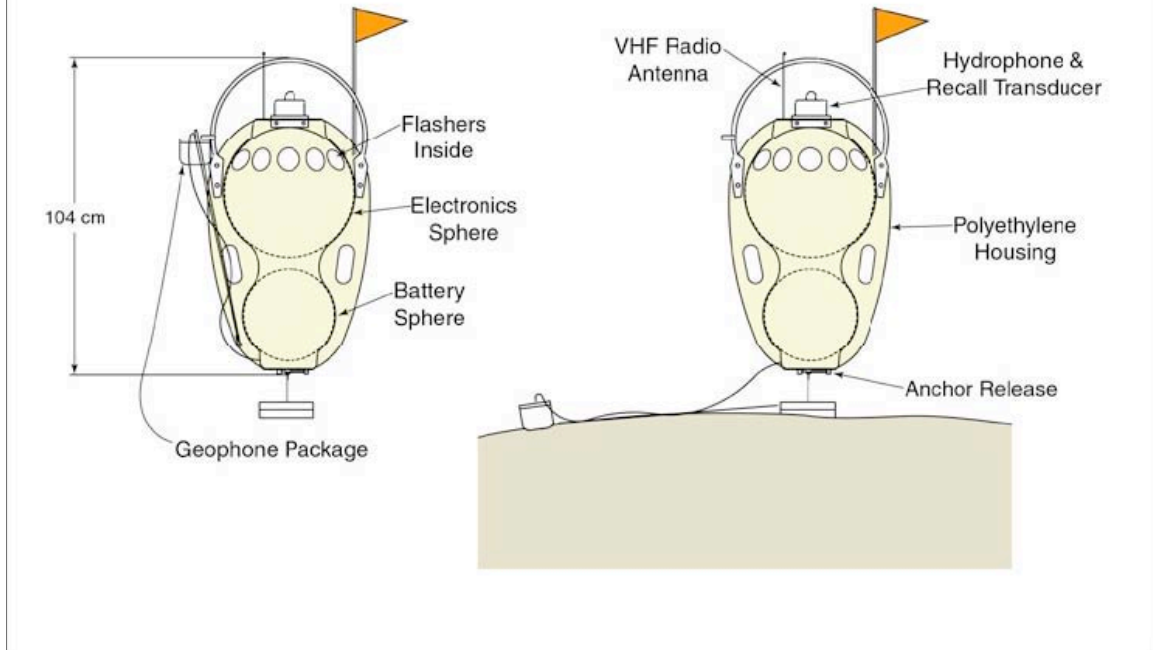
The WHOI short-period OBS, "D2", is a compact, relatively lightweight system, which allows recording of three components of ground motion and one of pressure at sampling rates of up to 200 Hz. Physically, the D2 is comprised of two glass balls containing electronics and batteries, enclosed within a rigid plastic housing. The system stands 39" high and weighs approximately 115 lb in air.

The upper glass ball (17" diameter) contains a Quanterra Q330 data engine, a Quanterra Packet Baler storage device with 20-GB hard disk and Ethernet hub, an EdgeTech acoustic release board, recovery aids, and custom electronics. A Seascan clock is located on a system control board and is accessible via a serial ASCII current loop. Recovery aids include four flashers, a programmable VHF radio with a minimum range at sea level of ~2 nm, and a high-visibility flag. The VHF antenna is attached to the inside surface of the glass ball. The Q330 includes operating software, a low-power analog-to-digital converter with 140 dB dynamic range, digital filters, clock, and 8-16 Mbytes of buffer memory. Engineering data and four channels of signal are continuously recorded and intermittently logged via an Ethernet connection onto the disk drive in mini-SEED format. For this experiment, we used a sample rate on all data channels of 200 Hz. In the lower glass ball (10" diameter) are battery packs comprised of both alkaline and lithium cells that supply power separately to the Q330 and hard drive, the recovery electronics board and aids, and to the EdgeTech release board (separate cells for acoustic ranging and releasing). Ethernet connections can be used to program the operating software and to recover data from the hard drive.

The external plastic case or "hard hat" provides protection for the glass balls and structural rigidity. An ITC 12 kHz acoustic transponder is attached to the upper cover of the case. Next to the transponder is a Hi Tech model HTI 1-90-U hydrophone. Three orthogonally mounted 4.5 Hz geophones are mounted in a 5" diameter (5.5" high) titanium case, which is attached by a weighted cable through the plastic case to the upper electronics ball. The case is filled with high viscosity silicone oil. Internal gimbals allow the geophones to passively orient themselves with respect to gravity through 180 degrees of motion. Prior to deployment, a bail is screwed to the seismometer case, and the bail is hooked to the tip of a 23" long fiberglass wand. The bottom of the wand is attached to the base of the plastic housing by a rotatable joint. The tip of the wand and the seismometer are raised and attached to the side of the plastic housing by a galvanic link that dissolves in seawater after ~4 hours. When the link dissolves, gravity carries the sensor can out and away from the D2. The sensor can slips from the tip of the wand, which is then pulled up and away from the can by a bungee cord.

The D2 has ~25 lb of buoyancy and is weighted by a 55 lb steel plate anchor (6"x15"x2"). A 9" length of stainless steel wire rope to a 2" diameter ring connects the anchor plate. The ring is held to the D2 by a lever arm. One end of the lever arm is attached to the D2 base plate by a burn-wire that can be severed by an electric current triggered by a coded acoustic signal to the EdgeTech transponder. A battery that is separate from the battery supplying power to the Q330 and the hard drive powers the burn wire and release electronics.

D2 Seismic Receiver



WHOI OBS

Hydrophone: Hi Tech® HTI-90-U
Geophone: Geospace® 4.5 Hz GS-11D
Data Logger: Quanterra® QA330 24-bit A/D. Dynamic Range: 135dB. Data Compression.
Sample Rate: 200 Hz

Ocean Bottom Seismometer Deployment Record

OBS	deployment		latitude	longitude	depth		
	date	time					
a1	7/28	23:27	33	37.77008	156	35.88005	5420
a2	7/28	22:09	33	33.00765	156	47.46612	5337
a3	7/28	20:51	33	28.23393	156	59.06065	5154
a4	7/28	19:21	33	23.35112	157	10.63500	4583
a5	7/28	17:54	33	18.49675	157	22.15655	4289
a6	7/28	16:49	33	13.63442	157	33.71268	3922
a7	7/28	15:26	33	8.73027	157	45.14823	4016
a8	7/28	14:04	33	4.32550	157	55.49785	3438
a9	7/28	13:05	32	58.90153	158	8.25485	3198
a10	7/28	11:24	32	55.23872	158	16.68805	2113
a11	7/28	10:19	32	51.46670	158	25.23218	2702
a12	7/27	23:55	32	46.52052	158	36.65648	2480
a13	7/27	15:54	32	42.26740	158	46.28695	2463
a14	7/27	14:51	32	39.02323	158	53.68970	2537
a15	7/27	13:08	32	32.74373	159	7.86650	3080
a16	7/27	11:33	32	27.21097	159	20.32465	3755
a17	7/27	9:57	32	21.40642	159	33.31370	4334
a18	7/27	8:30	32	16.32165	159	44.58832	4494
a19	7/27	7:04	32	11.25505	159	55.81475	4992
a20	7/27	5:41	32	6.08123	160	7.03549	5162
a21	7/27	3:50	31	59.72733	160	21.07258	5334
b1	7/28	6:03	32	8.19043	158	13.98265	2671
b2	7/27	4:35	32	17.90448	158	19.58452	2558
b3	7/28	2:52	32	27.56400	158	25.26890	2458
b4	7/28	1:23	32	37.22457	158	30.94437	2392
b5	7/27	22:23	32	56.54865	158	42.35098	2659
b6	7/27	21:11	33	6.20540	158	48.11145	2996
b7	7/27	19:28	33	15.86853	158	53.90003	3074

Ocean Bottom Seismometer recovery record

OBS	recovery		latitude	longitude	depth		
	date	time					
a1	8/30	10:43	33	38.52350	156	36.32896	5427
a2	8/30	13:40	33	33.64891	156	47.82293	5314
a3	8/30	17:03	33	28.78540	156	59.16820	5187
a4	8/30	20:02	33	23.88390	157	10.53810	4576
a5	8/30	22:51	33	19.01938	157	22.08677	4308
a6	8/31	1:37	33	14.06095	157	33.52627	3978
a7	8/31	4:24	33	9.01583	157	45.20893	4022
a8	8/31	7:20	33	4.73450	157	55.26660	3472
a9	8/31	10:13	32	59.33540	158	8.13820	3302
a10	8/31	12:36	32	55.40500	158	16.62250	2113
a11	8/31	14:49	32	51.67678	158	25.14765	2708
a12	9/1	2:25	32	46.63246	158	36.63470	2478
a13	9/1	16:45	32	42.18703	158	46.17086	2461
a14	9/1	19:14	32	38.76860	158	53.23310	2513
a15	9/1	22:05	32	32.38030	159	7.46148	(off)
a16	9/2	1:06	32	26.85220	159	19.90520	(off)
a17	9/2	3:43	32	21.22601	159	33.02161	4324
a18	9/2	6:24	32	16.14313	159	44.27570	4493
a19	9/2	9:11	32	11.16880	159	55.67300	4964
a20	9/2	12:19	32	5.96200	160	6.09010	5197
a21	9/2	15:28	31	59.32195	160	20.94921	5345
b1	9/1	10:53	32	8.28640	158	13.59490	2673
b2	9/1	8:44	32	17.91888	158	19.20793	2553
b3	9/1	6:40	32	27.62630	158	25.01090	2442
b4	9/1	4:25	32	37.32287	158	30.90233	2393
b5	9/1	0:19	32	56.62140	158	42.26700	2666
b6	8/31	22:10	33	6.34093	158	48.02615	2930
b7	8/31	19:48	33	15.71380	158	53.90940	3068

Ocean Bottom Seismometer Data Quality

OBS data quality check with all of refraction shots (*_RL.segy)

OBS	vertical	hori1	hori2	hydro	notes
A01_D31 scale(*)	noisy 400000	noisy 400000	noisy 400000	excellent 100000	vt,h1,h2 very noisy up to trace# 9000
A02_D07	noisy 400000	noisy 400000	noisy 400000	excellent 100000	vt,h1,h2 intermittently noisy
A03_D29	excellent 400000	excellent 400000	excellent 10000	excellent 100000	
A04_D25	weak 30000	excellent 400000	weak 20000	excellent 100000	
A05_D34	weak 20000	excellent 1600000	good 20000	good 100000	
A06_D18	noisy 400000	noisy 200000	noisy 100000	excellent 100000	vt,h1,h2 intermittently noisy
A07_D55	noisy 800000	weak 20000	noisy 400000	excellent 100000	
A08_D35	excellent 400000	excellent 400000	excellent 400000	excellent 100000	
A09_D03	excellent 400000	excellent 400000	excellent 400000	excellent 100000	
A10_D06	excellent 200000	excellent 400000	weak 40000	excellent 100000	
A11_D26	noisy/excel. 400000	noisy/excel. 400000	noisy/excel. 400000	excellent 100000	vt,h1,h2 very noisy up to trace# 9000
A12_D09	excellent 400000	weak 10000	weak 10000	excellent 100000	
A13_D11	noisy/excel. 400000	weak 1000	noisy/excel. 400000	excellent 100000	vt,h2 very noisy up to trace# 9000
A14_D51	excellent 200000	weak 4000	good 4000	excellent 100000	
A15_D49	weak 2000	weak 2000	weak 2000	excellent 100000	
A16_D19	excellent 200000	excellent 1000000	weak 5000	excellent 100000	
A17_D56	noisy 400000	noisy 400000	noisy 400000	excellent 100000	
A18_D39	weak 2000	good 400000	weak 5000	excellent 100000	
A19_D44	excellent 400000	excellent 400000	weak 2000	excellent 100000	
A20_D21	excellent 400000	good 400000	good 400000	excellent 100000	
A21_D10	excellent 400000	good 400000	good 400000	excellent 100000	
B01_D02	excellent 400000	excellent 400000	excellent 10000	excellent 100000	
B02_D40	excellent 400000	excellent 400000	excellent 10000	excellent 100000	
B03_D60	excellent 400000	excellent 5000	excellent 5000	excellent 100000	
B04_D50	excellent 400000	excellent 400000	excellent 400000	excellent 100000	
B05_D41	excellent 400000	excellent 400000	excellent 10000	excellent 100000	
B06_D08	excellent 400000	excellent 400000	excellent 400000	excellent 100000	
B07_D62	noisy 400000	noisy 400000	noisy 400000	good 100000	vt,h1,h2 very noisy from trace# 9000

(*) normalization factor used to plot data with pswiggle

Weekly Reports to NSF

Weekly Report

12 to 25 July 2010
W. W. Sager and J. Korenaga

Cruise MGL1004

Present Status:

Current position (0000 UT, 26 July 2010) is 30°30.73'N, 165°49.85'E and we are steaming NW on a course of 288° at a speed of 10.7 kt with fair wind and seas. We have made good time on our transit from Honolulu, which began at 1630 HST on 17 July 2010 (0230 UT, 18 July 2010). During that time, we have covered ~2030 nm. At our current course and speed, we will arrive at the Shatsky Rise study area tomorrow afternoon (ship's time) and will begin deploying OBS on the seismic refraction lines.

Operations:

During transit, we have been collecting underway geophysical data including multibeam bathymetry, echo sounder profiles, magnetic, and gravity field data. We experienced interference between the Knudson echosounder and the EM122 multibeam, so we reduced the echosounder ping rate in favor of the multibeam system. The multibeam has provided beautiful swaths of data as we cruise along showing ridges, troughs, seamounts, and seafloor spreading fabric. Technicians have spent their time readying equipment for a busy month of surveying over Shatsky Rise. The real work begins tomorrow.

Present Status:

Current position (0000 UT, 2 August 2010) is 33°53.8'N, 149°19.9'E and we are headed west toward Yokohama in Japan. We are about half-way between Shatsky Rise and Japan and expected arrival is noon on 3 August, Japan Standard Time.

Operations:

During the week, we finished transiting from Honolulu to the Shatsky Rise study area. The transit went without problems and many good multibeam bathymetry, magnetic, and gravity data were logged en route. On 27 July 2010 at 0337 UTC we arrived at the first OBS deployment station (near point A in figure), ending the transit. The total transit time was 217.1 hours (9.1 days), which was slightly less than the anticipated 231.4 hours (9.66 days).

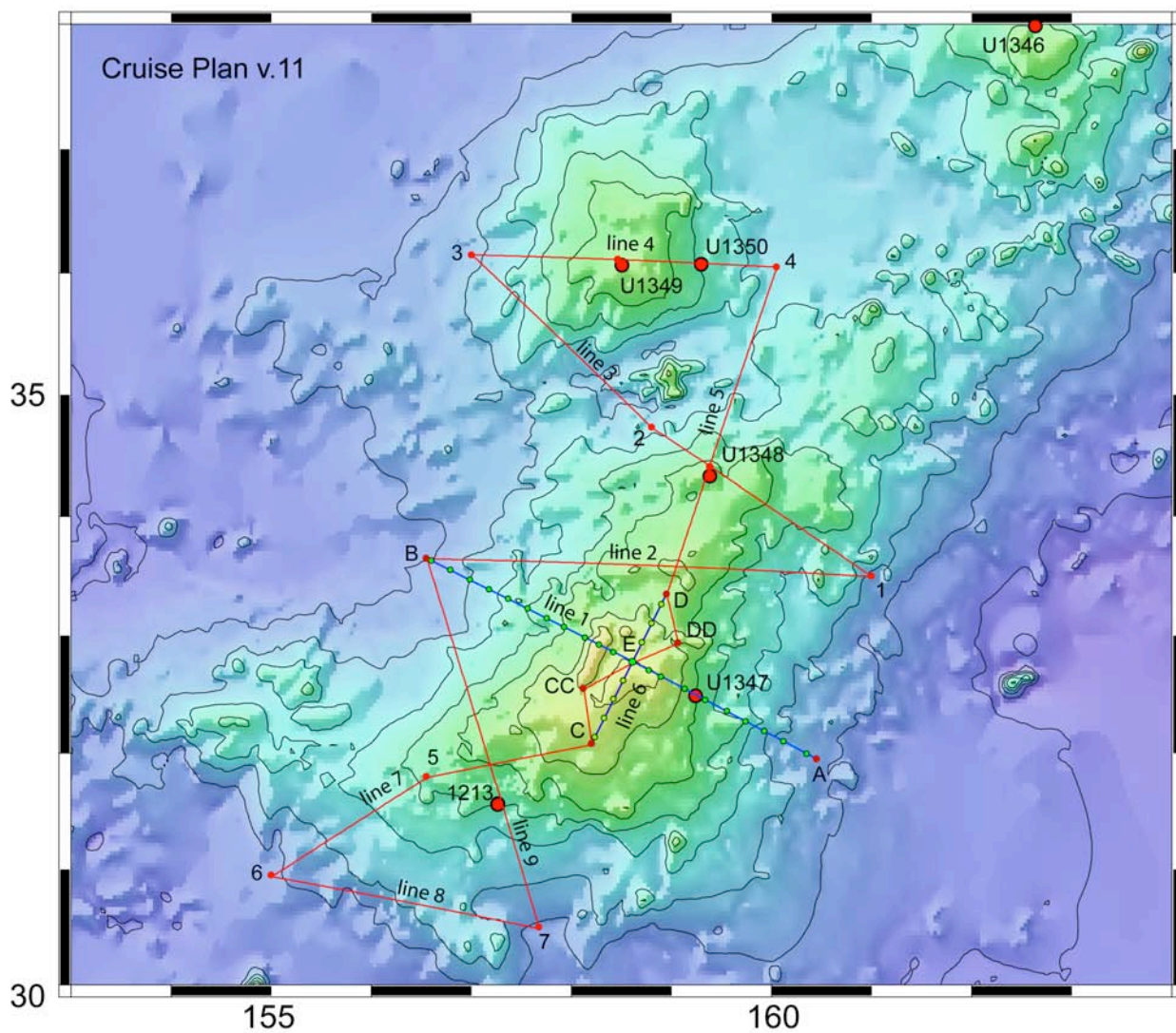
From 0337 UT, 27 July 2010, until 2327 UT, 28 July 2010, a total of 28 ocean bottom seismometers (OBS) were deployed by the Woods Hole Oceanographic Institution OBS team. Twenty-one OBS were dropped along the A-B line and 7 were dropped on the shorter, C-D line. Deployment took ~24 hours less than planned because of deployment contingency time.

By this point in the cruise, we had banked ~4.5 days in contingency time against weather and equipment delays. We left the dock with ~3 days in the bank and between the transit and OBS deployment, added another ~1.5 days.

From 2340 UT, 28 July, until 0201 UT, 29 July, the four air gun strings were deployed. Deployment went smoothly and the system worked adequately. Approximately 5 air guns were found to be not operating, but were mostly replaced by backup guns built into the deployed strings. At 0423 UT on 29 July, we began shooting the first seismic refraction line. The shot interval was set at ~70 seconds and the guns were placed slightly deeper than normal (12 m). This setup was to give more time between shots for deep sound propagation and the deeper air gun deployment accentuates lower frequency waves.

From 0423 UT, 29 July, to 0635 UT, 30 July, we shot line MGL1004_RL_B (points B to E). Turning NE, we next shot line MGL1004_RL_E (points E to DD) until 1318 UT, 30 July. Turning NW, we shot line MGL1004_RL_DD (points DD to D) until 1949 UT, 30 July. Reaching point D at the north end of the line D to C, the ship turned SW and started line MGL1004_RL_D at 2020 UT, 30 July. At approximately 0030 UT on 31 July, a medical emergency was declared and the seismic sources were brought aboard and we began transit to Japan.

At this point in the cruise (0000 UT, 1 August 2010) we have completed 92.9 hours (3.9 days) of science operations and we have been transiting 264.6 hours (11.0 days).



Map of planned tracklines for the Shatsky Rise Seismic Survey. Blue lines A-B and C-D are seismic refraction lines. Small dots on those lines are OBS stations. Red lines E-DD-D and E-CC-C are source only. All other red lines and the blue refraction lines will also be imaged with the MCS system.

Present Status:

Current position (0000 UT, 9 August 2010) is 32°21.3'N, 158°21.6'E. We are shooting seismic refraction to the OBS across Tamu Massif and finishing the line E-C (see figure in Week 1 report). All airguns in the array are firing properly and the shooting is going as planned.

Operations:

Most of the week was spent in transit to and from Japan owing to the medical emergency. The *Langseth* arrived at the dock in Yokohama at 0502 UTC on 4 August and departed a few hours later at 1010 UTC the same day. The transit back to Shatsky Rise took approximately 4 days.

With darkness approaching on 8 August, the airgun arrays were deployed beginning at 0530 UTC on 8 August and started before dark. By 1113 UTC, the *Langseth* was back on line MGL1004-RL-D, at the point where we stopped last week approximately 8.5 days previously. This seismic line is part of the 70-second interval shooting of the refraction lines with airguns only and is intended for the recording of deep refraction arrivals. At midnight UTC, we had shot an additional 105 km of seismic line.

Weather:

Until today the weather has been excellent. On 8th August, the ship finds itself in a small low-pressure cell that formed "out of nowhere", making the weather a bit less favorable, but not yet a problem. This low is expected to exit the region quickly. A tropical depression (TD-05W) has formed near Tawian and projections are that it will move north, perhaps as a typhoon, pass over Japan, and head eastward – to the north of Shatsky Rise - as a tropical system. Although gale warnings are issued for points farther north, this weather system does not appear a threat to *Langseth* operations.

Present Status:

Current position (0000 UT, 16 August 2010) is 30°40.94'N, 156°37.99'E. We are shooting seismic line MGL1004_ML_7, which is between points 6 and 7 on the planned track map (see figure with Week 1 report). All systems are working well and we are collecting excellent data.

Operations:

At 0000 UT on 9 August, the *Langseth* was shooting seismic refraction shots to the ocean bottom seismometers (OBS) located on the seafloor. On August 8, we picked up where we left off at the time of the medical emergency. The ship began shooting with 4 airgun arrays (36 guns) with a repetition rate of ~70 seconds to give time for long shot records from the OBS. The streamer was not deployed for these lines.

On August 9, we were shooting refraction line MGL1004_RL_DR, which is the NNE-SSW oriented, short refraction line between points D and E on the track plan. After this line was completed, we continued shooting to points C, CC, E, and then A where the refraction shooting was completed on 2056 UT on August 10. The OBS were left on the seafloor to record shots from multichannel seismic (MCS) lines at other locations on Shatsky Rise.

The airgun arrays were recovered and reconfigured with the guns at slightly shallower depth for reflection shooting. The 6-km streamer was deployed and the ship was ready to begin shooting MCS data on 1026 UT on August 11, after ~13 hours of deployment. The first streamer deployment was time consuming because it had not been used for a time and it was necessary to check connections.

The first MCS line, MGL1004_ML_A, between points A and B, was covered between 1026 UT on August 11 and 0644 UT on August 13, a period of 42.5 hours. The *Langseth* then took a wide, slow turn to allow two of the airgun arrays to be brought aboard for preventive maintenance. This process required ~3 hours. At 0953 UT on August 13, we began shooting line MGL1004_ML_B, the NNW-SSE line between points B and 7 on the track plan (see figure in Week 1 report). We made the decision to go south first because of a gale near the northern part of the survey. This line was completed after 46.2 hours at 0808 UT on August 15. Again the ship took a wide, slow turn so that preventive maintenance could be done on the other two airgun arrays. After 3.3 hours, the *Langseth* began line MGL1004_ML_7, connecting points 7 and 6 on the track map, at 1125 UT on 15 August. This line was in progress as the week elapsed.

Weather:

Weather was generally favorable during the week. For much of the week, the site was under a high pressure system and seas were very light, often <1 m. As the weekend approached, so did a low pressure cell. The weather has deteriorated throughout the day and seas of 3-4 m are expected.

Results:

At last we have some actual results to show. Appended at the end of this document are several figures produced from the MCS data of lines A and B. These figures only plot "near-trace" data, i.e., the output of the first hydrophone group, but they show a wealth of interesting detail at first glance. Line A crosses the backbone of Tamu Massif and intersects the summit. At the top of the massif is a deep sediment pond between two volcanic ridges, one buried and one emergent. Parasitic cones

are seen on the east side of the massif whereas deep canyons eroded into the sediment and two prominent fault scarps are noted on the west side of the line. The canyons are particularly spectacular in multibeam data as we have already crossed them several times. Scarps like those on the west side of the massif are often seen on the lower flanks of Shatsky Rise and may be important indicators of differential subsidence.

Line B crosses the backbone of Tamu Massif, but at a point down the flank from the summit. On the south side of the line, we note again another large erosional canyon and a large fault scarp. Another nick in the profile is seen on the north side of the line and it too, may be related to faulting.

The last figure shows enlargements of parts of these lines. The top panel is from Line A and shows a close-up of the summit ridge. Interestingly, volcanic basement seems to bow down beneath the ridge, suggesting flexural subsidence. The wavelength is so short that a very weak crust is implied, yet this ridge formed atop a volcano that is probably ~ 30 km in thickness. Beneath the strong reflection that corresponds to igneous basement, many nearly parallel layers are seen. These are probably intrabasement reflectors caused by lava flows. In this near-trace record, we can see ~ 0.5 seconds two-way traveltime into basement, which implies a depth of ~ 1 km (assuming seismic velocity of 4.0 km/sec).

The enlargement from Line B shows the escarpment, with a small parasitic cone at its top. This situation has been noted before on Shatsky Rise and the connection between the cone and scarp may indicate that the scarps formed while the volcano was active and are related to faulting. The multibeam bathymetry data are excellent and show that the cone has a crater in the top and it is breached on the south side, causing a submarine landslide, which shows up as the sediment bump at the base of the scarp. On this line, we also see intrabasement reflectors that are likely to be lava flows. Here we can see faint reflections almost 1 second beneath igneous basement (~ 2 km). We are hopeful that with proper processing, the MCS data will show details at even greater depths.

Present Status:

Current position (0000 UT, 23 August 2010) is 30°55.7'N, 155°34.2'E. We are nearing the end of transit back to Shatsky Rise from Japan. The plan is to slow down at 01:00 UT and deploy gear, to be back on line shooting by 1200 UT.

Operations:

We had to stop acquiring data at 0152 UT on 16 August because of a medical emergency declared by the captain. The seismic gear was recovered by 0532 UT and *Langseth* began a transit to Japan. At 1900 UT on 19 August (just after dawn local time), the ship met the tug *Amagi* several miles off Boso Peninsula and successfully transferred the sick crewman. *Langseth* immediately put to sea and maintained a good speed all the way back to Shatsky Rise.

Weather:

Although the weather was poor at the time we had to recover seismic gear, owing to a small low-pressure cell that passed over the site, conditions improved over the next 24 hours and weather was excellent for the trip to and from Japan.

Outreach:

Since the beginning of the cruise, Korenaga, Floyd, and the students have been posting entries to an online blog, "Life on Shatsky" (<http://lifeonshatsky.blogspot.com/>).

Present Status:

Current position (0000 UT, 30 August 2010) is 34°12.1'N, 154°53.9'E. We are currently proceeding to the end of the seismic refraction line to start recovering ocean bottom seismometers.

Operations:

The R/V *Langseth* arrived back at Shatsky Rise just after the beginning of the week at 0118 UT on 23 August. We deployed the seismic gear and picked up with the interrupted seismic line (MGL1004_ML_7) at 1057 UT. Since that time we have continuously collected multichannel seismic data.

All multichannel seismic lines completed on the cruise to date are shown in yellow. Lines MGL1004_ML_A and _B were completed previously. The rest were done during the past week. Upon returning to Shatsky Rise, we finished Line MGL1004_ML_7, which is a line that crosses a poorly understood low extension of the rise that is a parallel to the pre-Shatsky Rise magnetic lineations. After completing that line (0332 UT, 24 August), the *Langseth* turned NE to shoot a three part line up the southwest flank and across the summit of Tamu Massif. The three parts of the line are MGL1004_ML_6 (completed 0252 UT, 25 August), MGL1004_ML_5 (completed 2029 UT, 25 August), and MGL1004_ML_C (completed 0222 UT, 27 August). The latter line was interrupted by a pod of sperm whales that refused to yield right of way. We had to power down the airguns and turn around to reshoot the gap.

Realizing that we did not have time to go all the way to the north flank of Tamu Massif and still shoot seismics back to the location of the OBSs, we turned onto a cross line and shot down the west flank of the volcano as line MGL1004_ML_D2, completing it on 1500 UT on 28 August. Having a little time left over, we shot a seismic line that extends the transect of Line MGL1004_ML_A. The purpose of this extension was to find the edge of Shatsky Rise volcanism. In the first seismic line (Line A) we found that even though the line started and ended over what appears to be abyssal plain seafloor (depth >5200 m), the seismic data showed that we had not reached the end of the Shatsky Rise flank. Indeed, a preliminary MCS stack indicates that the crustal thickness at the end of Line A is ~9-10 km, which is thicker than normal. With line MGL1004_ML_B2, we extended the line ~200 km to the northwest. The seismic data show that we indeed found the edge of the rise and the beginning of abyssal seafloor. That seismic line was completed at 1815 UT on 29 August. Seismic gear was recovered until 2128 UT on 29 August, at which point the *Langseth* began steaming to the northwest end of the OBS array to start picking up seismometers. This operation is expected to continue for the next 4.4 days.

Results:

The seismic lines collected during the week show similar features to those that we reported previously. The seafloor, sediment layering, and igneous basement are easily identified. Reflectors within igneous basement are seen up to nearly 1.0 second two-way traveltime below the igneous basement surface on near trace plots, indicating significant penetration into the Shatsky Rise lava pile. We think that these reflections are representing stacked lava flows (see attached figures). We continue to find escarpments on the flanks and near the base. We also see buried volcanic cones with disturbed sediments ponded around them and this suggests that we should look at the onlap relationships for clues about their timing. On Line B2 (an extension of Line A; see attached figure), we were able to trace the lateral extent of Shatsky Rise lava flows to the west of the rise. We can

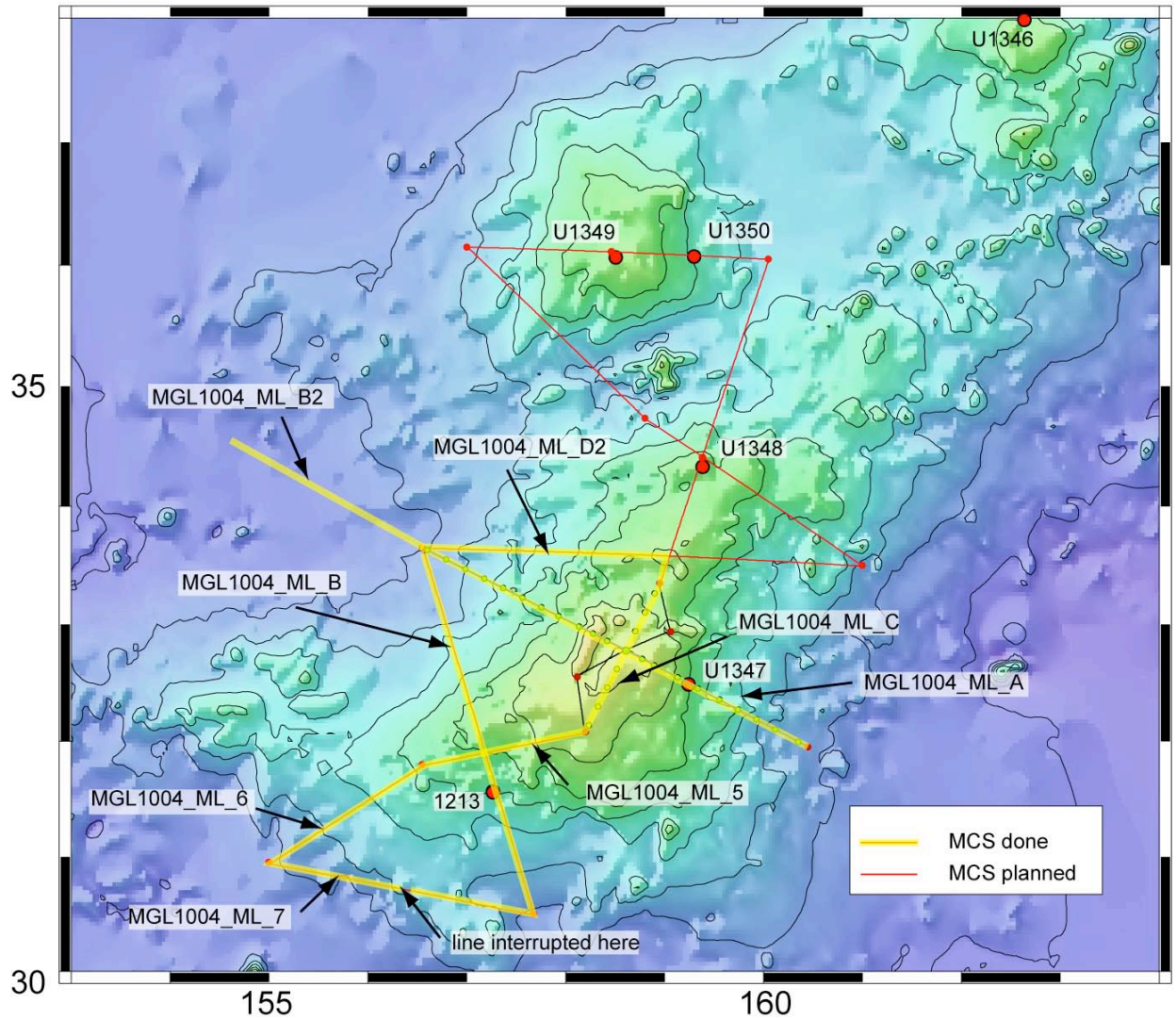
trace the flows to a stopping point against a buried ridge that appears to be ocean crust abyssal spreading fabric. This observation tells us that Shatsky Rise extends significantly farther from the rise than was previously thought and it means that previous estimates of volume are too low.

Weather:

The weather has been generally good and at times spectacularly good. After returning to Shatsky Rise, the seas were relatively calm with swells of ~1 m or less. A high pressure cell settled over the site and the result was that the winds died and we had several days of perfect weather for data collection with flat seas, including one day of glassy calm. The tail end of a front passing by to the north transited the study area and the seas have picked up slightly but have remained <1.5 m. The weather report looks positive for the OBS recovery period ahead. A typhoon has formed to the south of Shatsky Rise, but the predicted path takes it south and west of Japan and it does not appear to be a threat to our work.

Outreach:

Korenaga and the students continue to make daily entries on online blog, "Life on Shatsky" (<http://lifeonshatsky.blogspot.com/>). Jackie Floyd has created a web site for information and discussion of geophysics online, a.k.a. "The Galley" (<http://thegalley.ning.com>), and has posted articles and information from the cruise.



MGL1004 track plan and accomplished lines. Red lines show initial plan for MCS lines. Yellow lines have been completed. Lines MGL1004_ML_7, _6, 5, C, D2, and B2 were completed during the last week. Lines MGL1004_ML_A and _B were completed previously.

Present Status:

Current position (0000 UT, 6 September 2010) is 29°37.3'N, 168°36.1'E. We are currently transiting to Honolulu.

Operations:

At last report, the *Langseth* wrapped up multichannel seismic (MCS) profiling on 30 August and was headed to the refraction lines to recover ocean bottom seismometers (OBS). We left the OBS on the seafloor for the entire seismic experiment so that they would record shots from the MCS profiling of the seismic refraction lines as well as MCS profiling on other Tamu Massif seismic lines. This will provide extra data that can be analyzed to examine the lateral structure of the volcanic edifice. From 1043 UT on 30 August until 1528 UT on 2 September, the *Langseth* recovered the OBS that had been deployed in late July. Although hampered slightly by strong winds and seas up to 3 m, operations proceeded smoothly and 100% of the instruments were recovered. All data have been downloaded and initial examination continues. It appears that all OBS were functional and returned useful data.

From 1551 UT on 2 September to 0705 UT on 4 September, we used remaining contingency time to collect bathymetry and magnetic data over a series of interesting volcanic cones on the SE corner of Tamu Massif. Over the course of ~39 hours, we collected bathymetry data revealing partly buried volcanic cones. Their role in Shatsky Rise volcanism is not immediately clear, but it is clear that there are far more of these features than realized. The reason for their escaping notice is that they appear very subdued in satellite-derived bathymetry data and many fall in the gaps between the haphazard array of geophysical tracks in the area.

At 0705 UT on 4 September, the *Langseth* was back at the point where Shatsky Rise studies began 5.5 weeks ago. At that point, we turned toward Honolulu and the 9-10 day transit back.

Results:

During the week, we continued to work on processing MCS lines. Having Jaqueline Floyd on board has paid dividends because she has the students processing data with ProMax and most lines have gone through brute stacks, coarse velocity picks, several types of filtering, and some migrations. As a result, we are already able to see some important features. Shooting Line B2, the extension of the main refraction line (Line A), turned out to be a good idea because we have imaged a reflector that we think is Moho over the adjacent abyssal plain northwest of Shatsky Rise (see attached figure). Furthermore, this reflector is mostly continuous from Line B2 to adjacent Line A, and we can see it getting deeper towards Shatsky Rise. We would expect the Moho to get deeper where the original crust is isostatically depressed beneath the big volcano. Line B2 is also important because we identified the proximal limit to Shatsky Rise volcanics, which gradually thin out with distance from the center of the big volcano. What is very interesting here is that this is over a region with previously identified magnetic anomalies that are perpendicular to the trend of the seismic line. In other words, if the magnetic anomalies are not misidentified, they indicate that Shatsky Rise erupted on top of pre-existing seafloor that was significantly younger than previously thought (up to M17-M18, but we still need to verify the anomaly locations). This observation favors a model for the rise formation in which the eruptions from a distant center (hundreds of km distant) covered up seafloor all around the volcano, perhaps over a longer time period than previous studies have concluded.

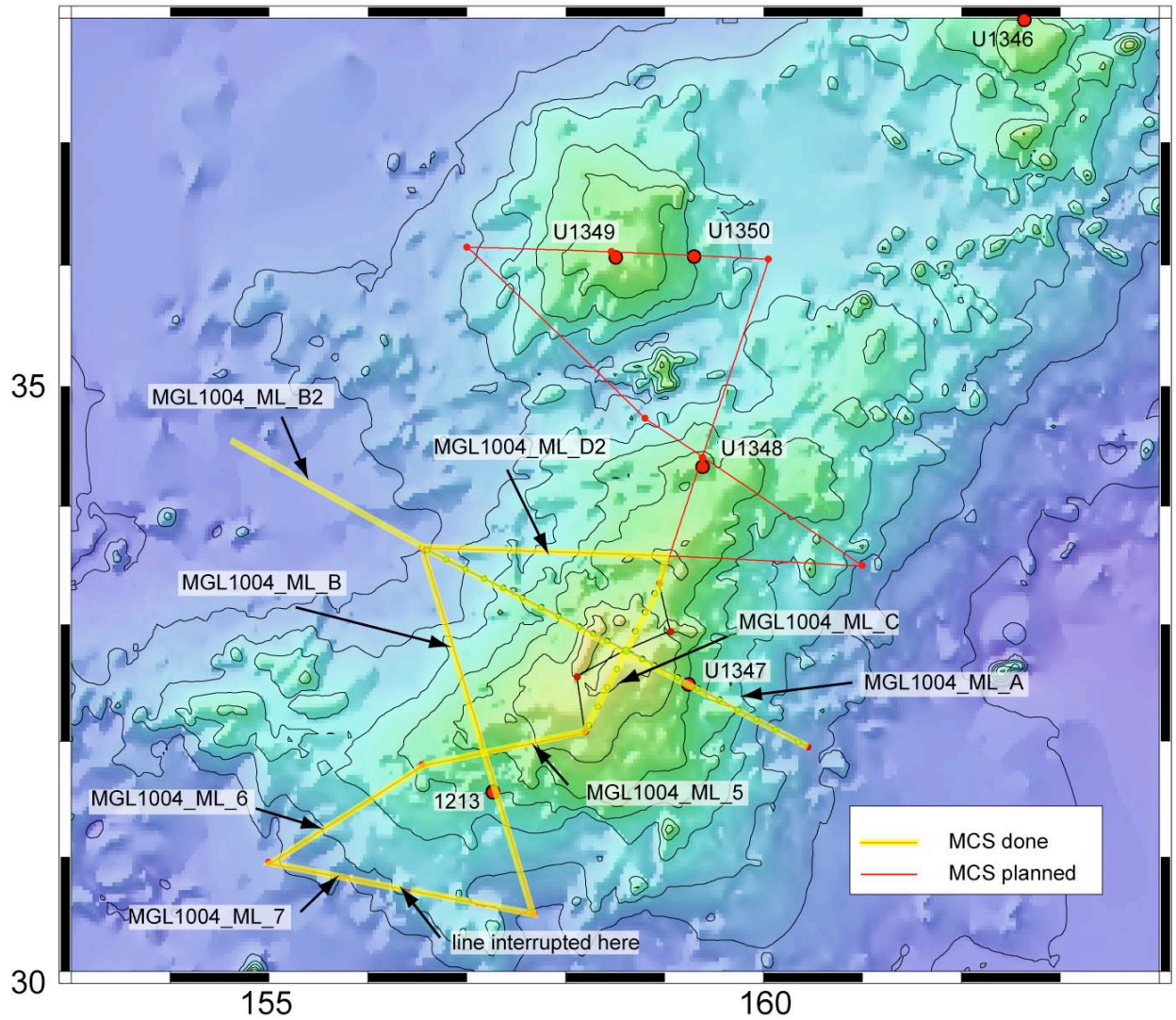
Korenaga has also begun the process of sifting through OBS data. This will take some time, but initial indications look good. The attached figure is from OBS12 (at the summit of Tamu Massif), after band-pass filtering and predictive deconvolution. It shows a reduced travel time plot that clearly shows refractions out to ~200 km from the OBS and beyond. In addition, a later phase with a velocity significantly faster than the reduction velocity (6.5 km/s) is seen. It eventually becomes a first arrival at long offsets. This is PmP, a diffraction from the Moho. We also see a faint signal at offsets greater than ~150 km that is probably Pn. Plots like this one imply that the data will provide the refraction results that were expected.

Weather:

The weather has been generally good; although, not quite as good as during the previous week. Seas have ranged from ~1 m to 2-3 m as the high pressure system in control in the previous week moved away and was replaced by a series of troughs related to higher latitude fronts. The weather has caused no delays.

Outreach:

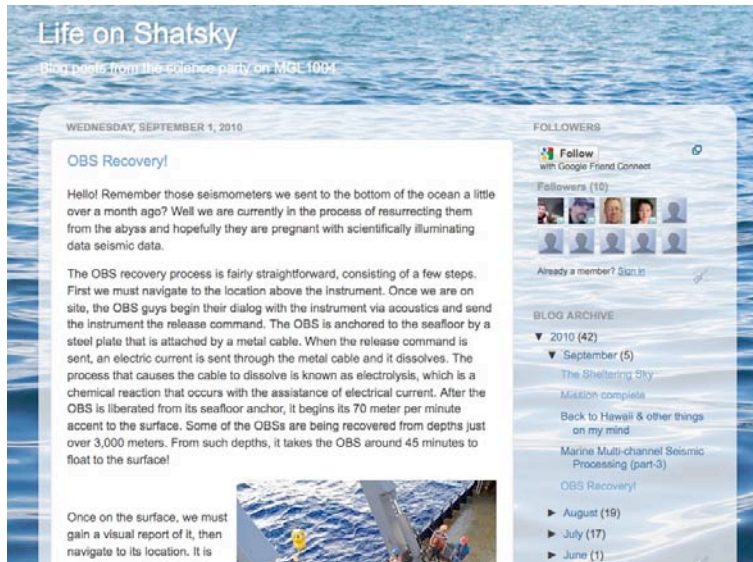
Korenaga and the students continue to make daily entries on online blog, "Life on Shatsky" (<http://lifeonshatsky.blogspot.com/>). Jackie Floyd has created a web site for information and discussion of geophysics online, a.k.a. "The Galley" (<http://thegalley.ning.com>), and has posted articles and information from the cruise.



MGL1004 track plan and accomplished lines. Red lines show initial plan for MCS lines. Yellow lines have been completed. Lines MGL1004_ML_7, _6, 5, C, D2, and B2 were completed during the last week. Lines MGL1004_ML_A and _B were completed previously.

Notes on Outreach Efforts

Prior to MGL1004, Korenaga set up a cruise blog for this cruise at www.blogger.com, which is a free blog site without any commercial advertisement. It was named "Life on Shatsky" (<http://lifeonshatsky.blogspot.com/>). At the beginning of the cruise, watchstanders were asked to sign up for the blog (requires a Google account) and post an article on a daily basis as a group. We have posted 17 articles in July, 19 articles in August, and 7 articles in September until the end of the cruise. Although we were unable to post on a daily basis, what we did may be close enough. The morale of watchstanders was understandably down during two medical diversions, and even Chief Scientist felt uncomfortable to post anything during the first diversion that involved the death of a crew member. Toward the end of this long cruise, everyone seemed to get exhausted, and most of watchstanders seemed to have forgotten their blogging duty.



The visitor's statistics were tracked by [blogger.com](http://www.blogger.com)'s own stats module as well as Google Analytics. The number of daily visits fluctuated around 30 to 50, and the countries from which we collected more than 10 visits during the cruise are USA (1740 visits), UK (64), Japan (37), South Africa (32), Germany (32), Australia (22), Canada (21), and India (16). The total number of page views exceeds 3,200. Though the significance of these statistics is unclear at this point, they should serve as a point of reference for future similar efforts. This type of outreach activity can be improved at least in the following two points:

1. We should more eagerly find a way to broadcast the existence of this cruise blog. We posted a link on the PIs' departmental web sites and emailed to our friends and colleagues, but we need to be more proactive.
2. At the same time, the blog has to have sufficient contents to warrant such broadcasting effort. Free, creative writing may not be easy for all of watchstanders, so to ensure a daily post, it may be better to prepare a large number of potential topics, from which watchstanders can choose.

We will maintain this blog for post-cruise activities and also use it again for a leg 2 planned in spring 2012. The effects of the above recommendations may thus be quantified by comparing the blog statistics of legs 1 and 2.

Summary of Pre-Cruise Twists and Turns

September 29, 2009 First UNOLS official ship schedule for year 2010 was published with the Shatsky Rise cruise dates of **June 17 (Apra Harbor) - July 31 (Dutch Harbor)**, 2010, with a note that "Cruise dates beyond April 2010 are subject to change and we do not recommend purchasing airline tickets at this time."

February 3, 2010 Second UNOLS schedule was published with the same cruise dates, but without the note.

February 22, 2010 During power washing of the Langseth hull, the yard workers hit the MB pod with 5000psi pressured water jets. Damages to the ceramics were deemed extensive. Within the same day, the NSF approved replacement of all damaged ceramics while the ship was in dry dock.

March 4, 2010 Third UNOLS schedule was published with the dates of **July 8 (Apra Harbor) - August 21 (Dutch Harbor)**.

April 8, 2010 Due to bad weather off Astoria postponing testing and a regulatory paperwork issue with the Coast Guard, Langseth's departure from Astoria was pushed back one week.

May 1, 2010 The Coast Guard center in DC had still in place a denial to sail. There were still some parts that needed to perform the final inspection test.

May 4, 2010 Fourth UNOLS schedule was published with the dates of **July 25 (Apra Harbor) - September 7 (Dutch Harbor)**. Korenaga lost all of Yale undergraduate watchstanders at this point.

May 6, 2010 Fifth UNOLS schedule was published with the dates of **July 23 (Apra Harbor) - September 6 (Honolulu)**.

May 22, 2010 Sixth UNOLS schedule was published with the dates of **July 24 (Apra Harbor) - September 7 (Honolulu)**. Due to pitch and engine control issues, Langseth was still in Honolulu.

May 26, 2010 Langseth still remained unable to set off to Guam, with more testing and analysis required.

May 28, 2010 The Rolls Royce techs and governor specialist onboard had exhausted options for fixing system as it existed, with the conclusion that the Engine Control PLC needed to be reprogrammed. In response, Rolls Royce sent one of their top technician from Bergen.

June 4, 2010 The Wiens cruise has been postponed until 2011, and the Shatsky Rise mission became the only Langseth expedition for 2010. The new cruise dates were set to **July 15 (Honolulu) - September 7 (Honolulu)**. Because the start date was pushed back, getting an IHA in time became an issue.

These difficulties, however, seem rather trivial details compared to what happened in the months of July and August.

Incidental Harassment Authorization (IHA)



UNITED STATES DEPARTMENT OF COMMERCE
National Oceanic and Atmospheric Administration
NATIONAL MARINE FISHERIES SERVICE
Silver Spring, MD 20910

Meagan J. Cummings
Marine Environmental & Safety Coordinator
Department of Marine Operations
Lamont-Doherty Earth Observatory
P.O. Box 1000
Palisades, New York 10964-8000

JUL 16 2010

Dear Ms. Cummings:

Enclosed is an Incidental Harassment Authorization (IHA) issued to the Lamont-Doherty Earth Observatory, under the authority of Section 101(a)(5)(D) of the Marine Mammal Protection Act (16 U.S.C. 1361 *et seq.*), to harass small numbers of marine mammals, by Level B harassment, incidental to the R/V *Marcus G. Langseth's* marine seismic survey at the Shatsky Rise in the northwest Pacific Ocean during July to September, 2010.

You are required to comply with the conditions contained in the IHA. In addition, you must cooperate with any Federal, state, or local agency monitoring the impacts of your activity and submit a report to the National Marine Fisheries Service's (NMFS) Office of Protected Resources within 90 days of the completion of the cruise. The IHA requires monitoring of marine mammals by qualified individuals before, during, and after seismic activities and reporting of marine mammal observations, including species, numbers, and behavioral modifications potentially resulting from this activity.

If you have any questions concerning the IHA or its requirements, please contact Jeannine Cody or Benjamin Laws, Office of Protected Resources, NMFS, at 301-713-2289.

Sincerely,

A handwritten signature in black ink, appearing to read "J. Lecky", written over a horizontal line.

James H. Lecky
Director
Office of Protected Resources

Enclosures





UNITED STATES DEPARTMENT OF COMMERCE
National Oceanic and Atmospheric Administration
NATIONAL MARINE FISHERIES SERVICE
Silver Spring, MD 20910

DEPARTMENT OF COMMERCE
NATIONAL OCEANIC AND ATMOSPHERIC ADMINISTRATION
NATIONAL MARINE FISHERIES SERVICE

Incidental Harassment Authorization

Lamont-Doherty Earth Observatory, Columbia University, P.O. Box 1000, 61 Route 9W, Palisades, New York 10964-8000, is hereby authorized under section 101(a)(5)(D) of the Marine Mammal Protection Act (MMPA) (16 U.S.C. 1371(a)(5)(D)) and 50 CFR 216.107, to harass small numbers of marine mammals incidental to a marine geophysical survey conducted by the R/V *Marcus G. Langseth* (*Langseth*) on the Shatsky Rise in the Northwest Pacific Ocean July through September, 2010:

1. This Authorization is valid from July 19, 2010 through September 28, 2010.
2. This Authorization is valid only for specified activities associated with the R/V *Marcus G. Langseth's* (*Langseth*) seismic operations in the following specified geographic area:
 - (a) The Shatsky Rise area, located at 30 - 37 °N, 154 - 161°E in international waters offshore from Japan, as specified in L-DEO's Incidental Harassment Authorization application and Environmental Assessment.
3. Species Authorized and Level of Takes
 - (a) The incidental taking of marine mammals, by Level B harassment only, is limited to the following species in the waters around the Shatsky Rise:
 - (i) Mysticetes – see Table 2 (attached) for authorized species and take numbers.
 - (ii) Odontocetes – see Table 2 (attached) for authorized species and take numbers.
 - (iii) Pinnipeds – see Table 2 (attached) for authorized species and take numbers
 - (iv) If any marine mammal species are encountered during seismic activities that are not listed in Table 2 (attached) for authorizing taking and are likely to be exposed to sound pressure levels (SPLs) greater than or equal to 160 dB re 1 µPa (rms), then the Holder of this Authorization must alter speed or course, power-down or shut-down the airguns to avoid take.



(b) The taking by injury (Level A harassment), serious injury, or death of any of the species listed in 3(a) or the taking of any kind of any other species of marine mammal is prohibited and may result in the modification, suspension or revocation of this Authorization.

(c) The methods authorized for taking by Level B harassment is limited to the following acoustic sources without an amendment to this Authorization:

- (i) a 36-Bolt airgun array that may range in size from 40 to 360 cubic inches (in³) with a total volume of approximately 6,600 in³ as an energy source;
- (ii) a multi-beam echosounder;
- (iii) a sub-bottom profiler; and
- (iv) the acoustic release transponder used to communicate with the Ocean Bottom Seismometers (OBS).

4. The taking of any marine mammal in a manner prohibited under this Authorization must be reported immediately to the Office of Protected Resources, National Marine Fisheries Service (NMFS), at 301-713-2289.
5. The Holder of this Authorization is required to cooperate with NMFS and any other Federal, state or local agency monitoring the impacts of the activity on marine mammals.
6. Mitigation and Monitoring Requirements

The Holder of this Authorization is required to implement the following mitigation and monitoring requirements when conducting the specified activities to achieve the least practicable adverse impact on affected marine mammal species or stocks:

(a) Utilize two, NMFS-qualified, vessel-based Protected Species Visual Observers (PSVOs) (except during meal times and restroom breaks, when at least one PSVO will be on watch) to visually watch for and monitor marine mammals near the seismic source vessel during daytime airgun operations (from civil twilight-dawn to civil twilight-dusk) and before and during start-ups of airguns day or night. The *Langseth's* vessel crew will also assist in detecting marine mammals, when practicable. PSVOs will have access to reticle binoculars (7x50 Fujinon), big-eye binoculars (25x150), and night vision devices. PSVO shifts will last no longer than 4 hours at a time. PSVOs will also make observations during daytime periods when the seismic system is not operating for comparison of animal abundance and behavior, when feasible.

(b) PSVOs will conduct monitoring while the airgun array and streamers are being deployed or recovered from the water.

(c) Record the following information when a marine mammal is sighted:

- (i) species, group size, age/size/sex categories (if determinable), behavior when first sighted and after initial sighting, heading (if consistent), bearing and distance from seismic vessel, sighting cue, apparent reaction to the airguns or vessel (e.g., none, avoidance, approach, paralleling, etc., and including responses to ramp-up), and behavioral pace; and
- (ii) time, location, heading, speed, activity of the vessel (including number of airguns operating and whether in state of ramp-up or power-down), sea state, visibility, and sun glare; and
- (iii) the data listed under 6(c)(ii) will also be recorded at the start and end of each observation watch and during a watch whenever there is a change in one or more of the variables.

(d) Utilize the passive acoustic monitoring (PAM) system, to the maximum extent practicable, to detect and allow some localization of marine mammals around the *Langseth* during all airgun operations and during most periods when airguns are not operating. One PSVO and/or bioacoustician will monitor the PAM at all times in shifts no longer than 6 hours. A bioacoustician shall design and set up the PAM system and be present to operate or oversee PAM, and available when technical issues occur during the survey.

(e) Do and record the following when an animal is detected by the PAM:

- (i) notify the PSVO immediately of a vocalizing marine mammal so a power-down or shut-down can be initiated, if required;
- (ii) enter the information regarding the vocalization into a database. The data to be entered include an acoustic encounter identification number, whether it was linked with a visual sighting, date, time when first and last heard and whenever any additional information was recorded, position, and water depth when first detected, bearing if determinable, species or species group (e.g., unidentified dolphin, sperm whale), types and nature of sounds heard (e.g., clicks, continuous, sporadic, whistles, creaks, burst pulses, strength of signal, etc.), and any other notable information.

(f) Visually observe the entire extent of the exclusion zone (180 dB for cetaceans; see Table 1 [attached] for distances) using NMFS-qualified PSVOs, for at least 30 minutes prior to starting the airgun (day or night). If the PSVO finds a marine mammal within the exclusion zone, L-DEO must delay the seismic survey until the marine mammal(s) has left the area. If the PSVO sees a marine mammal that surfaces, then dives below the surface, the observer shall wait 30 minutes. If the PSVO sees no marine mammals during that time, they should assume that the animal has moved beyond the exclusion zone. If for any reason the entire radius cannot be seen for the entire 30 minutes (min) (i.e., rough seas, fog, darkness), or if marine mammals are near, approaching, or in the exclusion zone, the airguns may not be

started up. If one airgun is already running at a source level of at least 180 dB, L-DEO may start the second gun without observing the entire exclusion zone for 30 min prior, provided no marine mammals are known to be near the exclusion zone (in accordance with condition 6(h) below).

(g) Establish a 180-dB exclusion zone for marine mammals before the 4-string airgun array (6,600 in³) is in operation; and a 180-dB exclusion zone before a single airgun (40 in³) is in operation, respectively. See Table 1 (attached) for distances and safety radii.

(h) Implement a “ramp-up” procedure when starting up at the beginning of seismic operations or anytime after the entire array has been shutdown for more than 8 min, which means start the smallest gun first and add airguns in a sequence such that the source level of the array will increase in steps not exceeding approximately 6 dB per 5-minute period. During ramp-up, the PSVOs will monitor the exclusion zone, and if marine mammals are sighted, a course/speed alteration, power-down, or shut-down will be implemented as though the full array were operational. Therefore, initiation of ramp-up procedures from shut-down requires that the PSVOs be able to view the full exclusion zone as described in 6(f) (above).

(i) Alter speed or course during seismic operations if a marine mammal, based on its position and relative motion, appears likely to enter the relevant exclusion zone. If speed or course alteration is not safe or practicable, or if after alteration the marine mammal still appears likely to enter the exclusion zone, further mitigation measures, such as power-down or shut-down, will be taken.

(j) Power-down or shut-down the airgun(s) if a marine mammal is detected within, approaches, or enters the relevant exclusion zone (as defined in Table 1, attached). A shut-down means all operating airguns are shut-down. A power-down means reducing the number of operating airguns to a single operating 40 in³ airgun, which reduces the exclusion zone to the degree that the animal(s) is outside of it.

(k) Following a power-down, if the marine mammal approaches the smaller designated exclusion zone, the airguns must then be completely shut-down. Airgun activity will not resume until the PSVO has visually observed the marine mammal(s) exiting the exclusion zone and is not likely to return, or has not been seen within the exclusion zone for 15 min for species with shorter dive durations (small odontocetes) or 30 min for species with longer dive durations (mysticetes and large odontocetes, including sperm, pygmy sperm, dwarf sperm, killer, and beaked whales).

(l) Following a power-down or shut-down and subsequent animal departure, airgun operations may resume following ramp-up procedures described in 6(h).

(m) Marine geophysical surveys may continue into night and low-light hours if such segment(s) of the survey is initiated when the entire relevant exclusion zones are visible and can be effectively monitored.

(n) No initiation of airgun array operations is permitted from a shut-down position at night or during low-light hours (such as in dense fog or heavy rain) when the entire relevant exclusion zone cannot be effectively monitored by the PSVOs on duty.

(o) If a North Pacific right whale (*Eubalaena japonica*) is visually sighted, the airgun array will be shut-down regardless of the distance of the animal(s) to the sound source. The array will not resume firing until 30 min after the last documented whale visual sighting.

(p) To the maximum extent practicable, schedule seismic operations (i.e., shooting airguns) during daylight hours and OBS operations (i.e., deploy/retrieve) to nighttime hours.


7. Reporting Requirements

The Holder of this Authorization is required to:

- (a) Submit a draft report on all activities and monitoring results to the Office of Protected Resources, NMFS, within 90 days of the completion of the *Langseth's* Shatsky Rise cruise. This report must contain and summarize the following information:
- (i) Dates, times, locations, heading, speed, weather, sea conditions (including Beaufort sea state and wind force), and associated activities during all seismic operations and marine mammal sightings;
 - (ii) Species, number, location, distance from the vessel, and behavior of any marine mammals, as well as associated seismic activity (number of power-downs and shut-downs), observed throughout all monitoring activities.
 - (iii) An estimate of the number (by species) of marine mammals that: (A) are known to have been exposed to the seismic activity (based on visual observation) at received levels greater than or equal to 160 dB re 1 μ Pa (rms) and/or 180 dB re 1 μ Pa (rms) with a discussion of any specific behaviors those individuals exhibited; and (B) may have been exposed (based on modeling results) to the seismic activity at received levels greater than or equal to 160 dB re 1 μ Pa (rms) and/or 180 dB re 1 μ Pa (rms) with a discussion of the nature of the probable consequences of that exposure on the individuals that have been exposed.
 - (iv) A description of the implementation and effectiveness of the: (A) terms and conditions of the Biological Opinion's Incidental Take Statement (ITS) (attached); and (B) mitigation measures of the Incidental Harassment Authorization. For the Biological Opinion, the report will confirm the implementation of each Term and Condition, as well as any conservation recommendations, and describe their effectiveness, for minimizing the adverse effects of the action on listed marine mammals.
- (b) Submit a final report to the Chief, Permits, Conservation, and Education Division, Office of Protected Resources, NMFS, within 30 days after receiving comments from NMFS on the

draft report. If NMFS decides that the draft report needs no comments, the draft report will be considered to be the final report.

8. In the unanticipated event that any taking of a marine mammal in a manner prohibited by this Authorization occurs, such as an injury, serious injury or mortality, and are judged to result from these activities, L-DEO will immediately report the incident to the Chief of the Permits, Conservation, and Education Division, Office of Protected Resources, NMFS, at 301-713-2289. L-DEO will postpone the research activities until NMFS is able to review the circumstances of the take. NMFS will work with L-DEO to determine whether modifications in the activities are appropriate and necessary, and notified the permit holder that they may resume sound source operations.
9. In the event that L-DEO discovers an injured or dead marine mammal that are judged to not have resulted from these activities, L-DEO will contact and report the incident to the Chief of the Permits, Conservation, and Education Division, Office of Protected Resources, NMFS, at 301-713-2289 within 24 hours of the discovery.
10. L-DEO is required to comply with the Terms and Conditions of the Incidental Take Statement (ITS) corresponding to NMFS' Biological Opinion issued to both NSF and NMFS' Office of Protected Resources (attached).
11. A copy of this Authorization and the ITS must be in the possession of all contractors and protected species observers operating under the authority of this Incidental Harassment Authorization.



James H. Lecky
Director
Office of Protected Resources
National Marine Fisheries Service

JUL 16 2010

Date

Attachments

Attachment

Table 1. Exclusion Zone Radii for Triggering Mitigation.

Source and Volume	Tow Depth (m)	Predicted RMS Distances (m)		
		190 dB	180 dB	160 dB
Single Bolt airgun 40 in ³	9-12*	12	40	385
4 strings 36 airguns 6600 in ³	9	400	940	3850
	12	460	1100	4400

*The tow depth has minimal effect on the maximum near-field output and the shape of the frequency spectrum for the single 40-in³ airgun; thus the predicted safety radii are essentially the same at each tow depth.

Table 2. Authorized Take Numbers for Each Marine Mammal Species in the Shatsky Rise Area.

Species	Authorized Take in the Shatsky Rise Area
Mysticetes	
North Pacific right whale (<i>Eubalaena japonica</i>)	1
Humpback whale (<i>Megaptera novaeangliae</i>)	10
Minke whale (<i>Balaenoptera acutorostrata</i>)	85
Bryde's whale (<i>Balaenoptera brydei</i>)	16
Sei whale (<i>Balaenoptera physalus</i>)	37
Fin whale (<i>Balaenoptera borealis</i>)	16
Blue whale (<i>Balaenoptera musculus</i>)	9
Odontocetes	
Sperm whale (<i>Physeter macrocephalus</i>)	22
Pygmy sperm whale (<i>Kogia breviceps</i>)	100
Dwarf sperm whale (<i>Kogia sima</i>)	244
Cuvier's beaked whale (<i>Ziphius cavirostris</i>)	212
Baird's beaked whale (<i>Berardius bairdii</i>)	27
Longman's beaked whale (<i>Indopacetus pacificus</i>)	14
Blainville's beaked whale (<i>Mesoplodon densirostris</i>)	40
<i>Mesoplodon spp.</i>	3
Rough-toothed dolphin (<i>Steno bredanensis</i>)	97
Bottlenose dolphin (<i>Tursiops truncatus</i>)	750
Pantropical spotted dolphin (<i>Stenella attenuata</i>)	2,200

Spinner dolphin (<i>Stenella longirostris</i>)	26
Striped dolphin (<i>Stenella coeruleoalba</i>)	3,721
Fraser's dolphin (<i>Lagenodelphis hosei</i>)	143
Short-beaked common dolphin (<i>Delphinus delphis</i>)	9,666
Pacific white-sided dolphin (<i>Lagenorhynchus obliquidens</i>)	1,137
Northern right whale dolphin (<i>Lissodelphis borealis</i>)	13
Risso's dolphin (<i>Grampus griseus</i>)	337
Melon-headed whale (<i>Peponocephala electra</i>)	41
Pygmy killer whale (<i>Feresa attenuata</i>)	0
False killer whale (<i>Pseudorca crassidens</i>)	64
Killer whale (<i>Orcinus orca</i>)	5
Short-finned pilot whale (<i>Globicephala macrorhynchus</i>)	156
Dall's porpoise (<i>Phocoenoides dalli</i>)	686
Northern fur seal (<i>Callorhinus ursinus</i>)	56